Alma Mater Studiorum - Università di Bologna

DICAM - Department of Civil, Chemical, Environmental and Materials Engineering

Ph.D. program in Civil, Chemical, Environmental and Materials Engineering

XXIX Cicle

08/A1 - Hydraulics, Hydrology, Hydraulic and Marine Constructions

ICAR/02 - Hydraulic Structures, Maritime Engineering and Hydrology

ANTHROPOGENIC DRIVERS OF FLOOD-RISK DYNAMICS OVER LARGE FLOOD-PRONE AREAS

Submitted by:

Francesca Carisi

Coordinator:

Prof. Luca Vittuari

Supervisor:

Prof. Attilio Castellarin

Final exam - Year 2017

Floods are acts of god,
but flood losses are largely acts of man.

(White, 1945)

Table of Contents

Abstract

Flood risk assessment and management witnessed an extremely significant progress and improvement during the last two decades due to the research efforts carried out by water engineers, climatologists, hydrologists, flood modellers, water authorities and stakeholders, who are pro-actively responding to the increasing impact of floods worldwide and, in Europe, to the promulgation of the European Flood Directive 2007/60/EC. The relationship between flood risk and other factors such as climate variability, population growth and social-economic changes is now a topical issue in the scientific literature. In spite of these efforts, the number of uncertainties associated with both components of flood risk (i.e. hazard and vulnerability) is still high. Also, several open problems need to be accurately investigated in order to better understand, assess and predict flood risk and its evolution in space and time. The present Thesis focuses on various aspects of flood risk assessment. Addressing three different Italian case studies, this Dissertation aims at shedding some light on the most important flood risk related issues for which current literature seems to be still sparse. Concerning flood hazard, the present research investigates the role of human-induced drivers of riverine flood hazard changes. In particular, we show that the influence of anthropogenic land-subsidence near the city of Ravenna is definitely less important than the impact of the linear infrastructures (i.e. reclamation channels, road embankments, etc.) in altering the inundation extent and distribution of flooded areas. Being flood vulnerability the combination of exposed assets and their susceptibility to be damaged by a flood event, these two components were addressed separately. Due to the scarcity of simplified literature procedures for evaluating flood exposure over large areas, this study proposes an innovative simplified tool which combines topographic and land-use information. This methodology proved to be reliable to preliminarily assess how and where (i.e. closer or farther from the river) a specific land-use class developed over time and to enable one to easily compare the suitability of alternative flood risk reduction strategies. By adopting these tools we investigated the evolution of exposure of private real estate sector over the entire floodplain of the middle-lower portion of the Po river during the last 50 years and we showed that the expected economic damages in case of a catastrophic flood event doubled during this time span. Finally, focusing on the assessment of flood susceptibility, which is a critical component of flood-risk assessment, we collected and analysed damage data for a real inundation event (i.e. the inundation event of January 2014 for the Secchia river in Northern Italy), using them to develop uni- and multi-variate damage models for flood losses evaluation over the study area. The performance of these models in estimating flood losses was compared with the performance of widely used and well known literature models. Our outcomes point out that literature damage models, which were originally developed for specific socio-economic

and geographical contexts, should not be exported to different contexts. Uni- and multi-variate models developed on the basis of the observed data set produced much more accurate estimations of flood losses than literature ones, with the multi-variate approach slightly outperforming the uni-variate one. Furthermore, our results highlight the need for a comprehensive collection of post-event data, aiming at validating existing models, or developing new ones in case existing literature models are proven to be unreliable.

Introduction

Hydrological disasters (i.e., natural disaster caused by river and coastal floods, flash-floods, stormwater, etc.) are the most frequently recorded natural calamities occurring worldwide in the last two decades (see e.g. D. Guha-Sapir, R. Below, Ph. Hoyois - EM-DAT: The CRED/OFDA International Disaster Database - www.emdat.be - Université Catholique de Louvain - Brussels - Belgium). Figure 1 shows the distribution of the natural disasters occurred around the world in 2016, subdividing the events into climatological (orange), geophysical (red), hydrological (light blue) and meteorological (green). As one can observe, the number of disasters caused by hydrological events occurred that year dominates comparing to other types of hazards.

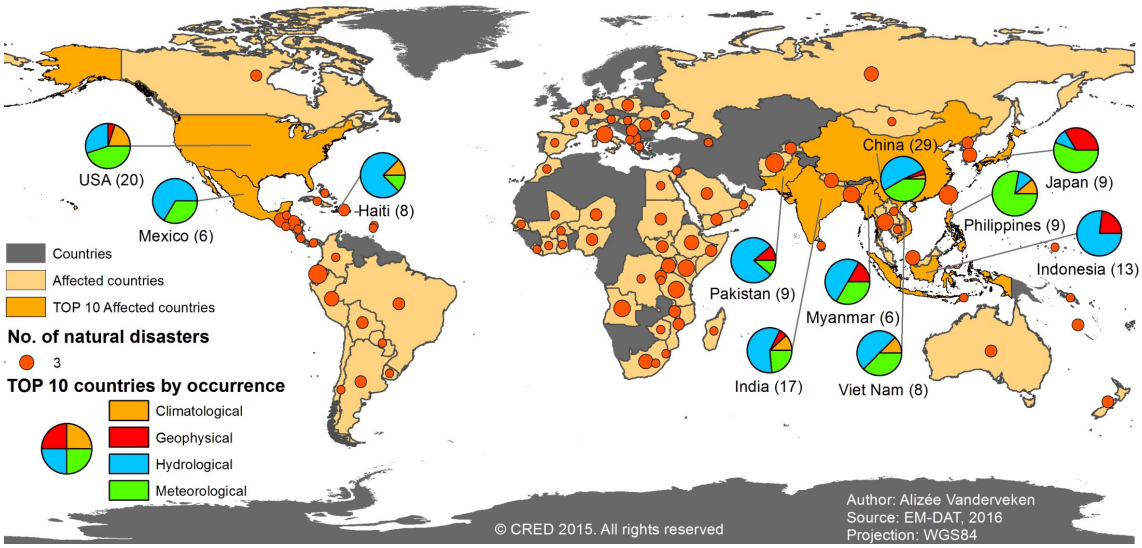

Figure 1: Occurrence and classification of natural disasters in the world in 2016 (see EM-DAT for further details).

Referring to the EM-DAT data-set, the number of hydrological catastrophic events occurred worldwide shows an increasing trend starting from the 1950s, which is more

accentuated relative to the trends reported for other natural disasters (see Fig. 2).

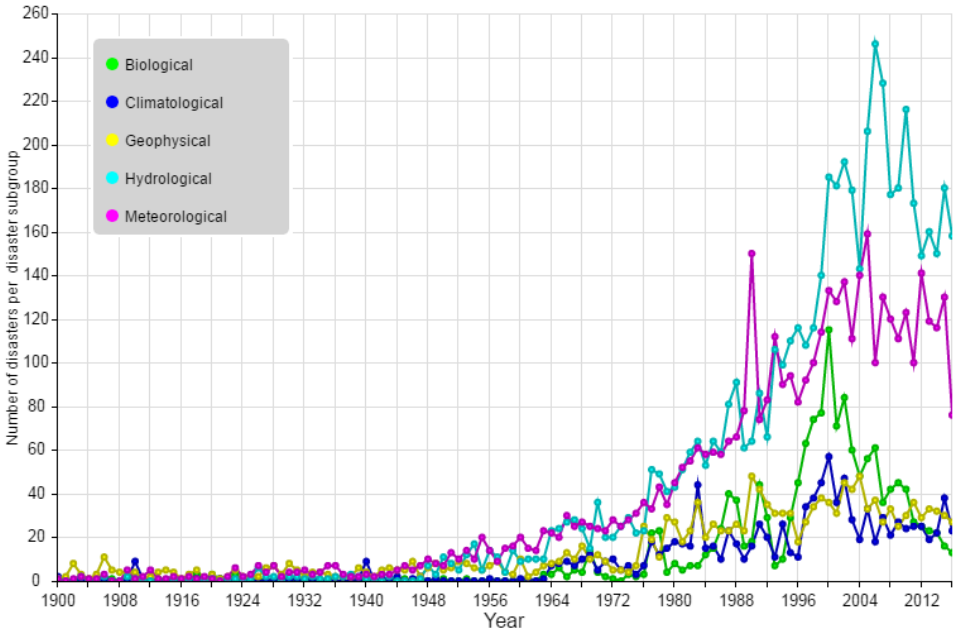

Figure 2: Number of natural catastrophes from 1900 to 2016, divided as per natural disaster subgroup (see EM-DAT for further details).

Analysing the weather-related disasters occurred over the time period 1995-2015, global EM-DAT data set shows that floods, in particular, represent the most frequent calamity, which is also the most impacting one in terms of number of people affected (see also Jonkman, 2005), although storms and extreme temperatures might be more significant in terms of loss of life (see Table 1).

Between 2006 and 2015, flooding was the third major cause of economic losses worldwide among all natural disasters (the firsts was earthquakes and storms), resulting in the total damage in excess of 300 billion $, and the first in terms of overall number of affected people (i.e. more than 0.8 billion people). During the same decade, flooding was ranked first in terms of both total damage (i.e. $\sim$51 billion $) and number of affected people (i.e. $\sim$4 million people) in Europe (EM-DAT). According to Amadio et al. (2013), Barredo (2009), Neumayer and Barthel (2011) and references therein, the occurrence frequency of flood events shows an increasing trend also in Europe for both average and major events. The EM-DAT findings about the increasing amount of economic losses agree with the analyses carried out by the Intergovernmental Panel on Climate Change (IPCC), which highlighted that flood damages in the past ten years were ten times higher than in

Table 1: Time period 1995-2015: number of people affected and killed by weather-related disaster type (see EM-DAT for further details).

	Number of people affected	**Number of people killed**
Flood	2.3 billion (56%)	157 000 (26%)
Drought	1.1 billion (26%)	22 000 (4%)
Storm	660 million (16%)	242 000 (40%)
Extreme temperature	94 million (2%)	164 000 (27%)
Landslide and wildfire	8 million (0%)	20 000 (3%)

the period 1960-1970 (IPCC, 2001, 2014).

According to these figures, floods severely impacts humans and their assets. This is not surprising as, for example, nine of the ten largest urban agglomerates worldwide are located in flood-prone areas (Di Baldassarre et al., 2013). This relationship highlights the importance of considering others factors in the calculation of the potential inundation losses, such as changes in socio-economic exposure (e.g. urban expansion along riversides, increased standards of living, higher individuals and population's well-being). This consideration represents the main background idea of Panta-Rhei "*Change in hydrology and society - Everything Flows*", the scientific decade 2013-2022 of IAHS dedicated to research activities on change in hydrology and society, emphasizing the importance of identifying people and water systems as two closely related components (see Koutsoyiannis, 2013; McMillan et al., 2016; Merz et al., 2014; Montanari et al., 2013; Sivapalan et al., 2012; Winsemius et al., 2015).

Future scenarios provided by IPCC (2014) and Jongman et al. (2012) suggest that future extreme flood events intend to increase in terms of frequency and magnitude on a global scale: by the end of 21^{th} century, world may experience more frequent events with a 100 year return period. Barredo (2009) drew an hypothetical scenario without any change in the meteorological forcing and found that losses would increase anyway in the future due to exposure and socio-economic changes (e.g. higher population, improved pro-capita wealth and living standards). According to Kvocka et al. (2016) and references therein, by 2050 66% of the population in the world will be living in urban areas and 40% of them will be located in areas with high frequency of flood

events. Therefore, the number of people potentially affected by floods is expected to significantly increase in the near future, also considering that 90% of the urban areas expansion will take place in Asia and Africa, where millions of people already live in areas with a high risk to be flooded.

All these considerations underline the importance of the accurate identification of flood-prone areas, in order to coherently design the urban planning and, consequently, implement adequate flood risk reduction measures (Luino et al., 2012). Here, we define *flood risk* as the damage expected for a given element due to a flood event characterized by a specific intensity at a given time period.

As a consequence of over 213 major damaging floods suffered in Europe between 1998 and 2009 (including the catastrophic floods along the Danube and Elbe rivers in summer 2002 and other severe floods in 2005, which caused 1126 deaths; see European Environment Agency, 2010), European Commission made a noteworthy effort to reduce flood risks in the future. In January 2006 the Commission proposed a law with the aim to "*establish a framework for the assessment and management of flood risks, aiming at the reduction of the adverse consequences for human health, the environment, cultural heritage and economic activity associated with floods in the Community*" (article 1, European Commission, 2007). The Directive 2007/60/EC was approved in October 2007 and finally published in the Official Journal in November 2007 under the name of "*Flood Directive (FD)*". In Italy, it is implemented through the Legislative Decree No. 49/2010.

The FD, through strict deadlines, requires Member States (MS) to first identify, for each river basin district, those areas for which potential significant flood risks exist or might be considered likely to occur. For such zones they would then need to draw up flood hazard and flood risk maps and establish flood risk management plans focusing on prevention, protection and preparedness.

Flood risk maps shall show the potential adverse consequences associated with flood scenarios and expressed in terms of the following:

- the indicative number of inhabitants potentially affected;
- the types of economic activities of the area potentially affected;
- installations concerning integrated pollution prevention and control which might cause accidental pollution in case of flooding and potentially affected protected areas;

- other information which the MS consider useful such as the indication of areas where floods with a high content of transported sediments and debris floods can occur and information on other significant sources of pollution.

The increasing impact of floods in the last twenty years and the promulgation of the FD in Europe led flood risk assessment and management to gain even greater interest (De Moel et al., 2015; Dottori et al., 2016b, and references therein). In addition to the classical issue of flood defence, higher attention has been reserved to the importance of mitigation, prevention, preparation, strategies, response and recovery of flood disasters, taking into account such factors as climate change, population growth and economic change in costs and benefits analyses (Merz et al., 2014, 2010b; Meyer et al., 2013).

Predicting current and future flood risk is a major challenge for water engineers, climatologists, hydrologists and flood modellers, who continuously develop new risk assessment methodologies and tools to strengthen hydrologic and hydraulic simulation (Aronica et al., 2013). However, there are still several open problems which need to be addressed and discussed in the scientific literature. For instance, flood risk assessments, due to the complexity of the relevant processes and the multi-aspect nature of the problem, are associated with considerable uncertainty, which can be either epistemic (reducible, due to the imperfect knowledge of the examined system) or aleatoric (irreducible, resulting from the variability and unpredictability of the considered natural processes) (Aronica et al., 2013). The following list sums up the principal sources of errors, inaccuracies or assumptions which can affect flood risk assessment:

- statistical analysis of extreme events from short time series with inherent measurement errors;
- spatial extrapolation of data;
- stationarity and homogeneity in performing flood frequency analysis, without taking into account changes in catchments and climate conditions;
- low resolution and accuracy of some digital elevation models;
- assumptions, simplifications and generalisations that lead to differences between models and reality;
- parametrisation and calibration of the models;

- scarce data for model development and validation;
- inaccurate up- and down-scaling methodologies.

Deep investigations and optimisations in all these fields are needed in order to enhance flood risk management from local to global scale (Messner et al., 2007; Meyer et al., 2013; Molinari et al., 2014a). The remaining uncertainties, however, need to be carefully evaluated and transparently communicated to decision makers (Aronica et al., 2013; De Moel et al., 2012; Kreibich et al., 2016c; Meyer et al., 2013) in a way that non-experts and stakeholders can understand, trust and get motivated to respond to uncertain knowledge (Büchele et al., 2006, and references therein).

Structure and contributions to the Thesis

Various aspects of flood risk assessment are explored in this Thesis. In order to organize its content in the clearest and most logical way, the Dissertation is structured as follows.

In Ch. 1, the concept of flood risk is explained. Aiming at better understanding its definition, an overview of the components that influence it (hazard, exposure and susceptibility) is provided, together with a sketch of the main related prevention measures which can be implemented in order to correctly manage the flood risk. An introduction about the most used approaches to flood risk assessment is included and, finally, the description of the hydrodynamic models used to assess the flood hazard is provided, distinguishing between one-, two- and three-dimensional approaches.

Chapter 2 goes deeply into the aim of the present Dissertation, providing the reader with an overview of the state-of-the-art of flood risk assessment. Open problems and largely discussed topics in the recent literature are examined, offering an overview of the most important issues to be addressed by present and future studies. In particular, the discussion focuses on drivers causing flood hazard and flood exposure evolution in the last decades and on the different literature approaches used to evaluate flood risk on large scale. Being vulnerability (considered as damage susceptibility) a significant component of flood risk, a part of this chapter is dedicated to the losses assessment methods mostly used in the literature and the uncertainties deriving by using one damage model rather than another. Chapter 2 ends with the main three research questions that this Thesis intends to give an answer.

Chapter 3, 4 and 5 present the results obtained assessing three different case studies addressed during the PhD activity.

Chapter 3 describes the potential role of anthropogenic land-subsidence in riverine flood hazard dynamics in the area near the city of Ravenna (cumulative land subsidence larger than 1.5 m in the last century over the historical center of the city), compared to the influence of other human-induced drivers, such as the construction of infrastructure). The study was performed by simulating the flooding dynamics in the study area by means of a 2D finite-element scheme, considering various inundation scenarios caused by four different breaches in the left embankment of the Montone River, South of Ravenna, and different topographic configurations.

The second case study is addressed in Ch. 4, where the reliability of simplified graphical tools, which we term Hypsometric Vulnerability Curves (HVCs), are proposed and investigated for assessing flood vulnerability and risk evolution over large geographical areas and for defining sustainable flood-risk mitigation strategies. These curves rely on the use of inundation scenarios simulated by means of a quasi-two-dimensional (quasi-2D) hydrodynamic model which reproduces the hydraulic behaviour of the floodable areas outside the main embankment system of the study river reach, the middle-lower 350 km stretch of the Po river (Northern Italy). We also compared the proposed simplified approach with a traditional approach based on simulations performed with fully-2D hydrodynamic models, in order to characterize the accuracy of the proposed methodology for flood-risk assessment over large geographical areas and different historical land-use scenarios.

In Ch. 5, the observed damage data for the area recently flooded by the Secchia River (January 2014) were used to assess losses prediction in the Italian context, characterised by the lack of damage curves valid over national scale, in addition to limited and fragmented losses data assessment. A comparison was performed between observed losses and damage data estimated by using both literature uni- and multivariate models and empirically obtained damage function. This allowed us to draw some general conclusions about the models performance and their transferability to different contexts compared to the one in which they are developed.

Parts of the research activity described in the present Thesis are reported in the following publications:

- Domeneghetti, A., Carisi, F., Castellarin, A., Brath, A., 2015. *Evolution of flood risk over large areas: quantitative assessment for the Po River*, Journal of

Hydrology, 527, 809-823;

- Carisi, F., Domeneghetti, A., Gaeta, M.G., Castellarin, A., 2016. *Is anthropogenic land-subsidence a possible driver of riverine flood-risk dynamics? A case study in Ravenna* (Hydrological Sciences Journal - under review);

- Brath A., Domeneghetti A., Carisi F., Castellarin A., 2014. *Percezione e realtà dell'evoluzione del rischio alluvionale. Il caso del bacino del fiume Po*, in Tecniche per la Difesa dallInquinamento, Proceedings of the XXXV course, Guardia Piemontese Terme (CS), Italy, 18-21 June 2014, EdiBios (CS), pp. 551-573;

- Domeneghetti, A., Carisi, F., Castellarin, A., Brath, A., 2014. *Evoluzione del rischio idraulico negli ultimi 50 anni: percezioni ed elementi oggettivi per il fiume Po*, Atti del XXXIV Convegno Nazionale di Idraulica e Costruzioni Idrauliche, Bari, Italy, 7-10 September 2014 (Zaccaria Editore), pp. 587-588;

- Carisi, F., Domeneghetti, A., Castellarin, A., 2015. *Simplified graphical tools for assessing flood-risk change over large flood-prone areas*, Proc. IAHS, 92, 1-7, 26^{th} IUGG General Assembly, Prague, Czech Republic, 22 June-2 July 2015;

- Carisi, F., Domeneghetti, A., Castellarin, A., 2015. *Assessing the historical flood-risk evolution over large floodable areas: testing the reliability of simplified graphical tools*, Proc. 36^{th} IAHR World Congress, Delft-The Hague, the Nederlands, 28 June-3 July 2015, pp. 1-11;

- Carisi, F., Domeneghetti, A., Castellarin, A., 2016. *Effects of anthropogenic land-subsidence on river flood hazard: a case study in Ravenna, Italy*, Proc. IAHS, 373, 161-166, 7^{th} International Water Resources Management Conference of ICWRS, Bochum, Germany, 18-20 May 2016;

- Carisi, F., Domeneghetti, A., Castellarin, A., 2016. *Effetti della subsidenza antropica sulle dinamiche di inondazione: il caso studio di Ravenna*, Atti del XXXV Convegno Nazionale di Idraulica e Costruzioni Idrauliche (Eds. A. Castellarin et al.) pp. 879-882, Bologna, Italy, 14-16 September 2016;

- Carisi, F., Domeneghetti, A., Castellarin, A., Brath, A. 2016. *Rischio alluvionale lungo lasta medio-inferiore del Po: valutazione dei danni potenziali e definizione*

di strategie di mitigazione, Atti del XXXV Convegno Nazionale di Idraulica e Costruzioni Idrauliche (Eds. A. Castellarin et al.) pp. 923-926, Bologna, Italy, 14-16 September 2016.

Chapter 1

Flood risk assessment

1.1 Fundamental concepts and definitions

The concept of risk in technical and scientific fields assumes different meanings depending on the analysis context (economic-financial, insurance, technology, etc.).

With regard to natural disasters, risk is generally described as the occurrence probability of natural disasters characterized by a certain intensity and causing a certain damage; more specifically, the concept of hydraulic risk related to flood, i.e. **flood risk**, is explicitly defined by the FD 2007/60/EC (European Commission, 2007) as *"the combination of the probability of a flood event and of the potential adverse consequences for human health, the environment, cultural heritage and economic activity associated with a flood event"* (article 2, paragraph 2).

From the analytical point of view, it is possible to express the hydraulic risk, R, as:

$$R = H \cdot V \tag{1.1.1}$$

where H is hydraulic *hazard* and describes the probability with which a flood event with a certain intensity can occur in a specific area and in a specific time period and V (*vulnerability*) provides information concerning which and how many elements can be affected by risk, and if and how much they are able to withstand a certain flood event. The second component is also called *damage*.

The flood risk is therefore defined as the damage expected for a given element due to a flood event characterized by a specific intensity at a given time period; it is therefore clear that it is a combination of two distinct aspects: the first one is related

to the description of the intensity and the characteristics of the inundation event, while the second aspect expresses the damage experienced by the elements exposed to flood.

According to Merz et al. (2007), in the literature flood *vulnerability* is often expressed by the *exposure* E, which indicates the quantification and qualification of the elements exposed to risk, multiplied by the *susceptibility* S, namely the attribution of a loss value to the given element, as a function of one or more hydraulic parameters (i.e. how much the element can be damaged). The hydraulic risk associated with floods, therefore, can be also expressed as:

$$R = H \cdot E \cdot S \tag{1.1.2}$$

The influence of these three factors is well represented by the concept of the risk triangle, introduced firstly by Crichton (1999) in the insurance field. Using a geometric analogy, he showed how its geometric area size strictly depends on each triangle size: if one gathers the area of the triangle to the flood risk size and its sides to the three risk influencing factors (hazard, exposure and susceptibility, see Fig. 1.1), it results evident that the flood risk decreases if at least one of the factor is reduced.

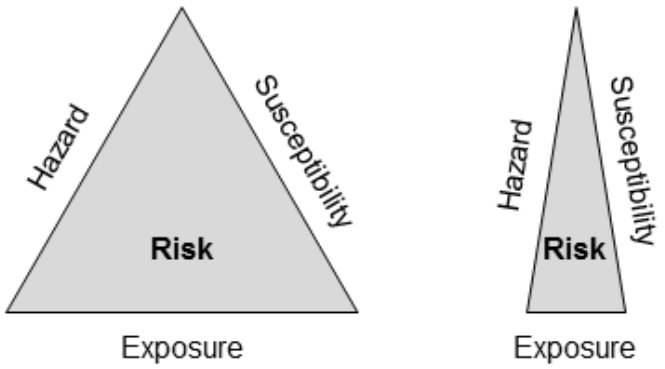

Figure 1.1: Risk triangle concept (Crichton, 1999).

In the next sections, a more detailed description of the factors having a role in the flood risk assessment is provided, together with a briefly overview of the measures that should be implemented, regarding each factor, for a proper risk management. According to Koks et al. (2015), the application of these strategies should not be homogeneous across large areas, instead it should take into account the different local socio-economic characteristics of each area of interest.

1.1.1 Flood hazard (H)

The flood risk is necessarily evaluated by considering a specific flood event, characterized, in the risk formula, through the hydraulic hazard.

According to article 6 of the FD 2007/60/EC (European Commission, 2007), one of the requirements to the MS is provide hazard maps, covering the geographical areas which could be flooded according to the following scenarios:

- floods with low probability, or extreme event scenarios;
- floods with medium probability (likely return period $\geq$ 100 years);
- floods with high probability, where appropriate.

For each scenario, the following elements shall be shown:

- the flood extent;
- water depths or water level;
- where appropriate, the flow velocity or the relevant water flow.

It is evident, therefore, that in the description of the intensity and the characteristics of an event, numerous variables come into play, named *alluvial intensity indices*. Among these, the most important and taken into consideration are:

- *Water depth*, which indicates the height of the liquid front interesting the element at risk and is the variable that mostly influences the damage processes (Apel et al., 2009; Kreibich et al., 2009; Merz et al., 2013; Penning-Rowsell et al., 2005; Smith, 1994);
- *Flooded area*, which defines the soil surface affected by flood and permits to distinguish potentially affected elements form *safer* ones;
- *Water velocity*, i.e. the speed with which the flood spreads, which can assume a great importance in high slope zones (mountain areas) or near embankment breaches and can increase the magnitude of the flood damage outcome compared to those only considering water depth (De Moel and Aerts, 2011); the element that can be most affected by the influence of this parameter is the human being, which loses stability and can be transported by flood already with a velocity equal to 0.5 m/s (Merz et al., 2007);

- *Flood duration*, indicating how long water dwells in the flooded areas; it is mostly used to evaluate losses due to activities interruption in the industrial, commercial and agricultural sectors, resulting in economic damages;
- *Water contamination rate*, which represents the concentration of pollutants in the water overflowed volume (coming for example by flooded industrial elements) that can increase the damage suffered by certain elements at risk such as people or environment.

Flood hazard is therefore described through the use of these indexes (not necessarily all at the same time) and can be mapped in order to create documents containing the main characteristics of the event (EXCIMAP, 2007), that can represent the reconstruction of a past flood event or be related to a specific return period. In fact, the value of H is closely connected to the event return period T_r (which expresses the time interval in which the event occurs once on average), through the relationship:

$$H = 1 - (1 - \frac{1}{T_r})^N \tag{1.1.3}$$

where N is the time frame, expressed in years, in which to assess the flood hazard.

Flood hazard mapping is a complex numerical task that can be accomplished by referring to various digital-hydraulic approaches existing in the literature and using numerous numerical models (for further details see Sec. 1.3), characterized by different degrees of complexity, according to the amount of data, resources and the technologies availability (Büchele et al., 2006), ranging from simple interpolation methods to sophisticated and spatially detailed models which solve the two-dimensional shallow water equations (Apel et al., 2009). Among the variety of these approaches, it is worth citing relatively new methodologies such as raster based models (Bates and De Roo, 2000; Bates et al., 2004; Falter et al., 2013, see e.g.), remote sensing techniques (Bates, 2012; Domeneghetti, 2014; Refice et al., 2015, 2013; Schumann et al., 2009), and methods based on geomorphic descriptors extracted from Digital Elevation Models (DEMs) (D'Addabbo et al., 2016a,b; Manfreda et al., 2011, 2015, 2014, 2008; Samela et al., 2015). However, the most common procedure for the hazard assessment still remain the use of hydrological-hydraulic models, which can be summarized in the following three steps:

1) Estimation of discharges associated with a specific occurrence probability: this phase, which is commonly performed by means of statistical analysis of historical

flow series, becomes more complex and uncertain in the absence of observations, thus making it necessary to use statistical procedures for regionalization and/or hydrological rainfall-runoff (RFRO) models; HBV, LISFLOOD, TOPKAPI and HEC-HMS are the most widespread hydraulic models in Europe, while MIKE11 and the EFFORTS system are to be cited among the most known hydrological/hydraulic model combinations, according to EXCIMAP (2007);

2) Conversion of estimated discharge values in the river bed into water level values: for this second step the adoptable procedures are multiple as well, ranging from the application of stage-discharge relationships for the determination of the water level in the river bed to the implementation of one- or multi-dimensional hydraulic numerical models for the flood propagation assessment;

3) Determination of the floodable areas and the associated water depth, crossing, section by section, the resulting liquid surface with the ground elevation contours of the flood-prone areas (this step is absorbed by the previous one in 2D hydraulic models).

This approach seems apparently simple, but presents a large number of uncertainties, which need to be considered. The most common error sources, according to Apel et al. (2009), are derived from the inappropriateness of the extreme value function for the given data series, violation of the underlying assumptions of the extreme value statistics, i.e. stationarity and homogeneity of the data series, shortness of the data series and large uncertainties in the extrapolation range. The selection of the appropriate model leads also to inaccuracies (e.g. due to the consideration of dikes and dike breaches), which can be only qualitatively evaluated in most cases, because of the lack of sufficient data on inundation extent and depths for the calibration and validation of the models.

Hazard maps enable authorities in charge of flood risk mitigation planning and management and stakeholders to compare different strategies for managing flood hazard (and flood risk, consequently). The most important protection measures that can be implemented in order to reduce flood hazard are:

- flow reduction (studies on runoff formation mechanisms and its drainage at the basin scale);
- structural measures for the outflows regulation (e.g. retention basins, reservoirs, etc.);

- measures affecting the flood dynamics (river sections, embankments and coverings maintenance, repair and adjustment, etc.);
- improvement of the urban areas drainage.

As mentioned above, the satisfying knowledge of hazard is anyway not sufficient in order to carry out a holistic flood risk analysis, but it is also necessary to define the other two risk triangle sides (exposure and susceptibility), described in Secs. 1.1.2, 1.1.3 and 1.1.4.

1.1.2 Flood exposure (E)

The flood exposure, and therefore the quantification and qualification of the elements exposed to risk, can be *directly* or *indirectly* evaluated. A direct analysis produces high quality data, as these data are obtained through an inspection carried out in the study area and thus report a faithful reconstruction of reality. This approach implicates very high resources costs, and for this reason it is often used only for hydraulic risk assessment at the local scale. In extensive study areas, instead, an indirect approach is preferred, in which exposure information can be obtained by referring to already existing data, for example by consulting geoportals and authorities databases. Obviously, this methodology is less demanding than a direct approach in terms of required resources, but the accuracy and the detail level with which these data are provided can vary significantly, influencing the flood risk assessment performance. In any case, the quality of the obtained results with an indirect approach is certainly lower than that obtained by directly analysing the flood exposure, but the indirect approach allows risk assessment at national or international scale that would be almost impossible with a direct analysis due to the difficulty of data availability.

In relation to the spatial resolution of the information, it is also possible to distinguish available data in *object-oriented data* and *aggregated land use data*. The first ones contain information about individual properties or buildings, such as location and typology (residential, industrial, etc.) and are retrieved from national and regional geoportals or by real estate registries; the latter ones return zones with homogeneous characteristics of the territory, resulting from grouping properties or areas having identical land use (e.g. the standardized classes aggregation adopted by the COoRdinated INformation on the Environment (CORINE) project, European

Environment Agency, 2007, based on satellite surveys). They have the disadvantage of leading to a large number of uncertainties, as an equal buildings and properties distribution within each area with homogeneous use destination is assumed.

Having a quite detailed knowledge of the elements distribution in an area exposed to risk inundation is also necessary in order to implement preparedness measures suitable to improve the population's, authorities' and emergency agency's capacity in addressing the flood event, such as:

- early warning systems and forecasting;
- emergency planning measures;
- training and preparation activities for citizens.

1.1.3 Flood susceptibility (S)

The susceptibility is usually estimated by means of damage models able to provide a damage value (or a percentage of it, compared to the value of the whole building) starting from one or more hydraulic parameters. As it occurs in the majority of literature cases (Green et al., 2011; Jongman et al., 2012; Messner et al., 2007), when losses are assessed only on the basis of one parameter, these functions are called *damage curves* or *susceptibility curves*: relating to the considered variable, they graphically return the damage value of a particular element at risk. According to Apel et al. (2009), Kreibich et al. (2009), Penning-Rowsell et al. (2005) and Smith (1994), among others, most of the models use as hydraulic parameter the water depth affecting the specific element. Other models are recently available (called multi-variate models), which potentially take into account at the same time all the variables that influence the the damage process (see e.g. Merz et al., 2013). In fact, recent studies pointed out the uncertainties of estimations based on stage-damage functions, since the water depth (and in some cases the building use) only explains a part of the data variance, while flood loss depends on many other factors, e.g. flow velocity, duration of inundation, availability and information content of flood warning, precaution and the quality of external response in a flood situation (Apel et al., 2009; Merz et al., 2013, 2004, and references therein). Multi-variate models showed important improvements in the damage estimation compared to the uni-variate models, but present some limitations so far, due to their complexity (Merz et al., 2013). For more complete and detailed damage models description, see Secs. 2.3 and 5.5.

In order to quantify the amount of economic damage suffered by an element at risk, it is necessary to retrieve information about its monetary value. Two approaches are commonly used to determine it:

- *full replacement value*, if it is assumed that, in case of flood, the asset and/or its movable properties have to be replaced with similar new goods, for which their market value is considered; this approach, however, leads to an overestimation of the damage, because the depreciation of the assets value due to their age is not taken into account.
- *depreciated value*, which considers the pre-flood value of each asset.

Because the evaluation of the goods' depreciate values requires detailed information about their age, although it is the most realistic approach, it is extremely complex and expensive: for this reason, average residual values are often considered (e.g. the 50% of the market value is considered, assuming a linear depreciation). It is worth considering that, depending on the type of approach adopted for damages estimation, the risk evaluation can differ significantly.

In order to manage the flood risk taking into account the flood susceptibility variable, the prevention measures that can be implemented are summarized in:

- buildings restrictions;
- relocation of elements at risk;
- updating and increasing knowledge on assets vulnerability in general.

1.1.4 Flood vulnerability ($V = E \cdot S$)

According to Merz et al. (2007), this parameter is often used in the literature in place of the product of exposure and susceptibility. It quantifies the losses expected for the elements (people, buildings, economic activities, ecosystem, etc.) exposed to risk. In the case of a flood event, all variables considered to describe the flood hazard combine together and cause various damage type to assets, people and environment. These different damages are conventionally divided in:

- *Direct damages*, which concern all those consequences caused by the direct contact between the water and the element at risk; for example, the life losses, damages to facilities or material goods fall into this category;

- *Indirect damages*, which consist of losses caused by the interruption of production activities or services and infrastructures related to productive sector, for example losses due to the traffic interruption and the consequent impossibility to reach the job location, causing lower profits and productivity for a specific company (Green et al., 2011); although they are quite difficult to evaluate and case and cite specific, some studies showed that assessment of indirect impacts is essential for a full understanding of the economic results of natural disasters, being a significant share of the direct losses (see e.g. Carrera et al., 2015; De Moel et al., 2015), but shifted in space and time (Green et al., 2011, see Fig. 1.2).

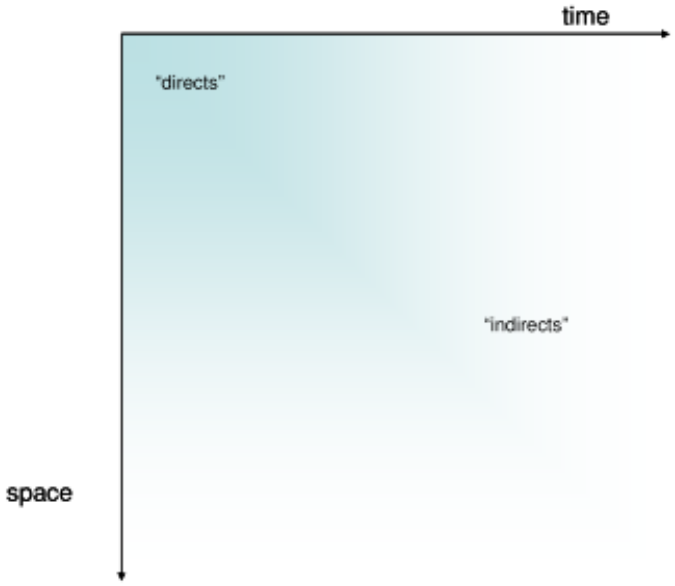

Figure 1.2: Representation of direct and indirect damages; the flood event is established at the beginning of the axis, both in space and time (Green et al., 2011).

Additionally, both the direct and indirect damages can be classified in:

- *Tangible damages*, i.e. with negative effects that are quantifiable from a monetary point of view, such as damages to buildings structure, or business interruption;
- *Intangible damages*, meaning losses for which an economic damage evaluation can not be done, or at least not as easily, such as in case of loss of life, damage to health, cultural heritage or environment (Markantonis et al., 2012).

Table 1.1 clarifies the classification explained above, providing damage examples for each typology.

Table 1.1: Typology of flood damages with examples (Messner et al., 2007)

	Tangible	**Intangible**
Direct	Physical damage to assets: - real estate - movable properties - infrastructure	- Loss of life - Health effects - Loss of ecological goods
Indirect	- Loss of industrial production - Traffic disruption - Emergency costs	- Inconvenience of post-flood recovery - Increased vulnerability of survivors

1.2 Approaches to flood risk assessment

Due to the increasing impact of floods in Europe and worldwide, in the last twenty years, flood risk assessment and management gained even much interest (De Moel et al., 2015, and references therein), leading to the promulgation of the FD 2007/60/EC (European Commission, 2007), which contributed to develop a different view of this topic. In fact, differently from the past, when the focus was mainly on the flood prevention, the FD launched a more holistic view to flood risk: strategies for the mitigation, prevention, preparation, response and recovery of flood disasters shifted from a *flood defence* approach to a *flood management* approach (Dottori et al., 2016b), taking into account also factors as climate change, population growth and economic change in costs and benefits analyses (Merz et al., 2014, 2010b; Meyer et al., 2013).

The FD, as explained in the previous sections, requires some goals to be reached by MS, i.e. the elaboration of hazard and risk maps, but leaves them great freedom on how to achieve these aims. This encouraged the development of different flood risk assessment approaches, which are briefly examined in this paragraph. All of them, however, refer to the same generalised structure, shown in Fig. 1.3:

1) Identification of flood hazard by investigating or modelling hydraulic parameters, i.e. water depth, water velocity, etc. in the areas exposed to flow;

2) Analysis of the exposed elements: creation of homogeneous classes in which potentially affected elements can be aggregated, description of the number and type of elements at risk and estimating their asset values;

3) Combination of information about flood impact and susceptibility of each element at risk, aiming at the quantification of the flood damages; if total damages are calculated for several events with different probabilities, it is possible to refer flood risk directly to an expected annual damage (Aerts et al., 2013; De Moel et al., 2015; Falter et al., 2015).

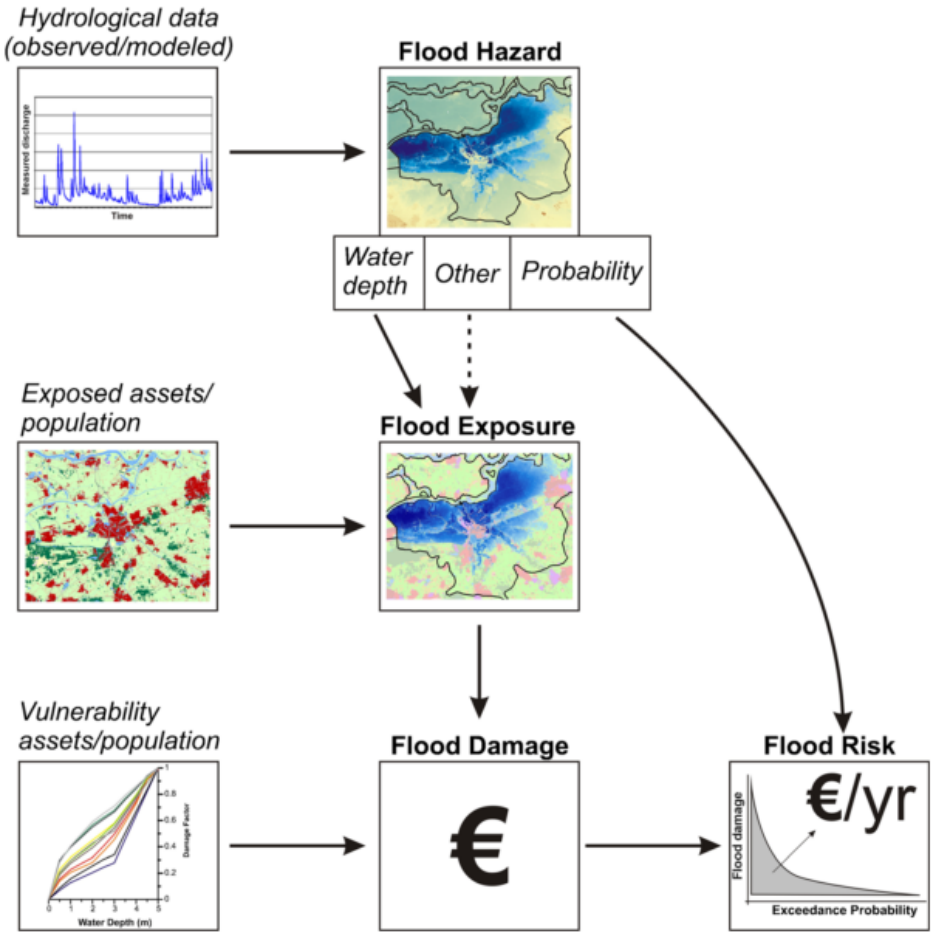

Figure 1.3: Conceptual overview of general flood risk assessment (Merz and Thieken, 2004).

Therefore, in a first step, meteorological, hydrological and hydraulic investigations to define the hazard and the estimation of flood impact to define vulnerability can be

undertaken separately, but are then combined for the final risk analysis (Apel et al., 2009; Di Baldassarre et al., 2013; Merz and Thieken, 2004).

Following this "holistic" trend, even more food risk modelling tools are becoming available, ranging from simpler approaches to sophisticated methodologies including hydrological and hydraulic models (Winsemius et al., 2013). Falter et al. (2013), for instance, developed an innovative complete chain model, which starts from a multisite, multivariate weather generator and through a hydrological model, a coupled one/two-dimensional hydrodynamic model and a flood loss model performs a comprehensive flood risk analysis.

Although the literature reports a noteworthy variability in the damage models field, regarding which and how many parameters are considered in the losses estimation (see e.g. Gerl et al., 2016; Jongman et al., 2012; Merz et al., 2010b, and Sec. 2.3 and Ch. 5 for datails), differences in flood risk methodologies are primarily a consequence of the recent development of several approaches to assess the flood hazard component. During the last decades, in fact, progresses made in the information technologies led to an enormous improvement of the hydrodynamic models available, for which now the modellers choice can vary from the easiest one-dimensional (1D) models to more complex two-dimensional (2D) and three-dimensional (3D) models (a more comprehensive models description is provided in Sec. 1.3). Moreover, starting from the late 1990s, advances in remote sensing techniques for mapping large prone areas, principally using airborne laser altimetry (LiDAR), provided easy and useful tools to calibrate and validate hydrodynamic models, which use became routine (Bates, 2012; Schumann et al., 2009). Beside 1D, 2D and 3D packages to assess flood hazard, or alternatively to them, remotely sensed data (e.g. synthetic aperture radar - SAR) are particularly useful and accurate to produce flood maps, thanks to relative insensitivity to the meteorological conditions during acquisitions (before, during and after the event), the use of microwaves as sensing radiation, and the possibility of acquiring imagery independently of solar illumination (Refice et al., 2015, 2013).

This kind of data are sometimes integrated by geomorphic and other ground information, in order to reduce uncertainties in flood mapping, mainly in flood events characterized by complex land cover ground conditions and time evolution (D'Addabbo et al., 2016a,b).

It is particularly important to cite recent studies (see e.g. Bates, 2012;

Domeneghetti, 2014; Schumann et al., 2009), which demonstrate that remote sensing data are feasible and potentially convenient for various hydrological-hydraulic applications especially in ungauged or poorly gauged areas. Aiming at developing simplified procedures for the delineation of flood-prone areas in scarcely monitored basins, other methods use linear binary classifiers based on several geomorphic descriptors extracted from DEMs (Manfreda et al., 2011, 2015, 2014, 2008; Samela et al., 2015). Although simple, fast and pretty accurate, outcomes of these models are often only qualitative (i.e. flood/no flood) and they are hardly usable where a high detail level is required (Dottori et al., 2016b).

Quite widespread and accurate (Falter et al., 2013) are also raster-based models, like Lisflood-FP (Bates and De Roo, 2000; Bates et al., 2004), in which channel flow is solved separately from the floodplain using either a kinematic or diffusive wave approximation. They use a grid covering the area of interest and each grid cell value corresponds to the characteristics of the geographic feature at that cell location.

If most of the literature assessment focuses on flood risk at micro- and meso-scale, few authors provide hazard models that can be applied globally. For instance, to cite two of them, it is the case of the analysis performed by Sampson et al. (2015), who does not aim to describe any single real event, but attempt instead to describe the areas affected by all events of a certain magnitude, and a study by Ceola et al. (2014), in which satellite night lights data proved that nocturnal lights close to rivers are consistently related to flood damages.

As disclosed before, "modern" flood risk assessments include concepts of climate change, population dynamics evolution and economic development, which are demonstrated to be important influencing factors, even more when considering future flood risk. Hence, recent studies developed new approaches, taking into account the mutual interactions and continuous feedbacks between floods and society (Di Baldassarre et al., 2013, 2015; McMillan et al., 2016; Montanari et al., 2013; Sivapalan et al., 2012).

1.3 Hydrodynamic models for flood hazard evaluation

Correct mapping of hazard and flood risk, as discussed in Sec. 1.1.1, needs tools that are able to reproduce hydraulic river operation and flood dynamics as realistic as

possible.

The higher diffusion of Geographic Information System (GIS) with a horizontal resolution up to 1 m, together with modern satellite observation techniques and the informatics progresses enhanced in the last decades, led to the improvement and easier availability of detailed topographical information (Bates and De Roo, 2000). Those information, being simply transferable to hydraulic applications, allowed a more detailed reproduction of the river geometry and water flow, permitting the rapid development of hydrodynamic models with increasing complexity, shifting from 1D to 2D and 3D modelling.

Thanks to the limited computational time and costs (Mukolwe et al., 2014), 1D models are still widely used (Di Baldassarre et al., 2009c; Pappenberger et al., 2006; Quiroga et al., 2013). They calculate discharge, water depth, flow velocity and other hydraulic variables at every computational node solving the Saint Venant (SV) system, which includes the one-dimensional continuity and momentum equations. Mike 11, Isis and Hec-Ras 1D, among others, are examples of 1D hydrodynamic models. They solve 1D system described above for river and wave propagation in the floodplains. The domain is considered as a series of cross-sections perpendicular to the flow direction, where areas between cross-sections are not explicitly represented. Inundation maps are generated by interpolating water surfaces between the computational nodes.

Some models have the possibility to connect delimited floodable areas (storage areas) to the one-dimensional river reaches, in order to simulate a quasi-2D behaviour of the model: it is the case, for example, of the software Mike11/Mike21 and Hec-Ras 1D/2D, in which overflowing water volume from the lateral embankments (represented by lateral structures that can be withstand a breach) is collected in the storage areas following an elevation-volume curve, on the bases of the topographic configuration of the area (see e.g. Castellarin et al., 2011b; Di Baldassarre et al., 2009b; Mani et al., 2014; Neal et al., 2012; Papaioannou et al., 2016; Vorogushyn, 2008; Vorogushyn et al., 2012; Yin et al., 2013b).

1D models, and even more so quasi-2D models, can represent a good compromise between complexity and satisfying results in some flood risk assessments. However, they are sometimes too simplistic in their treatment of floodplain flows, especially in areas with complex topographies (Apel et al., 2009). It is worth noting that important studies showed how the improvements in the topographic description of last decade are able to reduce the difference between 1D and more complex models,

highlighting at the same time their critical aspects and limitations in the hydraulic simulation and in the spatial representation of the outcomes (Costabile et al., 2015; Mukolwe et al., 2014). On the other hand, 3D models are still very detailed and complicated and the improvement in the additional information provided seems not to be compensate by the impact of their large computational time (Tsakiris, 2014). A satisfying compromise, therefore, is represented by 2D models (e.g. Telemac-2D, Mike 21,InfoWorks-2D, RiverFLO-2D, Isis-2D and Hec-Ras 2D), which avoid a large amount of attractive but dangerous simplifications adopted by 1D models and became more convenient than before thanks the higher actual availability of LIDAR data providing an almost continuous survey of the river reach (Di Baldassarre et al., 2010). 2D models are also commonly adopted for urban flooding modelling basin-scale flood assessment (Aronica et al., 2012; Costabile et al., 2015; Schubert et al., 2008; Tsakiris, 2014, and references therein).

Morphological characteristics of the study area are included in the 2D-models with a detail level that varies as a function of the topographic representation scheme adopted in the models, which defines the model calculation mesh. The most common topographic representations are:

- classic mesh pattern with square grid and a constant size on the computational domain, computed through a finite-different scheme;
- classic mesh pattern with square grid and variable size on homogeneous areas, computed through a finite-different scheme as well;
- unstructured triangular or quadrangular mixed mesh computed through finite-volume methods.

Floodplain topography allows computation of 2D flood extent with flow characteristics in every cell of the grid, e.g water depth and water velocity. Both finite-element and finite-volume methods solve the full-dimensional shallow water (SV) equations, obtained by averaging the three-dimensional Navier-Stokes equations for turbulent flow over the water depth. The finite-element method consists of the division of the domain into several subdomains, each represented by a set of element equations derived from the original problem that is then recombined into a global system of equations for the final calculation. Initial values of the original problem are necessary to reach a numerical solution. Finite-volume method, instead, calculates values in discrete parts of a meshed geometry, referring to the small volume around each node point of the

mesh. Using the divergence theorem, the method converts volume integrals in a partial differential equation containing a divergence term into surface integrals. These terms are then evaluated as fluxes at the surfaces of each finite volume. The flux entering a given volume is identical to that leaving the adjacent volume (conservative approach). Moreover, finite-volume methods are easily formulated to allow unstructured meshes. The finite-volume method is better suited for the inundations of large zones with initially dry areas and for simulations where hydraulic jumps and bores in the flow scenario need to be modelled, while the finite-element approach is efficient and more suitable for modelling large coastal areas and tidal estuaries.

To sum up, providing topographic data, boundary and initial conditions as input information, hydrodynamic models reproduce the inundation processes through different mathematical and numerical schemes, simulating various flood intensity indicators such as water depth, flow velocity and dynamics of the flooding front, depending on the complexity of the model. For example, 2D models map nearly automatically the flooded areas, while 1D models require a post-processing tool for that, usually combining simulation results with the DEM data (Costabile et al., 2015). The output of these simulations are then used to assess the expected amount of economic damages in the area of interest.

According to Mukolwe et al. (2014), the choice of one hydrodynamic model with respect to another is based on a compromise among the different factors of physical realism, computational efficiency, consistency with the quantity and quality of input and observation data, and objectives of the specific study.

Among all the available software and computer tools able to perform hydrodynamic simulations, the next paragraphs intend to give a brief overview of the two computational models for flood hazard assessment, used in the case studies of Chaps. 3, 4 and 5.

Hec-Ras

The software package Hec-Ras (River Analysis System, developed by the Hydrological Engineering Center of the United States Army Corps of Engineering - USACE), numerically solves the SV equations through an algorithm that uses a classical implicit four-point finite difference scheme (see e.g. Castellarin et al., 2009, and references therein).

Traditionally performing only 1D and quasi-2D simulations (used in the simplified flood risk assessment approach in Ch. 4), a new version of the model (i.e. Hec-Ras 5.0) has been recently released, which enables users to perform combined 1D and fully-2D unsteady flow simulations, that is by connecting 1D reaches and storage areas with 2D flow areas modelled through the 2D shallow water SV equations which are then numerically integrated by means of the finite-volume method. With the new release, it is also possible to run simulations by considering only one or more 2D flow areas and no 1D elements, which is what we performed in Ch. 4 to make a direct comparison with simulations performed by another fully-2D model, Telemac-2D.

Telemac-2D

Developed by the Laboratoire National d'Hydraulique et Environnement (LNHE), a research department of the French Electricity Board (EDF-DRD) and distribuited by SOGREAH, Telemac-2D is a fully-2D hydrodynamic model which solves the 2D shallow water SV equations using the finite-element method within a computational mesh of triangular elements (see Galland et al., 1991, for details). This computational model follows the recommendations of the International Association of Hydraulics Research (IAHR) for his validation and has been widely successfully applied to study cases (Brière et al., 2007; Hervouet and Bates, 2000).

In particular, Telemac-2D is used in our simulations to assess the inundation dynamics in the flooded areas of interest by using as boundary conditions either flow hydrographs retrieved by previous studies of the river reach (see Chaps. 3 and 5) or the overflowing flow-rates simulated with the quasi-2D model (see Ch. 4, where the Telemac-2D flood configuration is used as reference scenario to validate a flood risk approach based on the quasi-2D Hec-Ras model).

Chapter 2

Flood risk assessment and modelling: open problems, topical issues and future research avenues

The last couple of decades were characterised by an outstanding boost in development and enhancement of flood risk assessment and management approaches and procedures: flood risk deserved higher attention from people, authorities and stakeholders due to the increasing flood damages registered in Europe and worldwide (e.g. according to EM-DAT and IPCC reports) and the entry into force of the FD 2007/60/EC (European Commission, 2007); efforts have been done in order to find strategies and measures for managing risk instead of simply preventing events from occurring; much more (and more sophisticated) computing tools are available for different types of risk analyses, etc. In the vast and difficult field of flood risk management, however, there are still unresolved issues regarding all risk components (hazard, exposure, susceptibility, see Sec. 1.1) and an urgent need for addressing and discussing the interactions between society and floods (see e.g De Moel et al., 2015; Dottori et al., 2016b; Merz et al., 2014).

The next sections describe some key issues, which in our opinion are still open and deserve to be analysed because they are still unaddressed in the literature.

2.1 Flood risk drivers

Correctly interpreting the dynamics of flood risk components and identifying their major drivers are issues of paramount importance for a correct flood risk management (see also Ciullo et al., 2017).

The common perception of the increasing frequency of floods and inundation phenomena during the last decades (see e.g. Hall et al., 2015) is often supported by a growing concern on climate change (see European Environment Agency, 2005; Wilby et al., 2008). In fact, some studies in the literature seem to indicate that flood damages are expected to increase in the near future as a consequence of a global climate change (see e.g. De Moel and Aerts, 2011; Hall et al., 2005), especially in Western Europe (Feyen et al., 2012). A different point of view is given by other authors, who showed that flood risk changes mainly result from land-use and land-cover modifications increasing exposure to flooding, rather than climate variability and change (see e.g. Bouwer et al., 2010; Di Baldassarre et al., 2013).

However, climate change has increased worldwide the interest in understanding the interaction between human activities and the hydrological cycle. Flood damages are the result of a complex system of factors that influence the overall dynamics and impacts of flood events (see e.g. Elmer et al., 2012; Merz et al., 2010a), and the scientific literature seems to show a consensus on the most influential drivers of flood risk dynamics, identifying them in climate variability and human pressure (Merz et al., 2014; Winsemius et al., 2015). Numerous studies analysed long time series of hydrological variables (such as rainfall, river discharges, and temperature) to investigate the presence of significant trends in different contexts and at different scales (Hamed, 2008; Petrow and Merz, 2009; Villarini et al., 2011; Vorogushyn and Merz, 2013). In the Italian context, Domeneghetti et al. (2015) focused on long historical flood sequences observed for the Po River, demographic and land-use changes occurred in the last five decades and highlighted that major fluctuations in flood risk are associated with anthropization and urban sprawl within Po River floodplains (see Sec. 4.4 for details), confirming previous analyses on the same study area (see e.g. Montanari et al., 2013; Zanchettini et al., 2008).

Seventy years ago White (1945) affirmed that humans are responsible for, if not flood event itself, its consequences on the environment and settlements. It is right on the role that anthropogenic impact has (and had) on flood hazard and flood exposure that a consistent part of the research described in this Thesis focused on.

2.1.1 Flood hazard drivers

Focusing on the role and impact of anthropization occurred during the last century, the recent literature is addressing the understanding and representation of

complex interactions between society and flood hydrology. Several studies clearly show that these connections are particularly intense in floodplains around the world where residential, industrial and agricultural areas, infrastructures, flood control measures and river engineering have gradually co-evolved during centuries (see e.g. Castellarin et al., 2011a; Ciullo et al., 2017).

Among all human activities that can impact flood hazard dynamics in numerous floodplains and flood-prone areas of the globe, a still scarcely addressed aspect is the possible impact of the human-induced land-subsidence in densely populated areas, i.e. the accelerated ground-lowering due to the pumping of underground fluids.

Although Potok (1991) pointed out evidences of land-surface subsidence due to the withdrawal of oil and gas in the Baytown, Texas, already in 1918, this well known phenomenon was observed in different parts of the world, mainly during the second half of the 20^{th} century: Mexico (see e.g. Ortega-Guerrero et al., 1999), Japan (see e.g. Daito and Galloway, 2015; Gotoh et al., 2009), Thailand (see e.g. Phien-wej et al., 2006), Bangladesh (see e.g. Brown and Nicholls, 2015; Howladar and Hasan, 2014) and Philippines (see e.g. Rodolfo and Siringan, 2006) are some examples of severe human-induced ground-lowering which caused great problems to building foundations and to sewer and transportation systems, as well as the accumulation of storm water during the rainy season, resulting in extensive flooding of farmland.

The water problems induced by land-subsidence in coastal areas have been deeply investigated, see e.g. the studies regarding salt-water intrusion (see e.g. Giambastiani et al., 2007; Schmidt, 2015) or the decrease of the return period of coastal flooding (see e.g. Baldi et al., 2009; Potok, 1991; Yin et al., 2013a). The literature on possible alterations induced by anthropogenic land-subsidence on riverine flood risk in flood-prone areas, instead, is still sparse; yet the problem is worth investigating as, during the last decades, there has been a remarkable growth of urbanization in dyke-protected floodplains of major Italian (and European) rivers. In fact, the presence of levee systems encourages the development of residential areas and industrial/agricultural activities in areas that are close to waterbodies. In addition, it is worth noting that many existing embankment systems were built centuries ago; they prevented the riverbed to gradually adapt to changes of topography induced by natural (and anthropogenic) land-subsidence, and this may have resulted in significant modifications of the spatial distribution of flood hazard in case of embankment failure.

Our study, described in Ch. 3, focused on the most representative anthropogenic land-subsidence case in Italy, occurred near the city of Ravenna, and aims at better understanding whether and to what extent human-induced, or human-accelerated, ground-lowering can alter flood hazard associated with riverine inundations.

2.1.2 Drivers of flood exposure

According to the CRED/OFDA database (see D. Guha-Sapir, R. Below, Ph. Hoyois - EM-DAT: The CRED/OFDA International Disaster Database - www.emdat.be - Université Catholique de Louvain - Brussels - Belgium), during the three decades 1986-1995, 1996-2005 and 2006-2015 flooding affected a stable number of people worldwide (0.8-1.0 billion people), whereas the total damage increased dramatically (i.e. ∼100% per each decade).

Many studies highlighted that the economic and social development in flood-prone areas are key elements for the correct interpretation of the increase of flood losses observed during last decades (see e.g. Bhatta et al., 2010; Ceola et al., 2014; De Moel and Aerts, 2011; Di Baldassarre et al., 2013; Jongman et al., 2012; Ludy and Kondolf, 2012; Merz et al., 2014, and references therein). For instance, considering the flood-related costs recorded in Europe over the time period 1970-2006, Barredo (2009) showed that there is no evidence of a positive trend on normalized damages; that is, a large portion of the growth of nominal losses associated with floods can be explained by the evolution of exposure to floods and wealth in floodplains. Similar results have been found looking at the damages and costs associated with hurricanes in United States between 1900 and 2005 (see Pielke Jr. et al., 2008; Pielke Jr. and Landsea, 1998) and to globally observed disasters associated with water (see Barredo, 2009; Neumayer and Barthel, 2011). All these studies pointed out that there are no clear evidences of an increasing trend in the normalized economic damages, even though the difficulties in considering the overall mitigation measures enforced by authorities or individuals prevent one to infer that historical data do not show a clear positive trend in the frequency and/or intensity of weather-related natural disasters (Neumayer and Barthel, 2011).

These considerations are supported by investigations performed on flood risk projections over the future decades in different areas and contexts of the world (see e.g. Bouwer et al., 2010; De Moel et al., 2011; Elmer et al., 2012). These studies highlighted how land-use changes and economic development of hazard-prone areas

(i.e. flood risk exposure) may have an effect on the increase of flood losses that is comparable to, if not higher than, what is commonly associated with the expected climate change. For instance, according to Bouwer et al. (2010), population growth and the increase of exposed wealth in flood-prone areas may significantly increase potential damages during flood events. They may end up being the main factors controlling the increase in recorded damages, especially in areas where the *levee effect* is registered: the increase of the overall vulnerability of the areas (Di Baldassarre et al., 2015) may potentially result in higher damage in case of extreme flood events that cannot be restrained by the existing levee system, or in case of levee-system failures (i.e. what is usually identified as *residual flood risk*; see e.g. Castellarin et al., 2011a; Di Baldassarre et al., 2009b). Investigating a specific case study in California, Ludy and Kondolf (2012) clearly point out that the presence of a levee system changes the perception of the flood likelihood in people living in the dyke-protected areas, which are perceived as completely safe from inundations. This feeling ends up increasing the exposure and consequently the vulnerability of floodplains, even in areas that were already affected by inundations, where the demographic and economic growth experienced after the inundation, due to the enhancement of the levee system, led to a well-being condition that is higher than before the inundation (see Schultz and Elliott, 2013, and Fig. 2.1).

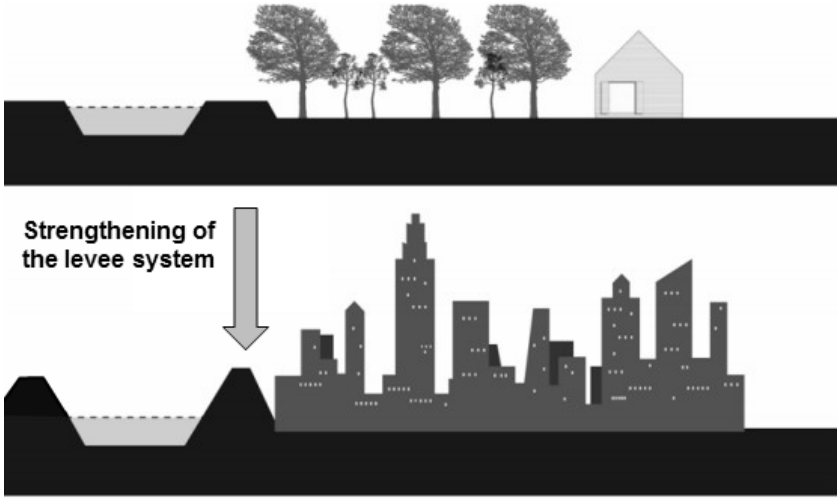

Figure 2.1: *Levee effect* phenomenon: increasing of the human settlements' inundation exposure in floodplain areas, where the levee system was strengthened (Di Baldassarre et al., 2013).

All these considerations underline the necessity to analyse flood risk and its evolution in time by means of holistic approaches, which take into account the exposure dynamics characterizing a large geographical areas and are poorly investigated up to now.

A better understanding of the interplay between social and hydrological factors represents a fundamental piece of information for the identification of robust large scale flood risk mitigation strategies and the definition of viable development plans for flood-prone areas (Di Baldassarre et al., 2013). However, although the *levee effect* phenomenon (Tobin, 1995), also named *call-effect*, is frequently mentioned, the literature on its objective quantification is still very sparse and many studies refer to estimates evaluated on each case study (see e.g. Di Baldassarre et al., 2015; Merz et al., 2009).

Chapter 4 aims at shedding some light on the role of anthropization in the Po river basin in the last half century, in terms of flood exposure evolution and its consequences on flood risk dynamics. In addition, some considerations about the *levee effect* in the study area are provided.

2.2 Flood risk evaluation

2.2.1 Spatial scales issues in flood risk assessment

Depending on the goals of the single studies, different spatial scales can be considered to perform flood damage assessments. Although the distinction between scales always conserves a margin of subjectivity, various authors agree to adopt this following general classification (De Moel et al., 2015; Merz et al., 2010b):

- *Micro-scale*, i.e. flood risk assessment is calculated on each single element at risk (building, infrastructure object, etc.) with a high level of detail with the aim of supporting the development of local flood management concepts and urban planning; it considers towns or specific river reaches in which detailed information about terrain elevation, hydraulic structures (e.g. dikes, weirs), building location/type/use, etc. are available (see e.g studies by Aronica et al., 2012; Costabile et al., 2015; Escuder-Bueno et al., 2012; Hammond et al., 2013; Schubert et al., 2008);
- *Meso-scale*: flood risk focused on regional flood risk management strategies, on re-insurance plans industry and on the impacts of climate change, socio-

economic growth, or both, is assessed by means of spatial aggregations of exposed assets, e.g. considering either land use units (residential areas), or administrative units (zip code areas) (federal states, provinces, or large cities; see Bubeck et al., 2011; Falter et al., 2015; Kreibich et al., 2016b,c; Vorogushyn et al., 2012)

- *Macro-scale*, or *large-scale*: municipalities, catchments, regions or countries, if with a consistent data availability, are considered in order to assess flood risk with a large range of aims (see e.g. Castellarin et al., 2011b; Falter et al., 2013; Neal et al., 2012);
- *Supra-national scale*: it allows continental or global flood risk assessment mainly related to the influence of climate change (see e.g. Jonkman, 2005; Sampson et al., 2015; Winsemius et al., 2015, 2013).

The general assessment structure for evaluating the three components of flood risk is common to all spatial scales (see Sec. 1.2, although diversities exist due to many factors, e.g. different data availability and the applicability of methods at different scales, with their limitation and potentiality (De Moel et al., 2015).

In case of models up- or down-scaling, although the increasing and improvements of computation tools make this process more automatic, it is very important to choose an appropriate procedure (De Moel et al., 2015; Merz et al., 2010b). The validation of flood risk assessments is another important issue which should be addressed in future studies, because it is often limited at all scales mostly due to the lack of detailed post-disaster information which could instead improve performance of flood risk models (De Moel et al., 2015).

Representing the large scale assessment a good compromise to explain and study the interaction of local and catchment-specific characteristics, such as meteorology, topography and geology (Green et al., 2011; Merz et al., 2014), this approach is becoming even more important and used in the literature, also thanks to the easy accessibility of most local information at the scale of regions, countries or river basins (Alfieri et al., 2015; Bubeck and Kreibich, 2011; Falter et al., 2015; Hall et al., 2005).

2.2.2 Simplified tools for flood risk evaluation over large spatial scales

Large scale hazard assessment can be performed by ranging from very basic approaches (simple intersection of flat horizontal water surface and Digital Elevation

Model of sufficient resolution) with numerous simplifying assumptions up to very sophisticated, data and calculation time demanding methodologies (e.g. 3D solutions of the Navier-Stokes equations with sophisticated turbulence closure), as far as what both hazard and vulnerability are concerned (Apel et al., 2009; Bates and De Roo, 2000). Literature procedures differ mainly due to the choice of the methodology aiming to perform hazard evaluations, for which several possibilities are available, each one with its advantages and limitations (see Sec. 1.2).

In current practice, however, large scale hazard assessment tends to avoid detailed hydrodynamic simulations mostly due to their high computation costs (De Moel et al., 2015; van Dyck and Willems, 2013, and references therein). If we consider, in addition, the large number of detailed data needed, among which topographic information, asset distribution, population density and potential damage functions, some simplification in large scale approaches are inevitably to be done, in order to reach a good compromise between results accuracy and contained implementation time (Alfieri et al., 2015).

Various authors in recent studies pointed out both strong points and limitations of simplified approaches used for large scale flood risk simulations. For instance, Manfreda et al. (2008), Samela et al. (2015) and following studies showed how the adoption of geomorphologic indexes computed from DEMs (and eventually considering the local slope and the distance from the closest river), without the need of any hydrological and hydrodynamic model, allow the rapid delineation of flood prone areas in scarcely monitored basins and in areas where it is impossible to perform expensive and time consuming simulations. Remaining in the poorly gauged basins field, Massari et al. (2015), instead, developed a simple kinematic-storage model (KSM) as a tool for a Decision Support System for the evaluation of probability inundation maps in near real time, which takes advantages on the very low computational times and its low sensitivity to the quality of the geometry representation of the channel and the floodplain. Starting from raster based models, some progresses was achieved by Falter et al. (2013), who applied an innovative grid coarsening procedure to cope with computational constraints aiming at the correct simulation of flood hazard dynamics, although the model accuracy seems to gradually deteriorate with the increasing size of the grids.

As highlighted in the previous considerations, a large number of reliable tools for predicting flood hazard over large geographical areas is available in the literature, while simplified approaches for assessing exposure to floods are still missing. Chapter 4

aims at filling this gap, developing and testing the reliability of simplified graphical tools, the HVCs, proposed for assessing flood vulnerability and risk evolution over large geographical areas based on land-use and topographic information. Considering the middle-lower 350 km stretch of the River Po (Northern Italy), flooded areas are identified by means of quasi-2D hydrodynamic model that reproduce the hydraulic behaviour of the floodable area outside the main embankment system of the study river reach in case of a catastrophic event.

A similar subsequent study by Dottori et al. (2016b) highlighted the benefits of the proposed methodology in providing simple and useful preliminary information about flood risk in different areas, which could be then analysed in depth by means of more sophisticated meso- and micro-scale approaches.

2.3 Damage models and uncertainties

Uncertainty exists in all flood risk components because of generalisations, assumptions and aggregation of information. Each source of error is accumulated and combined in the final damage estimate: hydrological models can bring uncertainties ascribable to numerical models, which lead to generalisations in parametrisations and input data; a simplistic schematization is also adopted to assess the elements at risk, as well, which are often represented by low-resolution land-use maps with a more or less limited number of land-use classes. These generalizations introduce large sources of uncertainty in the identification of the value of the elements at risk, in addition to errors due to spatial and temporal differences (i.e. market fluctuations; see De Moel and Aerts, 2011).

The literature from the last decade shows an increasing number of innovative studies about models able to estimate flood losses starting from one or more predictive variables. Nevertheless, several authors highlighted that damage models still provide the most important sources of uncertainty in flood damage estimates, leading to errors that are substantially larger than to the ones observed in the other components evaluation (Apel et al., 2009; De Moel et al., 2012, 2014; Gerl et al., 2016; Jongman et al., 2012; Merz et al., 2004, 2007). In particular, De Moel and Aerts (2011) tested the sensitivity of flood damage estimations to the flood hazard component (represented by water depth). Outcomes showed that, assuming the uncertainty in inundation depth is about 15% of the mean inundation depth, the total uncertainty surrounding the final damage estimate in the case study area

resulted to be equal to a factor 5÷6. The economic value of elements at risk and depth-damage curves are the most important sources of uncertainty, introducing about a factor 2 of uncertainty in the final losses estimation (Maatar, 2015).

The problem of uncertainties in vulnerability assessments seems to be a particularly important issue, assuming that the estimation of economic flood losses is gaining crucial importance in the flood risk management in recent years, becoming the dominant approach of flood control plans throughout Europe (Dottori et al., 2016a; Merz et al., 2010b; Messner et al., 2007; Schröter et al., 2014), instead of design standards and structural flood defence measures.

One of the larger source of uncertainty is certainly due to damage functions (Jongman et al., 2012). In most of the applications in the literature, in fact, the vulnerability of specific building type or land-use class is commonly related to only one variable, i.e. water depth in most of the cases (see e.g. Apel et al., 2009; Kreibich et al., 2009; Merz et al., 2013; Penning-Rowsell et al., 2005; Smith, 1994), providing a generalisation of the real situation and often excluding other factors, such as flood duration and flow velocity, which can have an important influence on damage processes (De Moel and Aerts, 2011; Merz et al., 2013). Recently, some authors (Kreibich et al., 2016a, 2010; Merz et al., 2013; Thieken et al., 2008) developed multi-parameter damage models including more than one predictive variable, such as other hydraulic parameters (e.g. streamflow velocity, duration of the inundation, etc.), resistance performance, precautionary measures and people experiences with floods (Meyer et al., 2013). These models were shown to perform better losses estimation with sufficiently large data set, compared to simple uni-variate models (Merz et al., 2013; Schröter et al., 2016). In order to improve these type of models, Bubeck and Kreibich (2011), (Cammerer et al., 2013), Messner et al. (2007) and Meyer et al. (2013), among others, highlighted the necessity of a better understanding of the damage processes.

The second largest contribution to the overall uncertainty can be associated with the lack of sufficient, comparable and reliable high quality losses data (Amadio et al., 2016; Green et al., 2011; Meyer et al., 2013; Molinari et al., 2014a; Scorzini and Frank, 2015): damage curves and model are in fact derived synthetically by experts (see e.g. Penning-Rowsell et al., 2005) or developed by empirical data of historical flood events (Kreibich et al., 2010; Merz et al., 2013, 2004; Thieken et al., 2008). The larger and more comprehensive the starting database, the more realistic the resulting model

(Messner et al., 2007).

In addition, post-damage collected data are essential to validate existing models (Cammerer et al., 2013; Meyer et al., 2013), to adjust them for the specific conditions of the assessment area, improving the consistency of the model itself (Amadio et al., 2016; Büchele et al., 2006; Gerl et al., 2016) and to provide information about their transferability in different analyses (Cammerer et al., 2013; Green et al., 2011; Molinari et al., 2014a). A lot of damage models developed up to now are in fact internationally accepted as standard methodologies of estimating flood damages (Merz et al., 2010b, 2007; Smith, 1994), without being neither tested nor calibrated for the specific study area (Amadio et al., 2016), thus leading to the incorporation of large errors by using them for different elements at risk, geographical areas and flood events from the ones for which they are derived (Merz et al., 2010b, 2004; Schröter et al., 2016). According to Gerl et al. (2016), validation analyses were performed only for about 45% of the existing literature models by means of comparisons with observed data, while for the remaining models either the evaluation status is unknown or the validation process is not explicitly described.

A minor, yet still important, source of error in flood losses estimation is the absence of standardized approaches and methodologies, that let preventing strategies and mitigation measures being compared, from regional to national scale (Gerl et al., 2016). For instance, a lot of models use replacement assets values instead of depreciated ones, thus overestimating the estimated damages (Jongman et al., 2012; Merz et al., 2010b; Messner et al., 2007); also, difficulties in models comparisons is due to the construction procedure of damage models, i.e. if original data are empirically obtained or defined on expert judgement in combination with artificial inundation scenarios (Jongman et al., 2012).

Dottori et al. (2016a) and Scorzini and Frank (2015) highlighted that a further limit to model applicability and transferability, as well as possible improvements, is the lack of transparency which characterises a significant amount of damage models, especially in some context.

Authors seem to agree that development and validation of loss models are currently the most urgent need to improve flood risk estimation accuracy (Elmer et al., 2010), in addition identifying and reducing the main sources of uncertainty previously discussed (Messner et al., 2007; Meyer et al., 2013; Molinari et al., 2014a). Assuming the difficulty to considerably reduce some of these errors in the near future

(De Moel et al., 2012), it is important to correctly account for them in flood damage assessments and transparently communicate residual uncertainties to decision makers (De Moel et al., 2012; Kreibich et al., 2016c; Meyer et al., 2013).

The aim of the analysis performed in Ch. 5 is therefore to make some progresses in the assessment of the estimation of flood damages. We focus in particular on the Italian context, where the the lack of standardised procedure and guidelines for collecting and analysing consistent and comparable data; this well known problem represents the primary issue to be addressed (see e.g. Amadio et al., 2016; Molinari et al., 2012, 2014b; Scorzini and Frank, 2015). Our study assessed the applicability and transferability of literature and empirically uni- and multi-variate damage models on losses estimation in an Italian context, taking advantages by a quite large damage data set collected after the flood event in January 2014.

2.4 Reasearch questions

Concluding and summarizing all previous considerations, this Thesis aims at shedding some light on the most important flood risk related topics for which we found that the literature is still sparse, mainly focusing on the Italian context. The research questions that sustain and motivated the activities of this dissertation are:

Does anthropogenic land-subsidence provide changes in flood hazard dynamics and, in case it does, how relevant are they?

Among all human-induced hazard drivers that potentially provide changes in flooding hazard dynamics, we focused on the anthropogenic land-subsidence, which is a well-known phenomenon in different parts of the world. Its influence on riverine flood dynamics was tested by comparing the inundation extent and the distribution of flooded areas in pre- and post-subsidence topographic configurations. Furthermore, the relevance of the potential alterations to the flood propagation was addressed by means of a comparison with the role of roads and railways embankments and land reclamation channels.

Can simplified and easy-to-use approaches for assessing flood risk evolution over large scale areas be developed? To what extent changes in exposure influence flood risk dynamics?

Because of the importance of flood risk assessment evolution over large scale floodplains, we recognized the value of disposing and testing a simplified tool to combine topographic and land-use information for the evaluation of flood risk evolution during recent decades. Moreover, focusing on the scarcely investigated flood exposure component in the literature, the simplified tool was thought with the aim to be suitable for evaluating the influence of exposure dynamics on the flood risk.

Are the literature uni- and multi-variate models capable of accurately reproducing flood losses in contexts that differ geographically and socio-economically from those for which the models were originally developed?

We addressed the open problem of transferability of empirically obtained damage models into contexts that differ from the one in which they were developed. Because of the lack of reliable literature damage models in the Italian context, we derived uni- and multi-variate damage models from post-event data collected in case of a real flood in Italy and tested their performance in estimating direct economic damages by means of a comparison with literature damage models.

Chapter 3

Flood hazard changes due to anthropogenic land-subsidence (case study 1: Ravenna, Italy)

3.1 Introduction

Our study aimed at better understanding whether and to what extent human-induced, or human-accelerated, ground-lowering can alter flood hazard associated with riverine inundations. To this aim, we focused on the area near the city of Ravenna (Northern Italy), one of the Italian most prominent cases of anthropogenic land-subsidence. The ground-lowering of the study area, which accelerated after World War II due to intense groundwater and natural gas extraction, reached peaks greater than 1.5 m in nearly 100 years close to the historical city center (Carminati and Martinelli, 2002; Gambolati et al., 1991). In order to quantify the potential influence of land-subsidence on the flood hazard dynamics and compare it with the influence of other anthropogenic drivers, we simulated several inundation scenarios resulting from possible levee failures in the proximity of the city of Ravenna through a fully 2D model. We implemented the 2D model considering current and past (i.e. reconstruction of 1897 ground elevation) topographies, as well as presence or absence of the main linear infrastructures (e.g. road and railway embankments and land-reclamation channels). Our comparison of the different inundation scenarios aimed at investigating whether or not anthropogenic land-subsidence can be regarded as a potential driver of riverine flood hazard change.

In particular, we addressed the following research questions:

1) can anthropogenic land-subsidence alter riverine flood hazard in a given flood-prone area?

2) can such subsidence significantly modify the inundation dynamics (e.g. extent and distribution of flooded areas; distribution of water depth, h, current velocity, v and/or intensity, $h{\cdot}v$, etc.)?

3) are human-induced land-subsidence's effects on flooding dynamics more intense than those resulting from the construction of roads, railways and artificial channels?

3.2 Study area

The study area covers 77 km^2 of the area around the city of Ravenna, in the Emilia-Romagna region Italy, which is about 60 km to South of the Po river delta (Fig. 3.1).

With a municipal area of 653 km^2 and a population of 160 000 inhabitants the city boasts a long and rich cultural history: historians set its foundation in the eighth century B.C., making it one of the oldest Italian towns. During the three centuries after 400 A.D., Ravenna became a capital three times: of the Western Roman Empire, of Theodoric King of the Goths and of the Byzantine Empire in Europe. Furthermore, after the invasion of the Lombards in 751, it was chosen as the seat of their Kingdom. The magnificence of this period left Ravenna with the great heritage of historical buildings: eight UNESCO World Heritage Sites are located in the city (source: Unesco).

The study area is a densely urbanized and commercial district, which is characterized by high population density (240 inhabitants/km^2, source: Wikipedia), as well as a complex network of human infrastructures. Although nowadays Ravenna is an inland city, it is still connected by the Candiano Canal to the Adriatic Sea, which is located a few kilometers East of the city. The Montone river and the confluence of Montone and the Ronco rivers (i.e. Fiumi Uniti river) flow through the city, which is entirely protected against frequent flooding by system of artificial embankments.

Like many other coastal lowlands and deltaic plains, the Eastern Po plain and, in particular, the area where Ravenna is located, lies on a subsiding sedimentary basin

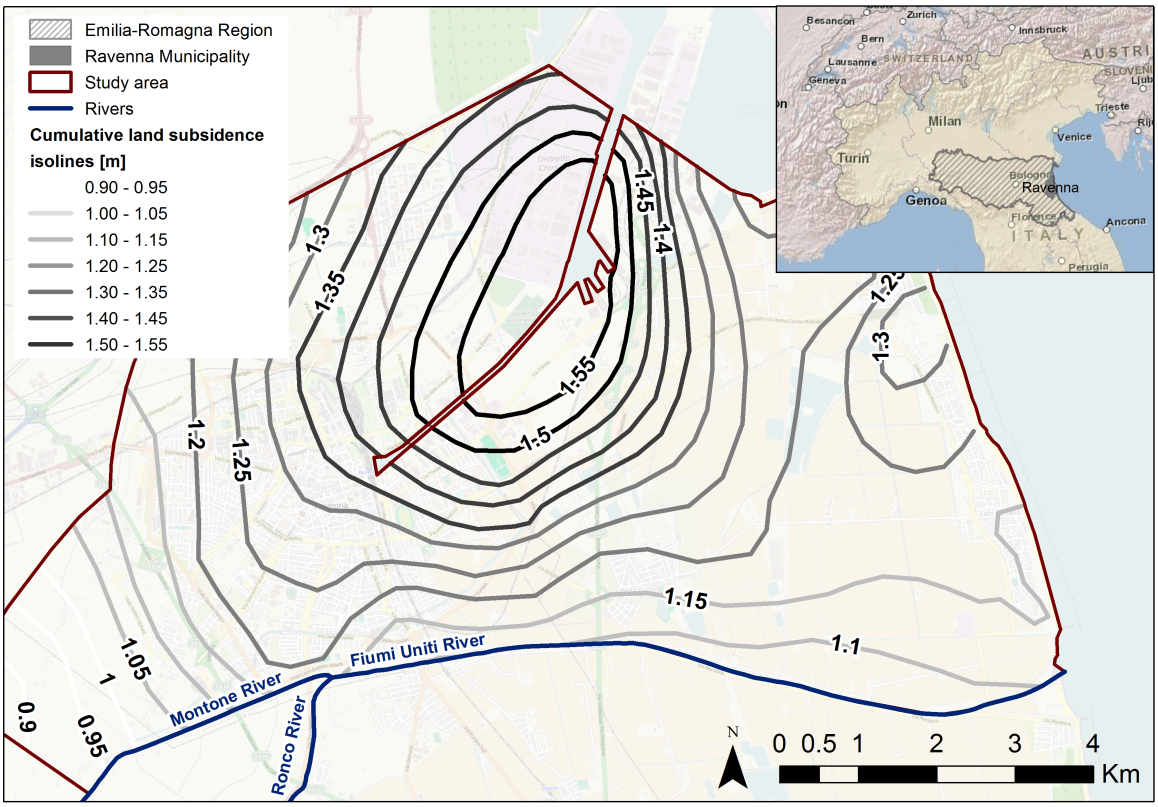

Figure 3.1: Study area and isolines of cumulative land-subsidence drops [m] between 1897 and 2002 (Teatini et al., 2005).

that experienced extremely significant changes over centuries in terms of ground elevation. The local rate of land-subsidence is naturally in the order of a few mm per year, but it increased enormously after World War II, as shown, for example, in the ground elevation analysis by Bitelli et al. (2000). This happened most likely due to an increase in the extraction of deep non-renewable groundwater associated with the economic growth and industrial expansion of the area. Gambolati et al. (1991) show how this and the subsequent exploitation of several on-shore and off-shore deep gas reservoirs in the Ravenna area increased the rate of land-subsidence up to some centimeters per year. The close relationship between groundwater pumping and land-subsidence is confirmed by numerous studies. Carminati and Martinelli (2002) show the link between the lowering of subsidence rate in recent years and the application of a national government law that enforced an important decrease of groundwater withdrawal. Baldi et al. (2009) and Teatini et al. (2005) affirm that

during the late 1970s and 1980s the construction of new public aqueducts exploiting surface water significantly reduced the subsurface water consumption and consequently the settlement rates reverted to the pre-war values, as already occurred in Houston, Texas (Potok, 1991). Teatini et al. (2005) also constructed a detailed georeferenced map of land-subsidence in the Eastern Po river plain over the period 1897-2002, based on the main levelling surveys available in the last century, i.e. Military Geographic Institute - IGM, Ravenna Reclamation Authority, Geological Service of the Ravenna Municipality, Regional Agency for Environmental Protection (ARPA) and National Hydrocarbons Authority - Exploration and Production (ENI-E&P).

Cumulative land-subsidence evaluated by Teatini et al. (2005) is illustrated in Fig. 3.1, which shows drops larger than 1 m over more than one third of the area. Peaks beyond 1.5 m over a 10 km^2 area are located between the historical center and the Adriatic coast. The patterns in Fig. 3.1 are particularly striking also in terms of subsidence gradients, which can be as high as 0.3 m/km, being therefore comparable with riverbed slopes of natural streams flowing in the area (e.g. bed slope of Montone-Ronco rivers system is approximately 0.7 m/km).

3.3 Topography of the study area

3.3.1 Current and past terrain elevation

The study-area current topography is described through a contemporary 5 m horizontal resolution DEM, made available as a GIS Service by the cartographic office of the Emilia-Romagna Region (see Fig. 3.2). The cumulative land drop observed up to 2002 and reported in Teatini et al. (2005) was summed to the current 5 m DEM, therefore obtaining another 5 m DEM that describes the ground elevation in 1897. We neglected changes in ground elevations in the last 15 years, which were minimal. According to Fig. 3.1, the backward-warping process increased the ground elevations the most in the North-Eastern portion of the study area (ca. 155 cm), and the least in the South-Western area, located approximately 4 km from the city of Ravenna (ca. 80 cm).

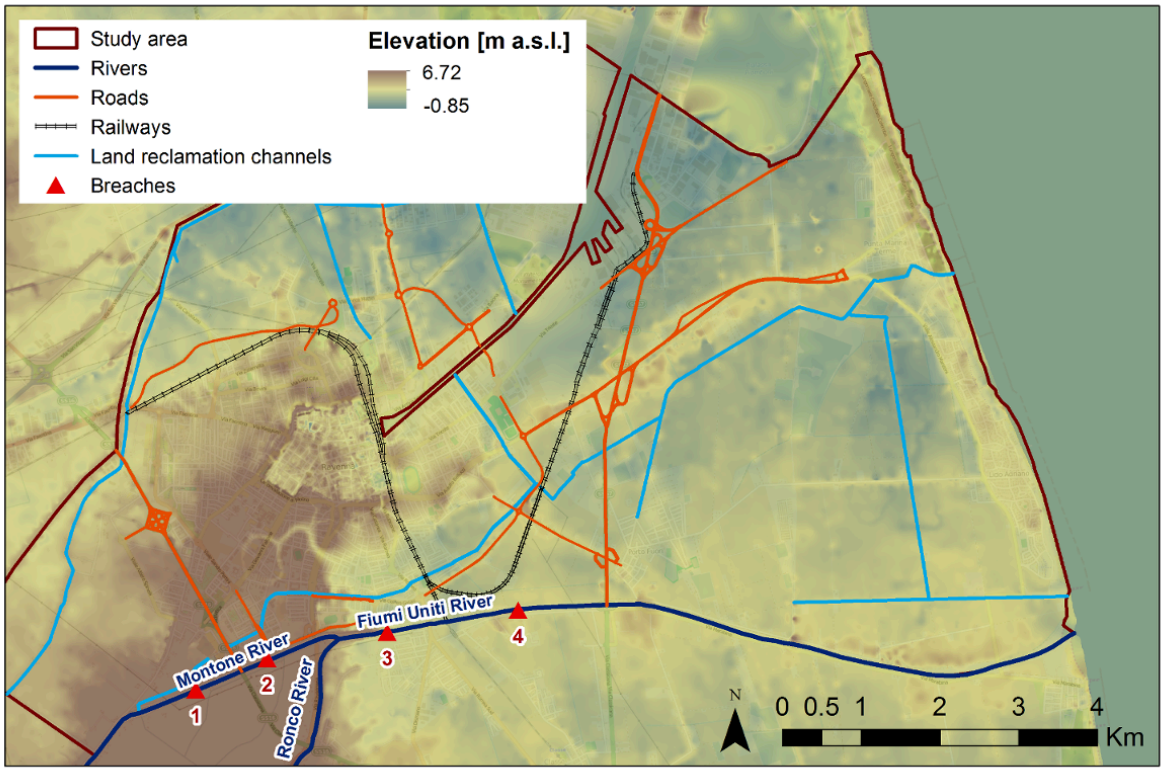

Figure 3.2: Current topography (5 m resolution DEM) of the study area, major infrastructures considered in the study and locations of the hypothesized levee breaches.

3.3.2 Main infrastructures

Even though the main focus of our study regards anthropogenic land-subsidence, human presence and activity on floodplains led to other kinds of topography alterations that are potential drivers of flood hazard and risk dynamics (e.g. construction of main road infrastructures, complex artificial drainage and land-reclamation networks, systems of secondary dikes, etc., see Domeneghetti, 2014; Dottori et al., 2013; Hailemariam et al., 2014). Possible changes in flooding dynamics and flood risk associated with land-subsidence and their significance need to be compared to changes that result from other anthropogenic alterations of the topography. Among these, we considered the main road and rail infrastructures and land-reclamation channels existing in the study area (see Fig. 3.2).

The DEM resolution (i.e. 5 m) cannot grasp the details of these existing discontinuities, apart from some of the larger ones; main railways and

land-reclamation channels could therefore be misrepresented and discontinuous due to the topology of the DEM grid. For this reason, two additional DEMs were created, one from the current DEM and the other from the backward-deformed DEM, in which major topographic discontinuities have been manually incorporated according to field surveys, digital databases and photos (sources: Google Street View; digital cartographic database of the Emilia-Romagna Region). In particular, continuous 1 m tall railway embankments were included in the topography and continuous 1.5 m deep land reclamation channels were carved to match the existing layout of main linear infrastructures (see Fig. 3.2).

3.3.3 Considered terrain configuration

Our study investigated the flooding dynamics in four different terrain configurations, obtained by combing two different topographies (past and present, related to land-subsidence) with the presence or absence of continuous linear infrastructures:

- ***Curr***, current morphology, as represented by the contemporary 5 m DEM;
- ***Curr_Infr***, current morphology with continuous infrastructures;
- ***Past***, 1897 topography obtained by backward-deforming *Curr* on the basis of cumulative land-subsidence illustrated in Teatini et al. (2005);
- ***Past_Infr***, 1897 topography obtained by backward-deforming *Curr_Infr* on the basis of cumulative land-subsidence illustrated in Teatini et al. (2005).

3.4 Implementation of the hydrodynamic numerical models

Hec-Ras was used in our study for simulating the hydraulic behavior of the Montone-Ronco Rivers system and the discharge outflowing hypothetical levee breaches, which in turn was used as an inflow boundary condition for reproducing the inundation dynamics with Telemac-2D, a fully-2D model briefly described in Sec. 1.3.

We implemented the numerical 1D hydraulic model of the middle-lower portion of Montone-Ronco Rivers system (nearly 28 km in total, to the mouth of the Fiumi Uniti River into the Adriatic Sea; see Fig. 3.2). River geometry was modelled on the basis of 85 cross-sections retrieved from the Regional River Basins Authority

(AdB-RR). It was simulated, that the maximum discharge that can flow in the lowest part of the Montone River without overtopping reached almost 550 m^3/s; this result was confirmed by independent analyses carried out by AdB-RR (2011). Therefore, the present study referred to a synthetic hydrograph with a flow peak of 550 m^3/s and a wave shape obtained by re-scaling a historical event observed at Ponte Vico streamgauge (located immediately upstream the considered river stretch). In addition, we adopted as downstream boundary condition a constant water surface elevation at river's outlet into the Adriatic Sea. We deemed these simplifications to be an acceptable working hypothesis; our study aimed at comparing flooding dynamics resulting from realistic flood events over different terrain configurations rather than performing a detailed reconstruction of historical flood events.

We hypothesized four different levee-breaching scenarios along the left Montone-Ronco embankment (Fig. 3.2 reports numbers to identify the breaches' locations). For each of them, we modelled an instantaneous breach formation concurrently with the transit of the flood wave peak, a breach width of 120 m and a full vertical breaching (from the levee crest to ground elevation). The breach width was set according to the sizes of historical breaches observed in similar Italian rivers (e.g. Serchio levee failure in December 2009, Secchia levee failure in January 2014 and others; see Govi and Turitto, 2000; Orlandini et al., 2015, catalogue of historical levee breaches along the Po River).

We focused on the embankment stretch close to the city of Ravenna, following the indications of the River Basin Authorities, that identify that particular stretch (overall length: 6 km) as the most exposed one to overtopping and stability issues (see Reno, Romagna and Marecchia-Conca Rivers Basins Authorities - AdB-Reno, AdB-RR, AdB-Marecchia-Conca, 2016). We modelled four different breaching events (see red triangles numbered from 1 to 4 in Fig. 3.2) for each terrain configuration identified in 3.3.3. There are two main reasons. Firstly, due to the morphology of the system (river and left-levee crest), the probability of levee overtopping is homogeneous along the 6 km stretch between points 1 and 4 (Fig. 3.2); hence it is impossible to identify a most likely breach location a priori. Secondly, we wanted the results of our study to be independent of the breaching location. Therefore, we considered four breaching locations that are approximately uniformly distributed along the critical 6 km stretch and located both upstream and downstream two large embankments. These levees can greatly affect the flooding dynamics in the flood-prone area (see Fig. 3.2): the first is

the embankment of a large state-road, which is accurately captured by the available 5 m DEM; the second is the railroad embankment that was manually represented in the terrain configurations that consider main linear infrastructures (i.e. *current morphology with infrastructures (Curr_Infr)* and *past morphology with infrastructures (Past_Infr)*).

Hec-Ras simulations of the four breaching events showed very limited differences in terms of the peak-flow and overall volume of the simulated outflowing hydrographs. Therefore, for the sake of simplicity and comparison among results, we referred to the mean outflowing hydrograph for all inundation scenarios. The mean simulated outflowing discharge (with an overall flood volume equal to $3{\cdot}10^6$ m^3) was adopted as liquid boundary condition for the Telemac-2D simulations focusing on the inundation dynamics in the 77 km^2 study area.

We constructed a non-structured computational mesh used for all the performed 2D simulations (see Fig. 3.3). The mesh consists of 133 722 triangular elements and 67 284 nodes and provides an accurate representation of natural complexities as well as linear infrastructures, when present. The element size varies from 350 to 0.5 m, moving from flatter zones to major discontinuities (see Fig. 3.3).

The elevation of each node in the mesh was then retrieved from the 5 m DEMss used to create the four terrain configurations (see 3.3.3): *current morphology (Curr)*, *Curr_Infr*, *past morphology (Past)*, *Past_Infr*. Floodplain Mannings roughness coefficient was mapped according to indications reported in the literature (see e.g. Domeneghetti et al., 2013; Vorogushyn, 2008) as the function of land-use characteristics retrieved from CORINE 2012 data set (Büttner et al., 2014; European Environment Agency, 2007). As for other simplifying assumptions of our study, we did not consider historical land-use changes in our analysis, thus enabling a direct comparison of flooding scenarios and better understanding the impacts of anthropogenic land-subsidence on flood hazard dynamics, regardless of any other factor. For the same reason, infrastructures and levees elevations have been modified only in accordance with the ground-lowering rate indicated by Teatini et al. (2005), without considering other modifications due to adjustments that the structures have suffered over the decades.

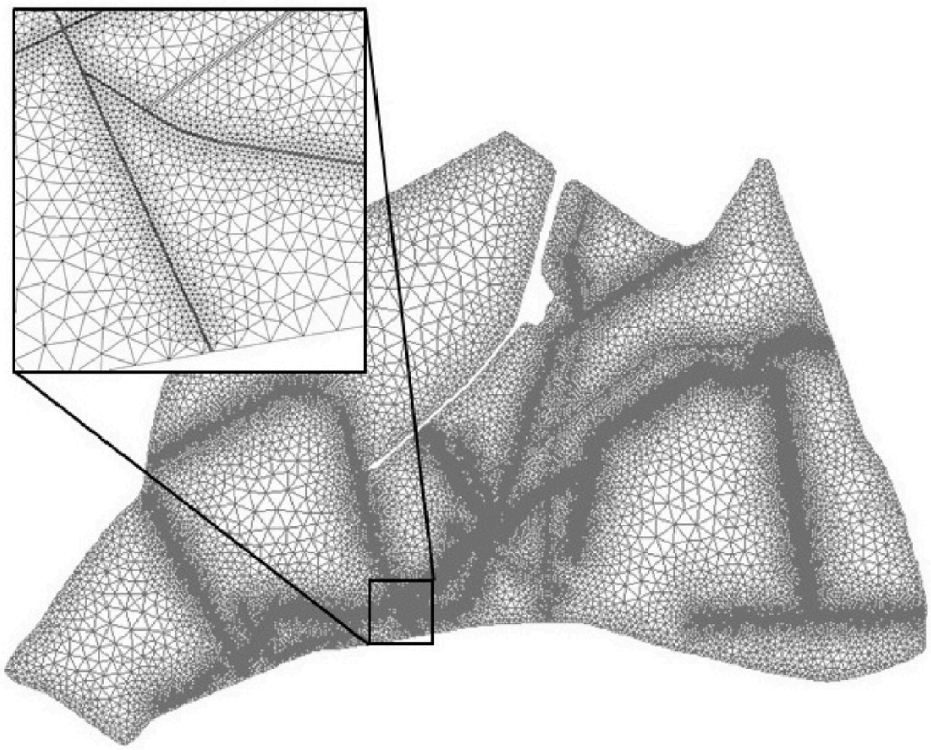

Figure 3.3: Non-structured computational mesh of the study area used for all 2D simulations in Telemac-2D.

3.5 Results and discussion

We present the results of our analysis focusing on the most representative hydraulic indices obtained from all simulations, namely:

- computed flooded area;
- maximum computed local water depth (h [m]);
- maximum computed local water velocity (v [m/s]);
- maximum computed local current intensity ($i = h{\cdot}v$ [m^2/s]).

For the sake of clarity, we organized the presentation and discussion of results by addressing the three research questions set in the introduction.

3.5.1 Can anthropogenic land-subsidence alter riverine flood hazard?

Figure 3.4 illustrates the flooded areas resulting from a given inundation event and two different terrain configurations. In this context, we defined the flooded area as a floodplain portion for which the computed maximum water depth resulted from the model simulations exceeds 0.1 m.

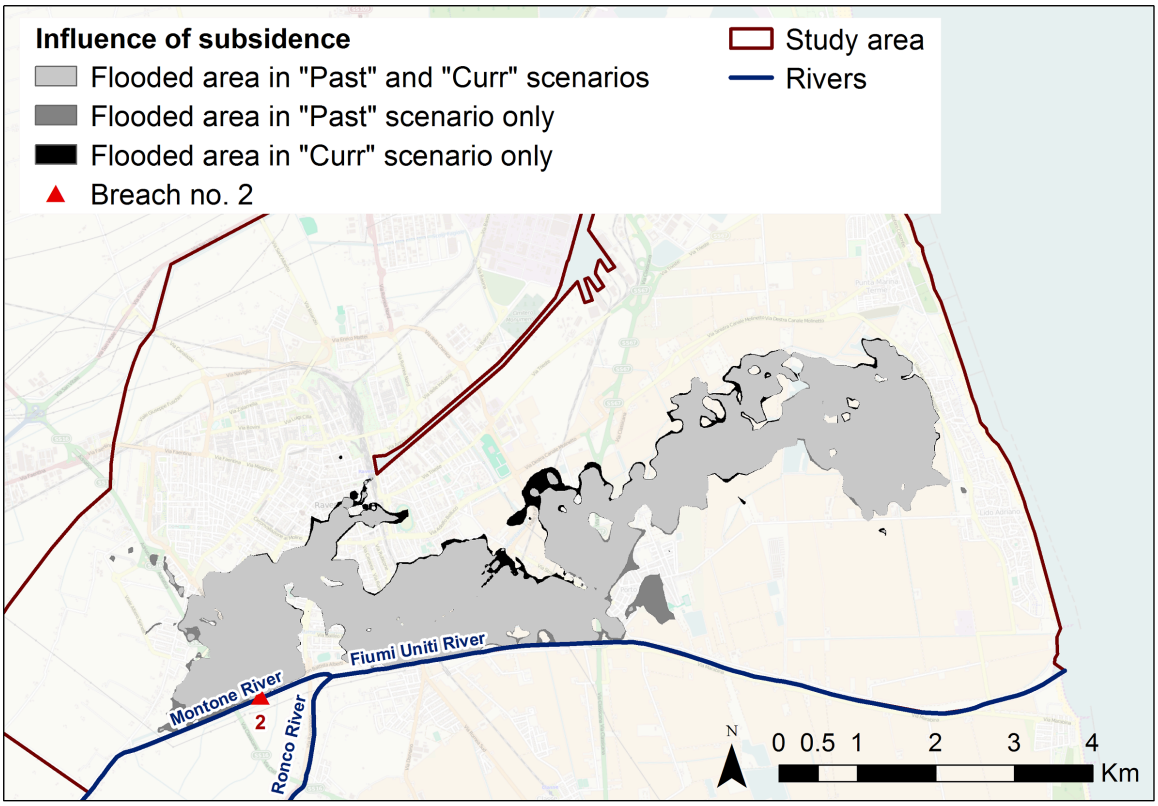

Figure 3.4: Example of different inundation patterns associated with the same levee breaching (breach No. 2, indicated in red) and two different terrain configurations: *Curr*, current topography, and *Past*, reconstruction of the pre anthropogenic land-subsidence topography (main linear infrastructures are neglected).

Figure 3.4 shows the comparison between flooded areas for *Curr* and *Past* terrain configurations under the same levee breaching (breach location No. 2 in Fig. 3.2). Light-grey areas in Fig. 3.4 were flooded in both *Curr* and *Past* configurations; dark-grey areas were flooded in *Past* configuration only, while black areas were flooded in *Curr* configuration only. The most striking feature of Fig. 3.4 is certainly the

fact that the majority of inundated areas was flooded in both terrain configurations. Nevertheless, it is worth noting that the current terrain configuration (*Curr*) was associated with larger inundated areas near the city of Ravenna (black area), where more damages are expected in terms of residential areas and industrial activities. Areas flooded only for *Past* terrain configuration, instead, were mainly located in rural zones in the Eastern portion of the study area (dark-grey areas).

Concerning *Curr* and *Past* terrain configurations, we obtained similar results by simulating the inundation scenarios based on the three remaining breaching events; additional simulations are not illustrated herein for the sake of brevity. Based on these outcomes, we can state that anthropogenic land-subsidence may have affected the inundation hazard in the study area, but the significance of these flood hazard alterations appears to be limited, at least in terms of floodable areas.

3.5.2 Can anthropogenic land-subsidence significantly modify the inundation dynamics?

The literature clearly indicates that tangible damages and economic losses caused by inundation events are associated with water depth, together with other hydraulic variables or indices (e.g. water velocity, see e.g. Green et al., 2011; Merz et al., 2013; Meyer et al., 2013). In addition, damages typically occur when at least one of these indices becomes significant. Significance in this context was identified empirically and is expressed in terms of threshold values. According to Kreibich et al. (2009), we adopted three definitions of significantly flooded area (i.e., flooding that produces more than slight structural damages and more than moderate non-structural damages when goods and assets are at risk), focusing in turn on one of the three different hydraulic indices:

- maximum local water depth (h) higher than 50 cm;
- maximum local water velocity (v) higher than 0.25 m/s;
- maximum local current intensity (i) higher than 0.1 m^2/s.

Therefore, considering one hydraulic index at a time (i.e. either h, v, or i), we compared the extent of significantly flooded areas associated with all four terrain configurations (i.e., *Past*, *Curr*, *Past_Infr*, *Curr_Infr*) by means of an adaptation of the Flood Area Index (FAI) (see Falter et al., 2013; Schumann et al., 2009).

In particular, for one breach event, we compared pairs of terrain configurations (e.g. *Curr* and *Past_Infr*) by means of:

$$FAI = \frac{A}{A + B + C} \tag{3.5.1}$$

where A is the extent of the area that is significantly flooded for both configurations (i.e. light grey area in Fig. 3.5); B is the extent of the area, that results significantly flooded in one of the two configurations only (i.e. dark-grey area in Fig. 3.5); C is the opposite of B, i.e. the area significantly flooded in the other configuration only (i.e. black area in Fig. 3.5).

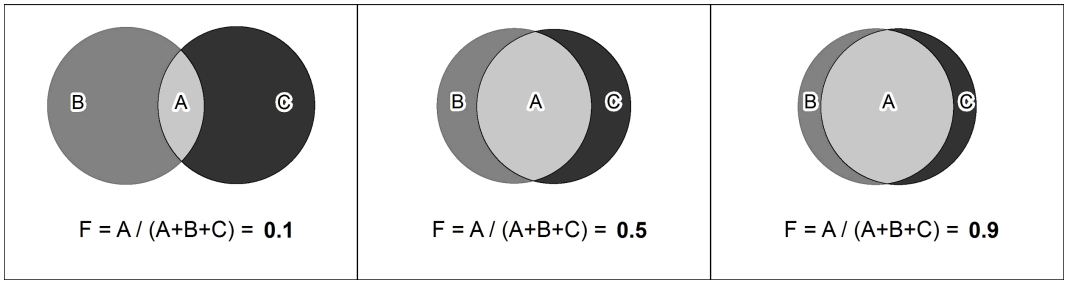

Figure 3.5: Schematization of FAI value calculation: A (light grey area) represents the area flooded in both terrain configurations; B (dark-grey area) is the area flooded in one of the two configurations only; C (black area) is the area flooded in the other configuration only; FAI value close to 1 indicates a high similarity between inundation scenarios.

Areas A, B and C are those in which one hydraulic index (either h, v, or i) satisfies the condition given above). The closer to 1.0 the FAI coefficient, the higher the similarity between the significantly flooded areas in the two terrain configurations.

Table 3.1 shows FAI values for the three hydraulic indices considered in the study, indicating the pairs of terrain configurations being considered. Specifically, once defined the terrain configurations that are compared, the value reported in Table 3.1 represents the average FAI value obtained from the comparison of all the inundations resulting from the four levee breaches (see Fig. 3.2). In particular, aiming at addressing the research question of the present section, we should focus on the first two rows of Table 3.1. These compare current and past terrain configurations in a consistent way as far as the presence of linear infrastructures is concerned, meaning that main linear infrastructures are either present or neglected in both terrain configurations.

Table 3.1: FAI values in terms of h, v and i resulting from the comparison of different configurations. Each value is the average of the values obtained, for the same pair of compared terrain configurations, in all the four considered levee-breaching scenarios.

	FAI (h)	**FAI (v)**	**FAI (i)**
Curr* vs. *Past (Effect of subsidence neglecting linear infrastructures)	0.88	0.81	0.83
Curr_Infr* vs. *Past_Infr (Effect of subsidence considering linear infrastructures)	0.93	0.77	0.87
Curr* vs. *Curr_Infr (Effect of linear infrastructures on current topography)	0.50	0.47	0.58
Past* vs. *Past_Infr (Effect of linear infrastructures on past topography)	0.51	0.49	0.58
Past* vs. *Curr_Infr (Effect of both subsidence and linear infrastructures)	0.50	0.49	0.58

The FAI values reported in the first two rows of Table 3.1 indicates that there were differences between the results obtained for compared terrain configurations, that is anthropogenic land-subsidence does alter the extent of significantly flooded areas. Yet, the modifications appear to be limited, being the FAI value always above 0.75 (i.e. differences were relative to less than 25% of the significantly flooded area), and close to 0.9 (differences were in the order of 10% of the flooded areas) when we define significantly flooded areas by looking at water depth only. Are these differences comparable with the alterations in flooding potential that result from the construction of linear infrastructures? We address this problem in the next paragraph.

3.5.3 Are the effects of anthropogenic land-subsidence more intense than those resulting from linear infrastructures?

Similarly to Fig. 3.4, Fig. 3.6 shows an example highlighting the differences in terms of flooded area simulated for two terrain configurations and a given levee-breaching scenario. In this case, we referred to the current topography. The two terrain configurations differed only in terms of main linear infrastructures (i.e., railways, roads and land-reclamation channels), which were either neglected, or correctly reproduced (i.e. *Curr* or *Curr_Infr* configurations, respectively).

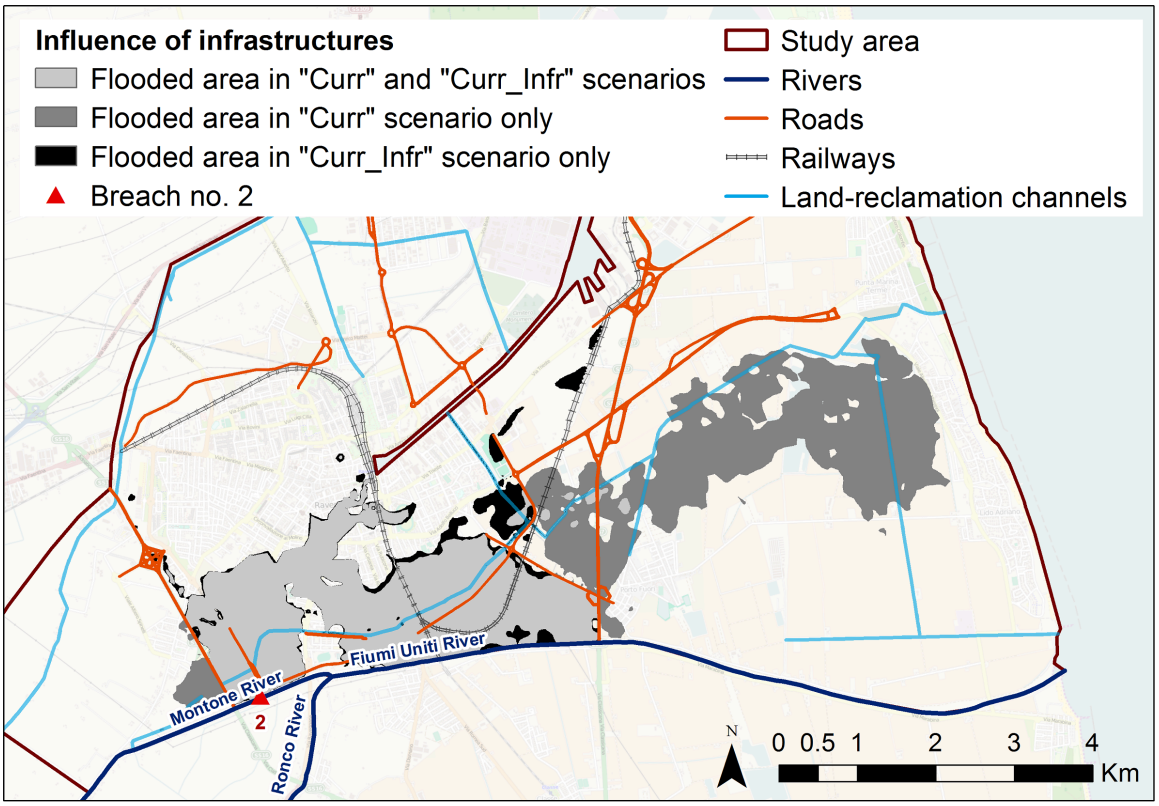

Figure 3.6: Example of different inundation patterns associated with the same levee breaching (breach No. 2, indicated in red) and two different terrain configurations: *Curr*, current topography, and *Curr_Infr*, current topography with main linear infrastructures (i.e. roads and railways embankments, land-reclamation channels).

Figure 3.6 clearly shows that the presence of linear infrastructures strongly affects

the flooding extent. The common flooded area in both the configurations (light-grey color) represents only a small portion (45%) of the overall inundated areas. Neglecting main linear infrastructures resulted in a significantly larger inundated region (i.e. 14 km^2 instead of 8 km^2 for *Curr_Infr* configuration), as the outflowing volume was not confined by man-made embankments, nor drained by the land-reclamation channel network (dark grey area in Fig. 3.6). Concerning *Curr_Infr* configuration, the barraging effects of transport infrastructures and the draining operated by artificial channels on the inundation dynamics are evident in Fig. 3.6 (black area); as a result, the computed water depths became higher in the central portion of the study area and the flooding moved Northern towards the city center.

These significant differences are even clearer if we consider the FAI values reported in Table 3.1. In particular, what is shown in Fig. 3.6 for one particular levee-breaching scenario (i.e. effects of infrastructures on current topography) is quantified by the values on the third row in Table 3.1 for the compound of four considered breaching locations. FAI values indicate that differences between the two terrain configurations in terms of significantly flooded areas relative to h, v or i varied approximately from 40% to 50%. Moreover, the FAI values resulting from the comparison between *Curr* and *Curr_Infr* (third row in Table 3.1) correspond almost exactly to the FAI values obtained from the *Past* vs. *Past_Infr* (fourth row in Table 3.1) or *Past* vs. *Curr_Infr* (fifth row in Table 3.1). This outcome highlights the overwhelming importance of considering or neglecting main linear discontinuities relative to anthropogenic land-subsidence observed in the study area. In conclusion, our analysis clearly showed that anthropogenic land-subsidence may have a role in altering inundation extent (or more precisely, the extent of significantly inundated area), but its effects are marginal if compared with the impact of linear infrastructures in area surrounding the city of Ravenna.

Does this conclusion hold also for the spatial distribution of relevant hydraulic indices (i.e. h, v, and i)? To draw a firm conclusion on the role of anthropogenic land-subsidence and infrastructures, we further analyzed all the flooding scenarios by assessing the changes in the spatial distribution of h, v and i. Referring to the one of the four breaching events, we compared the pairs of terrain configurations by looking at the spatial distribution of the difference of computed h (or v, or i) values, for all 5 m cells, included in the reference area. This area is defined as the merger of all areas significantly inundated in terms of h (or v, or i) at least in one of four configurations

(i.e. *Curr*, *Past*, *Curr_Infr*, *Past_Infr*). For instance, if we consider Breach No. 1 (see Fig. 3.2) and the water depth h as hydraulic index, the reference area is the merger of the four areas that are significantly flooded in terms of h (water depths higher than 50 cm) for four terrain configurations considered in the analysis.

Differences between flooding scenarios for two terrain configurations were evaluated in terms of empirical exceedance probability (or 1-F, if F is the empirical cumulative distribution function) of the absolute difference of computed water depths $|\Delta h|$ (or velocities $|\Delta v|$, or intensities $|\Delta i|$) over the reference area (i.e. merger of four significantly flooded areas) discretized at 5 m resolution. We adopted *Curr_Infr* as the basis for all comparisons, because it represents the terrain configuration closer to reality (i.e., current topography with a detailed representation of all major linear infrastructures). All other terrain configurations (i.e., *Past_Infr*, *Curr* and *Past*) are therefore compared with *Curr_Infr* in terms of exceedance probability of $|\Delta h|$, $|\Delta v|$, and $|\Delta i|$, constructed by grouping together results obtained for all four simulated levee-breaching scenarios.

Figure 3.7 presents the empirical exceedance probabilities for three different hydraulic indices on three separate panels. Black lines refer to the comparison between *Curr_Infr* and *Past_Infr* terrain configurations, which differ by means of anthropogenic ground-lowering only. Blue and red lines (*Curr_Infr* vs. *Curr* and *Curr_Infr* vs. *Past*, respectively) highlight, instead, the influence of major linear infrastructures by comparing two terrain configurations that differ at least in terms of representation of main linear infrastructures. Grey areas in all panels highlight significant values of $|\Delta h|$ and $|\Delta v|$ (differences within grey areas are higher than the typical uncertainty in variables modelled by Telemac-2D: $|\Delta h|$=0.2 m, and $|\Delta v|$=0.2 m/s; see Dimitriadis et al., 2016; Lim, 2011; Néelz and Pender, 2013); we calculated the uncertainty associated with simulated i (i.e. $|\Delta i|$=0.08 m^2/s) by taking into account the propagation of uncertainties in h and v. Therefore, the larger the portion of the curves inside the grey areas, the lower the similarity between two flooding scenarios in terms of spatial distribution of either h, v, or i.

Results in Fig. 3.7 are in accordance with the previous findings: black lines show limited differences and small portions of the lines within the grey areas for h and v, whereas intensity i shows a slightly larger portion of the curve within the grey area (i.e. significant differences) due to the non-linear dependence on h and v.

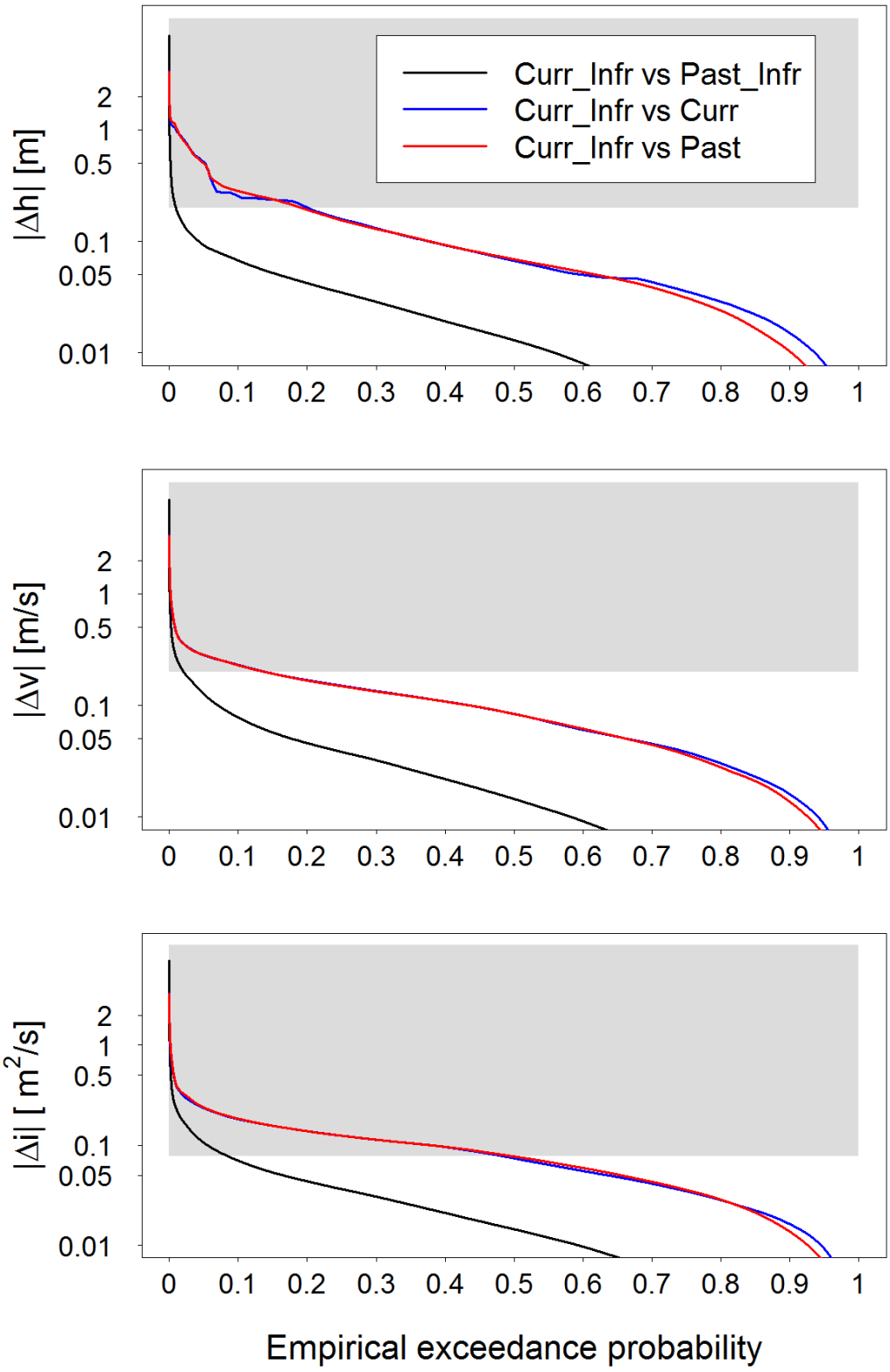

Figure 3.7: Empirical exceedance probability of $|\Delta h|$, $|\Delta v|$, and $|\Delta i|$ between the pairs of levee-breaching scenarios for different terrain configurations; grey areas denote the range of significant absolute differences.

Table 3.2 reports values of empirical exceedance probability for significant absolute differences (i.e. empirical probability associated with $|\Delta h|$>0.2 m, $|\Delta v|$>0.2 m/s, and $|\Delta i|$>0.08 m^2/s). These values can be interpreted also as the fractions of inundated areas in which differences between flooding scenarios on different terrain configurations in terms of computed water depth, velocity and current intensity are significant.

Table 3.2: Fraction of inundated areas that are associated with significant differences between pairs of terrain configurations in terms of computed maximum water depth $|\Delta h|$, velocity $|\Delta v|$, and intensity $|\Delta i|$.

	Curr_Infr **vs.** ***Past_Infr*** (Impact of subsidence)	***Curr_Infr*** **vs.** ***Curr*** (Impact of infrastructures)	***Curr_Infr*** **vs.** ***Past*** (Impact of subsidence and infrastructures)
$\|\Delta \boldsymbol{h}\|$	0.01	0.20	0.19
$\|\Delta \boldsymbol{v}\|$	0.02	0.14	0.14
$\|\Delta \boldsymbol{i}\|$	0.08	0.48	0.48

Figure 3.7 and Table 3.2 support our findings in terms of extent of flooded areas (i.e. values reported in Table 3.1) and further highlight the limited influence of land-subsidence on flood hazard alteration, as the effects in terms of spatial alteration of hydraulic indices due to subsidence are only limited relatively to the impact of linear infrastructures. The similarity between red and blue lines is evident in all panels of Fig. 3.7. These lines show the importance of main linear infrastructures, pointing out that differences between current configuration with and without linear infrastructures (red lines) are practically the same that one may obtain from the comparison between current topography with infrastructures and past topography without them (blue lines). It is, also, worth noting that portions of red and blue lines falling within grey areas in Fig. 3.7 are always significantly larger than the corresponding portion of black lines. This result is also evident from three columns in Table 3.2.

Finally, by looking at Fig. 3.7 and Table 3.2, it is also evident that the alteration in terms of water depth and velocity (i.e. $|\Delta h|$ and $|\Delta v|$) associated with the presence of linear infrastructures was limited in all considered cases. The presence of infrastructures mostly affected the spatial distribution of flood intensity ($i = h{\cdot}v$),

for which significant differences could be found in approx. 48% of flooded areas. In other terms, despite the alterations of computed water depth and velocity were significant only for small portions of the inundated areas (i.e. 14-20%), the product of the two variables was more sensitive to the terrain configuration and showed significant alterations over larger portions of inundated areas.

3.6 Concluding remarks

We studied the effects of anthropogenic land-subsidence on riverine flood hazard, comparing it with the impact on flooding dynamics of artificial channels, roads and railways embankments. We considered the area close to the city of Ravenna, as it is the most prominent example of human-accelerated land-subsidence in Italy. Due to the intense extraction of underground water and natural gas, the study area underwent an extremely significant ground-lowering during the last century, with a cumulative drop higher than 1.5 m a century in the historical center of the city, horizontal gradients above 0.3 m/km, and lowering rates larger than 110 mm/year, when the natural rate is estimated in a few mm/year (see Carminati and Martinelli, 2002; Gambolati et al., 1991; Teatini et al., 2005).

We simulated different levee breaches along the Montone-Ronco Rivers system and then assessed and compared the computed flooding dynamics of the adjacent flood-prone area resulting from four alternative terrain configurations, that is the current topography with and without main artificial road and railways embankments and channels, and the reconstructed topography for year 1897, with and without main artificial embankments and channels. Inundation scenarios were compared to each other in terms of computed flooded areas and spatial distribution of computed water depth (h), velocity (v) and flow intensity ($i = h \cdot v$).

The main outcome of our analysis is that large and rapid differential land-subsidence observed in the study area may have produced the modifications of riverine flood hazard, yet these alterations do not seem to be significant. In fact, the most significant and evident changes in flood hazard occurring in the study area seem to be associated with the construction of main linear hydraulic and transport infrastructures (i.e. man-made land-reclamation and irrigation channels, roads and railways embankments). These discontinuities introduce the macroscopic alterations of the inundated areas and flooding dynamics that are certainly more important than alterations resulting from man-induced, or man-accelerated, land-subsidence.

Consequently, under the main assumptions of our study, that for instance neglected the impact of land-use and land-cover changes, we can conclude for the study area that anthropogenic land-subsidence may be seen as the potential driver of riverine flood hazard and risk changes, but the construction of artificial canals and road embankments has a significantly stronger impact on flooding potential.

Although the limited relevance of anthropogenic land-subsidence relative to alteration in inundation dynamics, it is still necessary to consider its effect in terms of ground-lowering gradients. These could alter the safety level of rivers embankments, and hence flood hazard. This aspect deserves to be investigated in detail in future analyses.

Additionally, our analysis shows that the correct assessment and mapping of flood hazard and risk that rely on hydrodynamic inundation modelling cannot dispense with an accurate representation of major topographic discontinuities, such as artificial irrigation and land-reclamation channel systems, roads and railways embankments (i.e. resolution should be finer than 5 m). More in general, the results highlight the importance of the accurately identification of the specific topographic data that have to be considered in the modelling exercise (Domeneghetti, 2014; Dottori et al., 2013), which should represent the best compromise to balance model complexity, efficiency, and reliability.

Chapter 4

Simplified approach for assessing historical flood risk evolution (case study 2: the Po river basin, Italy)

4.1 Introduction

This case study aimed at analysing the residual flood risk evolution in the dyke-protected floodplain on the middle-lower portion of the Po river during the last half century. Several authors (see e.g. Montanari, 2012; Zanchettini et al., 2008, and references therein) studied the hydrological behaviour of the Po river basin, while the scientific literature does not report any comprehensive analysis of the historical flood risk dynamics for the entire middle-lower portion of the Po river nor of the influence of the main controlling factors (e.g. human activities that developed during last decades, climatic variability, etc.) on this dynamics. In particular, once proved the absence of trends in the flood hazard evolution by Domeneghetti et al. (2015), the investigation intended to develop a simplified and robust approach for the quantification of flood risk dynamics associated with the evolution of exposure to floods. As mentioned in Ch. 1, in fact, the flood risk of a given area is the combination of the probability of inundation (i.e. flood hazard) and the expected adverse consequences (i.e. flood exposure and damage susceptibility of the flood-prone areas).

Specifically, since the study area is protected against 200 year flood events (Po river Basin Authority, AdB-Po, 1999), we focused on the residual risk dynamics, thus referring to a specific low-frequency flooding scenario for which the protection measures are insufficient (see Sec. 4.6.1 for more details).

The proposed method consisted of developing simplified flood vulnerability indexes based on land-use and topographic information, particularly suitable for large spatial scale studies. They intend to be useful to assess the importance of the different elements contributing to the definition of flood risk and to represent the evolution in time of flood exposure and residual flood risk in the dyke-protected floodplain of the study reach, assessing the anthropogenic pressure by referring to land-use (i.e. focussing on residential areas) and demographic dynamics observed from 1950s.

Finally, we quantitatively assessed whether during the last half-century the study area experienced the so-called *levee-effect*, and to what degree it impacted the residual flood risk.

4.2 Study area

The study area consisted of the alluvial plain of the Po river, the longest Italian river that flows Eastward through the Northern part of Italy for about 650 km (see Fig. 4.1).

With the total extent of about 71 000 km^2, the Po river basin is the largest Italian catchment and covers a large portion of the Emilia-Romagna, Lombardy, Piedmont, Aosta Valley and Veneto. This area, in particular the Alpine foothills and flat portion of the basin, represents one of the most developed and populated areas in Italy: more than 45% of employed Italians live here producing almost 40% of the total Italian Gross Domestic Product (GDP) (Po River Basin Authority, AdB-Po, 2006).

The middle-lower reach of the Po river flows across a flat and fertile alluvial plain, named Pianura Padana (overall extent of around 46 000 km^2), where the flood-prone areas that are closer to the Po river, or its major tributaries, are protected from frequent inundations by means of a complex system of embankments and other hydraulic structures (e.g. pumping stations, sluice gates, etc.) that are monitored and maintained by the Interregional Agency of the Po River (AIPO) and by the Po River Basin Authority (AdB-Po).

The current embankment system represents the result of the people's struggle during the last centuries to prevent the loss of their properties and assets due to floods. From 1705 to 1951 Pianura Padana was hit by 18 major floods with 225 embankment failures along the main river or its major tributaries (Govi and Turitto, 2000). In the inundations aftermath the embankment system was continuously

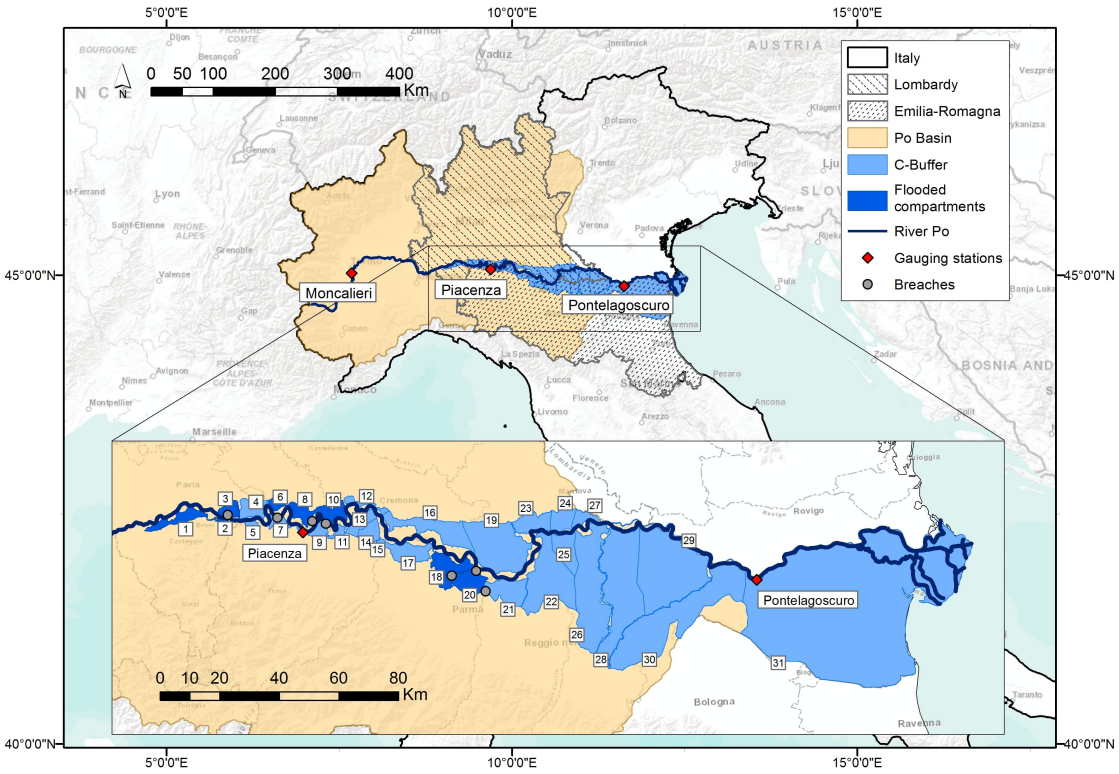

Figure 4.1: Study area: Po river basin with gauging stations (red dots) and Regions of interests (Emilia-Romagna and Lombardy); the numbered compartments (blue polygons) represent the area outside the levee system that is exposed to a residual flood risk (i.e. C-Buffer zone; AdB-Po, 1999; Castellarin et al., 2011b).

strengthened and extended, increasing from a total length of about 1500 km in 1878, to more than 2900 km after the flood event of 1951, that inundated an area of ∼1080 km^2 (see Masoero et al., 2013) and caused severe damages (e.g. 100 victims, 900 houses seriously damaged and around 200 000 refugees; Amadio et al., 2013).

Castellarin et al. (2011a) and Di Baldassarre et al. (2009b) clearly showed the evolution in time of the overall length of the embankment system along the Po river and major tributaries between 1800 and 1950s-1960s and the associated increasing trend in the sequence of annual maximum water level at the Pontelagoscuro streamgauge (see Fig. 4.1), located at the catchment outlet. During the last decades (i.e. from 1960s) the actions of adjustment of the levee system along the lower portion of the river mainly focused on the strengthening of the existing embankment, while further

embankment widening and raising were implemented after the flood event of October 2000 (see Castellarin et al., 2011a; Coratza, 2005). The current river configuration is reported in Fig. 4.1 (box), which shows the main river reach, the main embankment system, as well as the area that can potentially be flooded in case of catastrophic flood events (blue polygons). This area, named *Fascia-C* (literally *C-Buffer*, which we consistently use in the remainder), is characterized by the overall extent of ∼6100 km^2 and is identified by the Po River Basin Authority (AdB-Po, 1999) as the envelope of all areas associated with a non-negligible residual flood risk. It represents the areas that can be flooded in case of the sudden and unpredictable failures of the embankment system or in case of flood event with a return period higher than the one adopted for the design of the embankments (i.e. ∼200 year, AdB-Po, 1999). The box on Fig. 4.1 shows the C-Buffer area divided into different compartments defined referring to the layout of natural and man-made structures (e.g. embankments for the Po river and its main tributaries, rivers, roads, etc.; see also Castellarin et al., 2011b).

Despite the existence of a non-negligible residual risk in the C-Buffer (i.e. the levee failure occurred in 1951 is the evidence of the residual risk that still exists in the flood-prone area), the feeling of safety ensured by the embankment system attracted human settlements and the area itself went through a significant economic development during the 20^{th} century. In the light of these considerations, together with the availability of historical land-use information (see Sec. 4.3 for details), we investigated the driver factors of the evolution of the residual flood risk in the flood-prone areas during the last decades, focusing in particular on the period that goes from 1950s up to now.

4.3 Available data

Data of various type retrieved from different sources were used in this study, briefly summarized by the following list, while further information on the utilization of these data are provided in Secs. 4.4, 4.5 and 4.6:

- *Land-use maps*: land-use maps are available for the C-Buffer and different time periods from cartographic offices of Emilia-Romagna and Lombardy administrative districts (see Fig. 4.1). In particular, land-use information is retrieved from aerial imagery available for 1954 (G.A.I-Gruppo Aereo Italiano and WWS flights) and 2008 (AGEA-2008), with a resolution of about 150 m and 75 m, respectively, and classified referring to the standardized classes

aggregation adopted by the CORINE project (European Environment Agency, 2007);

- *Demographic dynamics*: number of inhabitants available throughout Italy since 1861; the Italian National Statistical Institute (ISTAT) makes available information on the population dynamics with ten-year frequency at each census sections;
- *Economic values of the assets*: the economic values of residential buildings in the alluvial area; the Agenzia delle Entrate (Italian Revenue Agency) (AE) provides the open-market values for different assets, taking into account different classes for residential and industrial buildings and the overall economic well-being of the region (see Sec. 4.6.2 for more details);
- *Topographic information*: topography of the study area is retrieved from TINITALY/01 (Tarquini et al., 2007); created by using heterogeneous elevation data sets (i.e. contour lines, elevation points, etc.), TINITALY/01 represents the most accurate DEM covering Italy. It is characterized by a horizontal resolution of 10 m and a vertical accuracy (i.e. root mean square errors ranging from 0.8 to 6 m) higher relative to other global DEMs (i.e. SRTM, ASTER; see Tarquini et al., 2012).

4.4 Previous studies

A previous assessment by Domeneghetti et al. (2015) concerned the evolution of flood hazard in the middle-lower reach of the Po river. Being this one a complementary analysis to the evolution of exposure in the same area of interest, it deserves to be briefly described, in order to provide general conclusion on the evolution of flood risk in its entirety. Domeneghetti et al. (2015) analysed long streamflow series available at different gauging stations located along the study reach, statistically falsifying the hypothesis of changes in flood hazard during the last half century similarly to what have been shown for some other regions of the world (see e.g. Kundzewicz et al., 2005; Svensson et al., 2005).

Many studies investigated the streamflow regime of the Po river: to cite one of them, Zanchettini et al. (2008) analyzed the long-term daily streamflow variability at Pontelagoscuro (see Fig. 4.1) by referring to a time series longer than 200 years, in which some daily streamflow values were re-constructed from the historical

information on water surface. The analysis highlighted an increase in the streamflow values observed at the streamgauge of Pontelagoscuro during last decades: the authors concluded that this increase is mainly ascribable to the massive embankment works implemented along the river network during previous decades, rather than to climate changes. The study also pointed out the existence of perturbation periods (mainly associated with droughts) lasting for several years. More recently, Montanari (2012) reached similar conclusions by investigating the variability of daily streamflows observed along the Po river and some of its major tributaries. The study highlighted the presence of local perturbations (i.e. periods characterized by water scarcity or water abundance), which memory lasts for long periods of time (i.e. several years), which can be associated with the size of the drainage area. Even though this evidence suggests the presence of long-term persistence that would be worth investigating, the research of trend interested only the gauged section of Pontelagoscuro and was made by means of a linear regression application.

Domeneghetti et al. (2015) further analysed the variability of the daily streamflow regime of the Po river by testing the existence of trends of the daily streamflow series collected at three gauging sections along the main stream: Moncalieri, Piacenza and Pontelagoscuro (see also Fig. 4.1), which are statistically correlated to each other (being the streamgauges located along the same river) but refer to rather different drainage areas and periods of time (see Fig. 4.1). In particular, performing a two-sided trend test at 5% significance level through the MK-TFPW procedure (to remove serial correlation from time series) on the sequences of Annual Maximum Series (AMS), mean (MEAN) and Standard Deviation (SD) of daily streamflows, the results highlighted the absence of significant and consistent long-term trends: considering Moncalieri and Piacenza cross-section, Sen's slopes appeared to be limited for all considered statistics, pointing out a small increase in the annual maxima and mean discharge values. The river daily streamflow variability, instead, is almost constant over the period. Moreover, p-values reported for Moncalieri and Piacenza indicated the absence of statistically significant long-term trends at 5% level. The slight increase of annual maximum daily discharges in the upstream cross-sections of Moncalieri and Piacenza was confirmed at Pontelagoscuro, where this feature appeared to be emphasized. AMS at Pontelagoscuro were associated with a slight trend which, if not negligible, was insignificant from a statistical viewpoint. Furthermore, concerning the

non-significant positive trend associated with the last 90 years of observations, it was worth highlighting that the same analysis repeated for the data observed after 1950 resulted in a statistically non-significant negative trend.

The extended analysis of historical stream flow series carried out by Domeneghetti et al. (2015) confirmed the findings of previous studies (e.g. Montanari, 2012; Zanchettini et al., 2008) and highlighted the absence of statistically significant trends within streamflow series along the overall river reach. The impact of the flood hazard variability in the assessment of the residual flood risk dynamics during the last half century appeared to be practically negligible and statistically insignificant, making the hypothesis of the stationarity of the streamflows data set reasonable. On the basis of these considerations, the likelihood of extreme flood events responsible for the residual flood risk in the area of interest (such as flood events with return period higher than 200 years) can be considered not significantly changed during the last half century. For this reason, our analyses of the flood risk evolution in the Po plain focused on the exposure evolution trends only.

4.5 Exposure evolution

4.5.1 Land-use dynamics

The investigation of the land-use evolution in the Po river basin focused in particular on Emilia-Romagna and Lombardy administrative districts (see Fig. 4.1), which entirely cover the C-Buffer (i.e. the floodable area in case of the $T_r 500$ flood event; see box in Fig. 4.1). Our analysis considered land-use maps available for 1954 and 2008 (see Sec. 4.3). The maps were constructed on the basis of historical aerial photographs with different spatial resolution (150 m and 75 m for the 1954 and 2008 maps, respectively), however the land-use classifications adopted in both cases were consistent and enabled one to compare the two data sets. The land cover data in both maps used a hierarchical structure similar to the one adopted by the CORINE project (European Environment Agency, 2007), in which different soil-uses are organized by means of several levels of aggregation. In this study the evaluation of the flood exposure evolution was performed referring to urban and residential areas only.

We evaluated the expansion of urban and residential areas by referring to two different spatial scales. Firstly, we considered a local scale by referring to C-Buffer

compartments only (see Fig. 4.1). Secondly, we evaluated the land-use evolution at a larger scale (i.e. regional analysis), comparing the overall extension of urban areas in 1954 and 2008 in Emilia-Romagna and Lombardy districts. Results obtained for the local (C-Buffer) and regional (large-scale) analyses were then compared to gain a deeper understanding of the evolution of exposure to floods, providing interesting insights to foster the discussion on the effectiveness of the *levee-effect* (or *call effect*) on the floodplains areas (see Secs. 4.7 and 4.8).

We derived a large scale assessment on the exposure to floods in the C-Buffer using the land-use maps described above. In particular, we combined the land-use class of interest (i.e. urban settlements) of each compartment with the digital description of the topography using DEM with 10 m resolution (see Sec. 4.3) to retrieve a simplified altimetric description of urban and residential areas through a so-called hypsometric curve, which we named Hypsometric Vulnerability Curve (HVC). The HVC of a given area reports the percentage (or the portion) of area (on the x-axis) characterized by elevations lower than the value reported on the y-axis. HVCs of each compartment of the C-Buffer combine land-use information with information on the elevation retrieved form the 10 m DEM. Zhang et al. (2011) firstly proposed the use of hypsometric curves in the Florida Keys for the evaluation of the impact of different scenarios of sea level rise on human population and real estate property.

We constructed the urban and residential areas HVCs for each compartment for 1954 and 2008 in GIS environment. HVCs represent a valuable tool for the preliminary assessment of the exposure to floods for each compartment, and, when land-use information related to different time periods is available, as in our case, these curves can be particularly useful for characterizing the dynamics of urban areas over a given historical period (e.g. in the dike-protected floodplain of the Po river over the last half century). The schematic representation (Fig. 4.2) illustrates HVCs for a specific land-use type.

The HVCs graphically represent the altimetric characteristics of a specific land-use class in a given compartment (e.g. residential settlements). HVCs related to different periods enable one to assess how and where (i.e. closer or farther from the river) a specific land-use class developed over time (see Sec. 4.7 and Fig. 4.6 for details). Furthermore, assuming the dashed line of Fig. 4.2 as a hypothetical inundation level, its intersection with the HVC identifies the extent of the affected area and may be particularly useful for the prompt assessment of flood damages (see Sec. 4.6.2 for

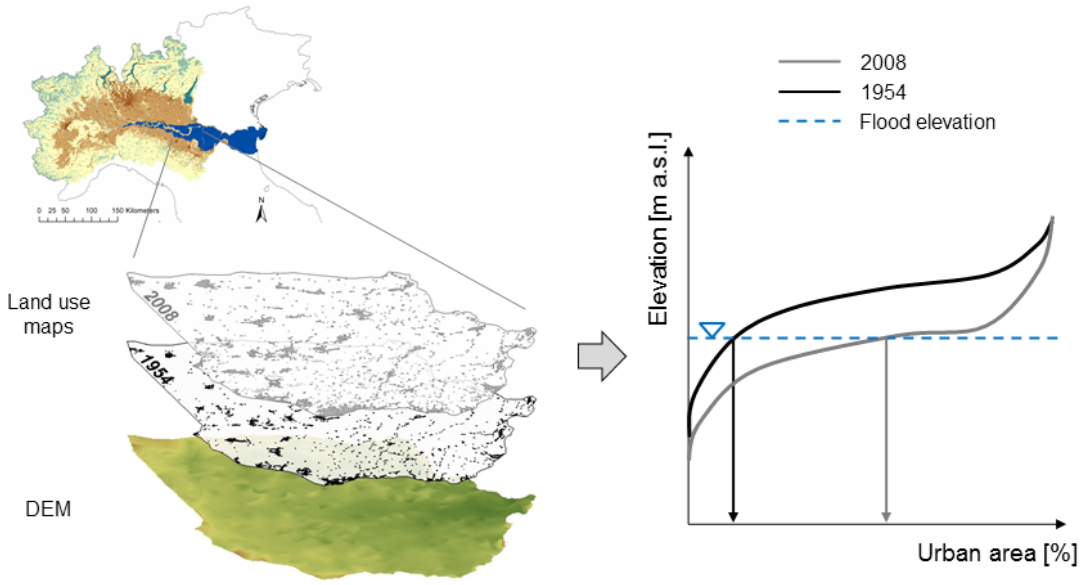

Figure 4.2: Examples of Hypsometric Vulnerability Curves for a specific C-Buffer compartment for 1954 and 2008.

details).

4.5.2 Population dynamics

The number of people living in flood-prone areas represents a fundamental element for the evaluation of the exposure to floods and is a key factor of the *levee effect* phenomenon (see e.g. Barredo, 2009; Di Baldassarre et al., 2009a, 2013). Accordingly, we analysed the population dynamics in the Po river basin, assessing if the strengthening of the levee system registered during last century (see Sec. 4.2 and also Castellarin et al., 2011a; Di Baldassarre et al., 2009b) is associated with any population growth in the flood-prone areas in spite of the residual flood risk. In particular, we evaluated the population dynamics from 1861 to 2011 considering the number of inhabitants recorded by the Italian National Statistical Institute (ISTAT) (census data are provided with a 10 year frequency for each Italian municipality). Once collected, the population data were gathered together distinguishing between Emilia-Romagna and Lombardy regions and all of the compartments of the C-Buffer (see Fig. 4.1). Given the extent of urban areas and the overall number of inhabitants living in a specific municipality within a C-Buffer compartment, we estimated the population density under the hypothesis of a uniform distribution over the urban

extent. The population density of a specific compartment was calculated as the weighted average among different municipalities, proportioning that data to the extent of urban areas. Then, we derived the Hypsometric Inhabitants Curves (HICs) for 1954 and 2008 by combining the average population density with the altimetry of the urban area in a given compartment (same procedure as the one adopted for the HVC construction; Fig. 4.2). HICs are the curves that report the overall number of inhabitants living in a compartment below a given elevation: they integrate information on the number of people living in a specific compartment with the overall extent of urban areas, obtained from land use maps, and elevation retrieved from a DEM of the area of interest. The curves may serve as useful tools for the preliminary evaluation of the exposure to floods of a specific area. For instance, HICs may enable one to estimate the number of people that could be affected by a given inundation scenario over a floodplain area; alternatively, HICs constructed for a given inundation scenario and floodplain compartment by considering census data and land-use maps for different years may effectively summarize the impacts of demographic dynamics on flood risk.

4.6 Damage evolution

Flood risk management recently shifted its main focus from flood hazard (i.e. hazard reduction) to a risk-based view (i.e. risk reduction) (see e.g. De Moel et al., 2012; Merz et al., 2010a; Vis et al., 2003). This approach considers the interplay between hydrological and socio-economic factors. The calculation of the expected flood damage represents a fundamental piece of information for the overall flood risk mitigation process. The evaluation of the overall costs of natural hazards, such as flood events, is a challenging task due to the variety of damage types that may be directly or indirectly related to the hazard. Meyer et al. (2013) recently summarized these costs distinguishing four different categories identified in relation to their nature and to the methodologies adopted for their assessment: direct and indirect costs, business interruption and intangible costs. Considering flood events, direct costs represent the damages occurred to properties (e.g. buildings, stocks, cars, infrastructure, etc.) physically hit by the flood. Business interruption costs result from the interruption of the economic activities in the flooded areas, for example because of inaccessibility or because of the destruction of the working instruments (see Meyer et al., 2013). Indirect costs summarize all the economic losses that can be related to direct and indirect (e.g.

business interruption) damages, occurred both inside and outside affected area, even considering the effects on a broad timeframe after the event (see Carrera et al., 2015, for more details). Finally, intangible costs consider the impact on services, goods or human beings which have not a market value and for which the damage estimation in monetary terms is not trivial, if not impossible (e.g. health and environmental impacts, damages to cultural heritage, etc.; Markantonis et al., 2012; Meyer et al., 2013).

Concerning the estimation of different types of flood losses the literature provides a series of methodologies of various complexity based on different type of data and assumptions, and suitable for different scales of application (see Sec. 2.3 Meyer et al., 2013, for a comprehensive review of these approaches). Traditionally, the flood damage assessments mainly refer to direct losses, because of the easier way to estimate them. In particular, more often suggested models by the scientific community estimate the expected direct flood damages by means of depth-damage functions (also named susceptibility functions), where the economic damage of a specific element (e.g. a building) is a non-decreasing function of the water depth, which is sometimes integrated with some other hazard factors (i.e. flow velocity, duration, pollution, etc.; see Jongman et al., 2012, and Secs. 2.3, 5.5.1 and 5.5.2). Recently, sophisticated multi-parameter models have been proposed for the local estimation of losses in private households and companies (e.g. Elmer et al., 2010; Kreibich et al., 2010; Merz et al., 2013; Thieken et al., 2008). Even though the former approach is less accurate and associated with a higher degree of uncertainty (see Sec. 2.3), in the light of the large spatial scale of interest (i.e. overall C-Buffer area) we estimated the expected flood damage referring to a simplified approach based on the joint use of a depth-damage curve and the previously defined HVCs.

Differently from previous applications, where hypsometric curves were used only for identifying the extent and amount of affected properties (see Zhang et al., 2011, for sea level rise scenarios), we proposed an original application of HVCs in combination with a given inundation scenario and specific depth-damage curves (e.g. accurately identified for a specific land-use or buildings type, see Sec. 4.6.2 for a detailed description about flood damage estimation) that enables the user to calculate the flood losses. We focused on direct tangible damage for residential building, while neglecting all other costs in this preliminary application.

4.6.1 Inundation scenario

For the evaluation of the flood hazard we refer to the inundation scenario generated by the numerical model developed by Castellarin et al. (2011b), who implemented a quasi-2D model for the Po river stretch considered herein (from Isola S. Antonio to Pontelagoscuro, ∼350 km; see Fig. 4.1). The model describes the main river reach by means of cross-sections retrieved from a detailed digital elevation model (LiDAR, with a spatial resolution of 2 m), while all dike-protected floodplains are represented as storage areas connected to each other and/or the main channel by means of weirs representing the minor levees system. Adopting a similar modelling strategy, all C-Buffer compartments are represented as storage areas and connected to the main river, or dike-protected floodplains, by means of lateral structures that reproduce the main embankment crests. Volume-level curves regulate the hydraulic behaviour of all storage areas, and, in case of inundation of a dyke-protected floodplain or C-Buffer compartment, the simulated water level is computed as a function of the water volume exchanged with the main river and/or adjacent storage areas. Volume-level curves were estimated referring to the cited LiDAR imagery for the dyke-protected floodplains and to a 10 m resolution DEM (Tarquini et al., 2007) for C-Buffer compartments. The quasi-2D model was calibrated referring to the historical flood event occurred in October 2000 and then used for simulating a major flood event, hereafter referred to as T_r500, which represents a low frequency/high intensity event associated with the return period of ∼500 years (see Castellarin et al., 2011b, for details).

The main embankment system of the middle and lower portion of the Po river is designed to contain flood events associated with return periods up to ∼200 years, which are significantly less intense than the T_r500 event identified in Castellarin et al. (2011a) and Castellarin et al. (2011b). Considering the homogeneous protection level ensured by the major embankment system along the entire study reach, we referred to the T_r500 event as the reference flood scenario, thus limiting the estimation of the residual flood risk to the likelihood of this extreme event, neglecting the hazard related to flood events associated with return periods lower than 500 year but not contained by the embankment system or to possible levee failures. Considering these latter cases (e.g. breaches on the embankment due to seepage, piping, etc.), in this study the possibility of levee failures for more frequent events was not explicitly considered. Nevertheless, the proposed approach is perfectly suitable for applications that for example adopt comprehensive multivariate Monte Carlo resampling techniques for

the through characterization of the flooding hazard in the region of interest (see e.g. Domeneghetti et al., 2013; Vorogushyn et al., 2010).

The T_r500 inundation scenario is modelled by simulating failures along the embankment system, i.e. formation of breaches in case of the overtopping of the main embankment, see configuration *BREACHBL* in Castellarin et al. (2011b). Dike overtopping may occur in *BREACHBL* if the water level exceeds the crest elevation of the embankments; under this circumstance, as a consequence of the flow erosion on the out-board side of the levee, the quasi-2D model simulates the formation of a levee-breach according to literature information on width, depth and time of full development recorded for the Po river (see e.g. Govi and Turitto, 2000). The numerical model enables the simulation of multiple breaching events as a result of concurrent overtopping phenomena along the main embankment system, thus enabling the inundation of several C-Buffer compartments during a single major flood event (see details in Castellarin et al., 2011b). In order to better highlight the role of the exposure to floods on the evolution of the flood risk, the numerical simulations were performed, for both years of interest (i.e. 1954 and 2008), referring to the actual levee system configuration, thus neglecting the strengthening of the levee system eventually occurred during the last 50 years. Furthermore, the absence of consistent and statistically significant long-term trends on the streamflow series recorded along the Po river (see Domeneghetti et al., 2015, and also Sec. 4.4) enabled the use of the same inundation scenario for the entire period of interest (i.e. from 1954 to 2008), thus facilitating the evaluation of the flood exposure evolution and the overall flood risk.

4.6.2 Damage modelling for urban areas

It is well known that the estimation of direct damages associated with a flood event is a challenging task which is affected by a large amount of uncertainties (Cammerer et al., 2013). Concerning Italy, Molinari et al. (2014b) related this uncertainty with the lack of high quality post-flood event damage data, which are necessary for a proper calibration and validation of damage models. In our analysis, considering the scale of interest (i.e. large scale analysis: middle-lower portion of the Po river) and the nature of the proposed approach (i.e. simplified numerical tools to evaluate the flood risk), the quantification of the flood exposure was performed by referring exclusively to the economic value of private buildings prone to inundation events, neglecting other direct

(e.g. damages to public or commercial buildings) and indirect costs.

The AE publishes the economic value [€/m^2] of different types of private buildings (e.g. civil houses, offices, stores, etc.) in each Italian administrative district (spatial scale of municipality) every six months. Focusing on residential buildings and assuming a unique building type (i.e. civil houses), we defined the reference economic value [€/m^2] for urban settlements within any given compartment of the C-Buffer as the average of the economic values provided for all the municipalities, weighted proportionally to their urban extent located within the C-Buffer (see Table 4.1). Therefore, the overall value of urban properties could then be approximated by the product of the average economic value and the overall urban area extent in the compartment, which we obtained from the land-use maps available for 1954 and 2008 (see Sec. 4.5.1). It is worth noting that the damage evaluation relies on the assumption of a constant economic value for urban buildings over the period of interest (i.e. from 1954 to 2008). Without lack of generality, our analysis considered two different land use maps, yet, for the matter of comparison, we referred to 2014 economic value of buildings for both historical land-use scenarios.

Table 4.1: Average economic values of civil buildings provided by the AE in the C-Buffer compartments flooded in case of the T_r500 event.

Compartment	**Average economic value [€/m^2]**
1	$\sim$ 840
2	$\sim$ 970
3	$\sim$ 865
6	$\sim$ 870
8	$\sim$ 935
10	$\sim$ 850
18	$\sim$ 1105
20	$\sim$ 1245

The literature provides a wide set of depth-damage curves that offer different covering applications contexts, considering different types of buildings (i.e. residential, commercial, industrial, etc.; see e.g. Thieken et al., 2008) and the effect of factors which may influence the expected damages (i.e. contamination, levels of private precaution, etc.; see e.g. Kreibich et al., 2010). These curves generally express the percentage of damage of a specific asset as a function of the water depth and are constructed on empirical damage data (i.e. historical inundation) or using expert judgement and synthetic analysis (Jongman et al., 2012, and Sec. 5.5.1 for more details).

Among the available curves, we referred to the damage-curve implemented in the Multi-Colored Manual (MCM) (Penning-Rowsell et al., 2005, 2010) which estimates the expected losses for residential buildings as a function of the local water depth (see Fig. 4.3). According to Jongman et al. (2012), the MCM is one of the most advanced models for flood damage estimation within Europe and represents a possible tool for the estimation of direct flood damages.

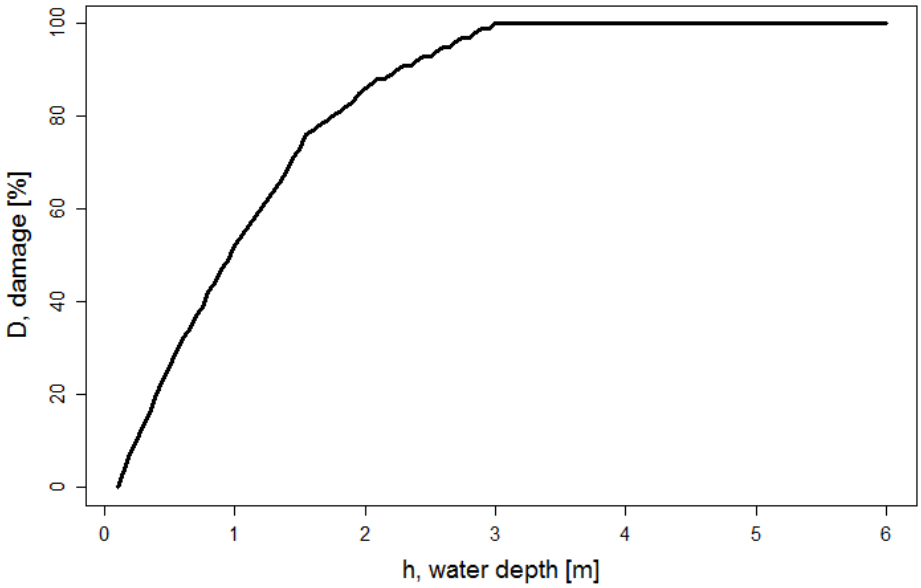

Figure 4.3: Depth-Damage curve adopted for urban areas and provided by MCM (Penning-Rowsell et al., 2005, 2010).

Combining the MCM damage curve and the overall economic value of residential buildings, we computed the expected damage in a given C-Buffer compartment for a given inundation scenario through a procedure that is schematically illustrated in Fig. 4.4.

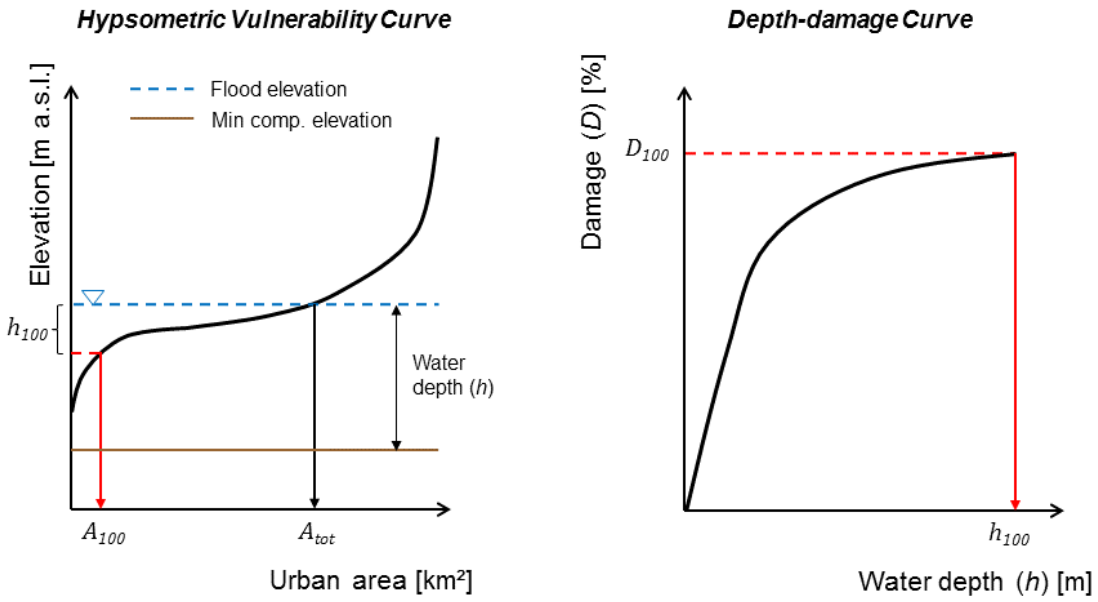

Figure 4.4: Schematic representation of the combination of a Hypsometric (left panel) and a depth-damage (right panel) curve for estimating flood damages in urban areas.

The horizontal blue line of Fig. 4.4 (left panel) represents the maximum water level [m a.s.l.] resulting from the quasi-2D simulation of the inundation scenario of interest (see also Sec. 4.6.1). As explained in Sec. 4.5.1, the extent of the inundated urban area (A_{tot}) can be easily retrieved from the intersection between the elevation of the maximum water level (blue line in Fig. 4.4, left panel) and the HVC of the flooded compartment. The damage (D) to urban settlements is associated with the local water depth (h) by means of the depth-damage curve (see Fig. 4.4, right panel for a schematic example). This curve also identifies water-depth value (h_{100}) associated with 100% of damage, meaning that, for buildings hit by water depths equal or higher than h_{100}, the flood loss coincides with the entire value of the buildings. Based on this hypothesis, one can estimate the extent of urban area where the damage is maximum (A_{100} [km^2] in Fig. 4.4, left panel) by subtracting h_{100} (i.e. water depth equal to 3 m for the MCM depth-damage curve; see Fig. 4.3) to the maximum flood elevation (blue

line in Fig. 4.4, left panel). Everywhere in A_{100} the water depth is higher than h_{100} and therefore the flood damage can be estimated as:

$$D_{100} = E \cdot A_{100} \tag{4.6.1}$$

where E [€/m^2] indicates the overall average economic value of residential buildings in the compartment (see Table 4.1).

In the remaining portion of the inundated urban area (A_{tot} - A_{100} in Fig. 4.4, left panel) the flood damage, D_h, depends on the local water depth and can be expressed as:

$$D_h = \int_{A_{100}}^{A_{tot}} E \cdot d[h(A)]dA \tag{4.6.2}$$

where the percentage of losses *d[·]* is a function of *h(A)* through the depth-damage curve (see Fig. 4.3).

According to Eq. 4.6.1 and 4.6.2, we calculated the total direct damage in the compartment, D, as:

$$D = D_{100} + D_h \tag{4.6.3}$$

It is worth noting that the damage estimate provided by Eq. 4.6.3 could be easily extended to other buildings typologies or land-uses by considering a better knowledge of these assets within a given compartment and their economic values, that is resorting to a set of different hypsometric and depth-damage curves, possibly differentiated within the same compartment.

4.7 Results and discussion

4.7.1 Results for land-use dynamics evolution

Table 4.2 summarizes the main results of the *T_r500* inundation scenario, listing the C-Buffer compartments that were flooded due to the overtopping of the levee crests and consequent levee breaching (see Sec. 4.6.1 and Castellarin et al., 2011b, *BREACHBL* scenario, for details). For each flooded compartment, the first columns

of Table 4.2 report maximum water depth, maximum water inundation level and total overflow volume simulated by the quasi-2D model (see also Fig. 4.4, left panel, for a schematic representation of these terms). Table 4.2 also reports the estimate of the overall extent of urban areas flooded in 1954 and 2008 (last two columns) under the inundation scenario *T_r500*, which were obtained by combining maximum water inundation levels computed in Castellarin et al. (2011b) with the HVCs proposed in this study (A_{tot} in Fig. 4.4).

Table 4.2: Flood inundation of C-Buffer area for the *T_r500* event. Inundation characteristics simulated by the quasi-2D model in each flooded compartments (see also Fig. 4.4).

Compartment	**Max. water depth [m]**	**Max. water level [m a.s.l.]**	**Volume [10^6 m^3]**	**Flooded urban area 1954 [ha]**	**Flooded urban area 2008 [ha]**
1	5.3	58.9	4.58	2.62	3.89
2	10.5	60.7	1.89	15.49	21.74
3	8.8	62.1	135.84	53.12	90.80
6	6.9	55.7	61.19	22.19	31.61
8	8.4	51.3	143.68	112.84	227.04
10	7.1	44.6	81.08	101.88	143.78
18	6.0	29.2	27.29	43.56	92.11
20	5.6	31.5	207.14	144.25	453.23
8 Compartments	-	-	**∼663**	**∼496**	∼1064

Inundation occurred in 8 compartments as a consequence of just the same number of levee breaches; estimates of the overall urban extent affected by the inundation scenario were equal to 1064 ha in 2008 and 496 ha in 1954.

According to Eq. 4.6.1, 4.6.2 and 4.6.3 and the MCM depth-damage curve (see Fig. 4.3 and 4.4), Fig. 4.5 illustrates the overall losses, D [billion €], estimated for the flooded compartments by referring to the average economic value of urban buildings E [€/m^2] reported in Table 4.1.

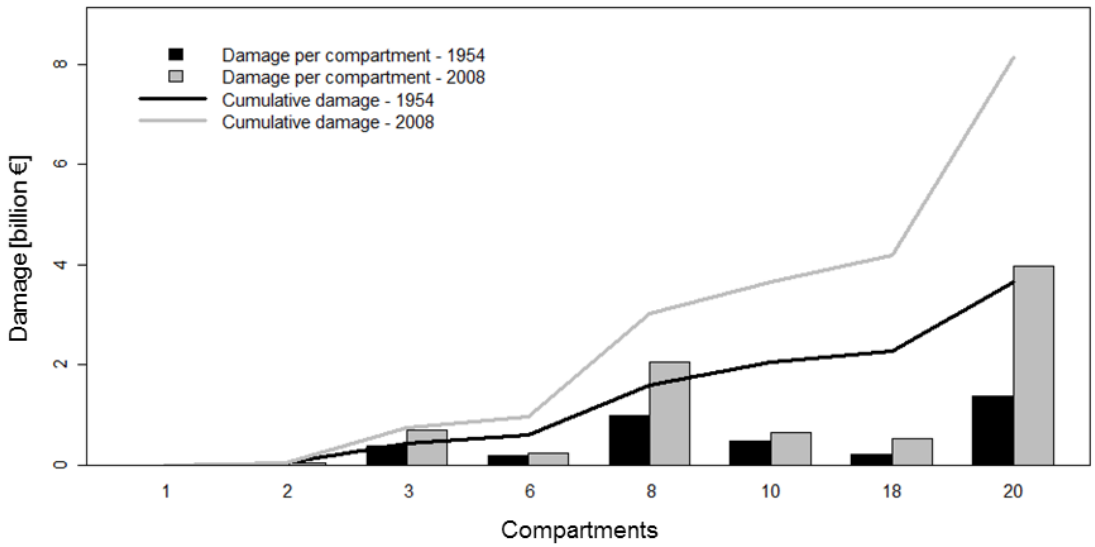

Figure 4.5: Bars indicate the expected economic losses in billions € (left axis) for the C-Buffer zone compartments and the $T_r 500$ event with urban extent of 1954 (black) or 2008 (grey); solid lines (right axis) report the cumulative economic losses from the first to the last flooded compartment for 1954 (black) and 2008 (grey).

In particular, considering the urban extent mapped for 1954 and the related HVCs, the overall damage associated with urban buildings was equal to ∼3.6 billions €, with around 65% of the total losses concentrated in the compartments number 8 and 20 (see Fig. 4.1 and 4.5). As a consequence of the urban expansion, the losses estimated for the 2008 urban extent rose to ∼8.1 billions €, more than twice the 1954 damages. Compartments 8 and 20 were responsible for ∼74% of the total damage in 2008. The higher damage in these compartments can be justified by considering the high economic value of urban settlements (compartments 20 and 8 have the highest and the fourth-highest economic values among those provided by AE for the residential buildings, respectively; see Table 4.1) and the amount of urbanized areas exposed to flood. In fact, looking at Table 4.2, the flooded urban areas of these compartments are larger than the others for both reference years (1954 and 2008), thus resulting in high damages. Furthermore, the striking flood risk evolution observed in these compartments in the period 1954-2008 (see Fig. 4.5) can also be explained by considering the spatial evolution of the urban areas, that is the location where this urban extension predominately occurred. As an example, Fig. 4.6 reports the HVCs for urban areas of compartments 8 and 10 in 1954 and 2008, while

the blue dashed lines in both panels represent the maximum inundation levels obtained from the quasi-2D model (see also Fig. 4.4, left panel).

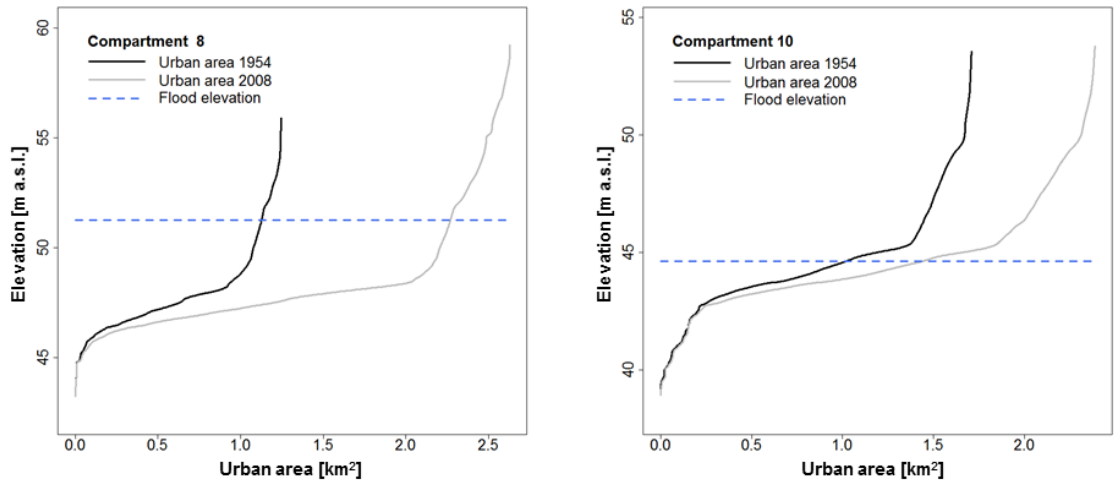

Figure 4.6: Hypsometric Vulnerability Curve (HVC) expressed in terms of total urban area extent [km^2] for Compartment 8 (left panel) and 10 (right panel) in 1954 (black line) and 2008 (grey line) with the maximum inundation level for the $Tr500$ event (blued dashed line).

The comparison of those HVCs highlighted that the urban expansion within the compartment 8 mainly occurred in the most depressed portion of the compartment, thus exacerbating the flood exposure of urban settlements (a similar land-use evolution characterized the compartment 20). On the contrary, referring to the compartment 10, the urban development occurred in the most elevated portion of the compartment (i.e. mainly above 45 m a.s.l.; see Fig. 4.6) with the consequence that the flood exposure did not increase significantly during the reference period.

The analysis of these different dynamics clearly emphasized the importance of the correct land-use planning for flood risk mitigation and highlights the suitability of HVCs as a tool for the identification of alternative risk attenuation strategies (see Sec. 4.8 for a more comprehensive discussion).

4.7.2 Results for population dynamics evolution

Left panel of Fig. 4.7 illustrates the temporal dynamics of the number of inhabitants of Emilia-Romagna and Lombardy administrative districts (grey line), where the C-Buffer is located (see Fig. 4.1), showing a nearly constant grow rate from 1861 to 2011.

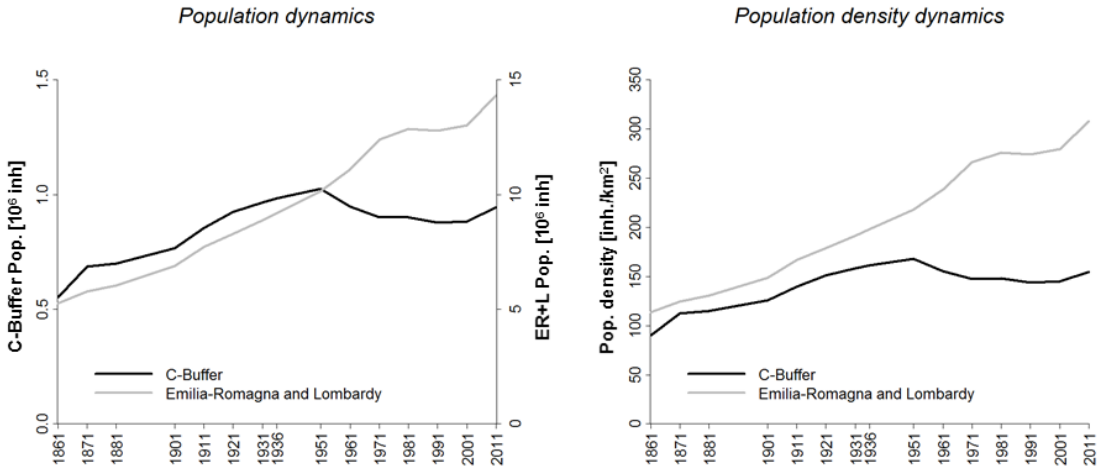

Figure 4.7: Demographic dynamics in the main administrative districts of the Po basin (Emilia-Romagna and Lombardy, see Fig. 4.1, grey line right axis) and in the C-Buffer zone (black line, left axis) in terms of number of inhabitants (left panel) and population density (right panel).

Focusing on the C-Buffer, the black line on Fig. 4.7, left panel, highlights a different evolution, with a negative population trend that started during 1950s and lasted since 2001. A similar pattern can be seen looking at the right panel of Fig. 4.7, which compares the population density in the C-Buffer and in Emilia-Romagna and Lombardy.

Figure 4.8 reports the estimated number of people living in the C-Buffer that are potentially affected by the $T_r 500$ inundation scenario. These values were estimated by combining the maximum water level simulated for one of the 8 flooded compartments with its corresponding HIC (see Sec. 4.5.2). Black and grey bars in Fig. 4.8 represent the simulated number of people affected by the inundation scenario in 1954 and 2008, respectively.

As shown in the figure, the number of inhabitants exposed to flood in 2008 (grey bars) is lower than the one estimated for 1954 for all compartments but 20, where the increase in the number of inhabitants is mainly due to the presence of Parma, which is a rather large city. The cumulated number of potentially affected people that can be computed moving downstream along the study reach (i.e. going from Compartment 1 to 20) is illustrated as a black line for 1954 and grey line for 2008, scoring ∼30 400 people in 1954 and ∼29 400 people in 2008.

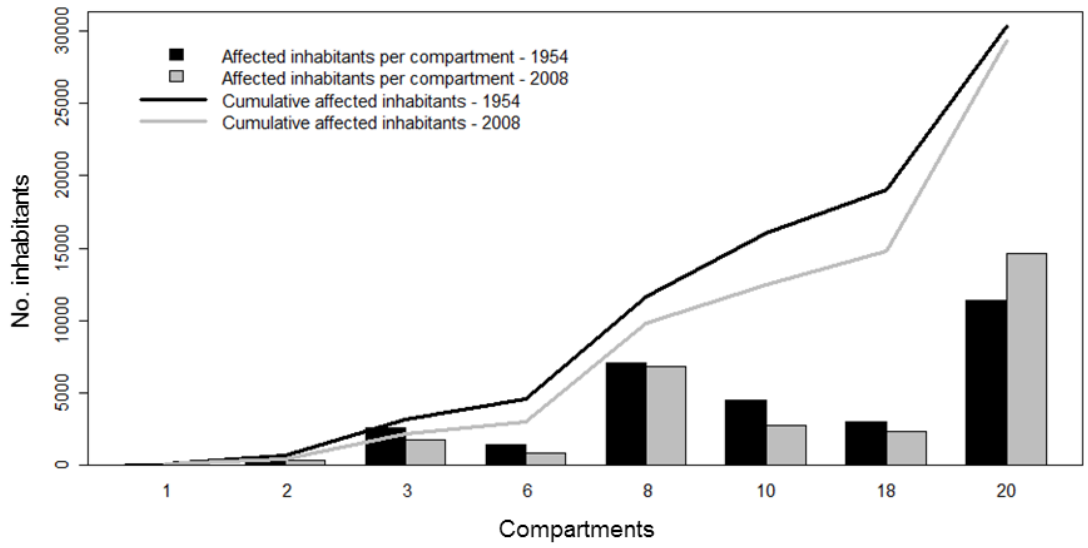

Figure 4.8: Estimated number of inhabitants that are potentially affected by the $T_r 500$ inundation scenario for each flooded C-Buffer compartment (bars) and cumulated moving downstream (lines) considering the population living in the flood-prone area in 1954 (black) and 2008 (grey).

We show that coupling HVCs with inundation scenarios simulated by means of a simplified hydraulic model (e.g. quasi-2D) may represent a suitable and effective tool for the approximated quantitative assessment of direct damages to residential settlements over large geographical areas. Generalized expansion of urban areas notwithstanding, the number of exposed inhabitants decreased in all C-Buffer compartments but No. 8 and 20, where it remained the same (compartment 8) or increased (compartment 20) during the study period (see Fig. 4.8). This result might be a consequence of inaccuracies of land-use maps adopted in this analysis, but it also might be representative of an inefficient land planning and utilization (see e.g. Bhatta et al., 2010). The consequences of this phenomenon, usually known as *urban sprawl*, can be seen through changes in land-use and land-cover of a specific region, increasing the built-up and paved area (Sudhira and Ramachandra, 2007), without a corresponding increase of inhabitants (see also Fig. 4.7). In fact, the birth and growth of residential settlements in rural areas is a common phenomenon in Northern Italy, even though the expansion of metropolitan areas is definitely more evident (ISTAT, 2009; Settis, 2012). ISTAT (2009) found that the urban areas mapped during the 2001 census covered nearly the 6.4% of the Italian territory with

an increase of about 15% compared to 1991, whereas, in the same period, the population grew only by 0.4%. Differently from metropolitans area characterized by high population density, rural areas in the North-Eastern part of the country (i.e. Lombardy, Veneto and Romagna) experienced an unbridled soils consumption due to a low density urban development (*urban sprawl*; ISTAT, 2009). These new settlements represent, in some cases, the outcomes of inefficient and speculative urban, and industrial in some cases, expansion plans, which did not result in economic (i.e. well-being) and social developments (see Settis, 2012). As a consequence, the extent of residential areas reported in land-use maps are not always representative of a higher number of inhabitants.

4.7.3 Discussion on the validity of the simplified approach

As inundation processes on floodplains have a markedly 2D nature, another approach that is traditionally used for flood risk assessment resorts to the application of 2D models for a quantification of hydraulic hazards. Based on topographic information, boundary and initial conditions and different mathematical and numerical schemes, 2D models reproduce the inundation processes, simulating various flood intensity indicators such as water depth, flow velocity and dynamics of the flooding front. The output of such models for reference inundation scenarios or sequences of hydraulic loads that are stochastically generated within a Monte Carlo framework (see e.g. Vorogushyn et al., 2010) are then used to assess the expected amount of economic damages in the study area, in combination with the wide set of literature depth-damage curves, in which the loss percentage of a specific asset is mainly related to the water depth or takes into account more damage influencing variables.

Although these models are not necessarily slower in terms of computation time than simpler models, their implementation requires difficult numerical solutions and time consuming pre-processing steps (Falter et al., 2013, and references therein). At large scale, this complexity is not always compensated in terms of accuracy, when compared to less complex schemes considering inundation extent and risk estimates (see e.g. Castellarin et al., 2011b, and references therein). Nevertheless, thanks to the high reliability of state-of-the-art fully-2D hydraulic models, they are useful in order to validate new approaches like the one we developed and described above.

Traditional flood risk assessment: application for two different fully-2D models

Among several existing numerical modelling systems, in this study we considered the inundation scenarios simulated by two fully-2D hydrodynamic models: the well known Telemac-2D and Hec-Ras 5.0, a new version of the Hec-Ras quasi-2D model, extended to the 2D simulations. Both models are briefly described in Sec. 1.3. Telemac-2D, thanks to its diffusion, was considered in this part of the study as a reference scenario, testing the performance of the new version of Hec-Ras software. According to the inundation scenario, eight compartments were flooded due to eight different breaches in the main embankments system (see Sec. 4.6.1). In order to validate the simplified approach we developed, we chose to focus on the four most representative compartments, from a the morphological and residential viewpoint, out of eight flooded compartments.

Considering a constant Gauckler-Strickler's roughness coefficient of 25 $m^{1/3}/s$ (calculated as the weighted average of the roughness coefficients associated with the CORINE land use classes in the compartments; see Domeneghetti et al., 2013; Vorogushyn, 2008), the topographic information available for each compartment and the outcomes of the reference scenario (i.e. overflowing flowrates, the width and position of the breaches simulated with the quasi-2D model) as boundary conditions, we reproduced the detailed inundation processes with the 2D models (i.e. Telemac-2D and Hec-Ras 5.0). For each model and each compartment, similar to the procedure adopted in the previous sections, we firstly analysed the results in terms of evolution of the flooded urban areas extent in 1954 and 2008 and, secondly, we compared the inundation extents simulated by Telemac-2D in both years with the corresponding extents retrieved from Hec-Ras 5.0. We quantified the agreement between total flooded areas, flooded urban areas in 1954 and 2008, by means of the adaptation of the FAI (see Falter et al., 2013; Schumann et al., 2009, and similarly used in Sec. 3.5.2), defined as:

$$FAI = \frac{A}{A + B + C} \tag{4.7.1}$$

where A is the extent of the areas simulated as flooded by both models (blue areas in Fig. 4.9, lower panels), B is the extent of the urban area that is flooded in Hec-Ras schematisation and dry according to the Telemac-2D one (i.e. the Hec-Ras model

overestimates the flooded areas simulated by the Telemac-2D model; green areas in Fig. 4.9), while C is the opposite of B (i.e. the Hec-Ras model underestimates the flood extent simulated by the Telemac-2D model; red areas in Fig. 4.9).

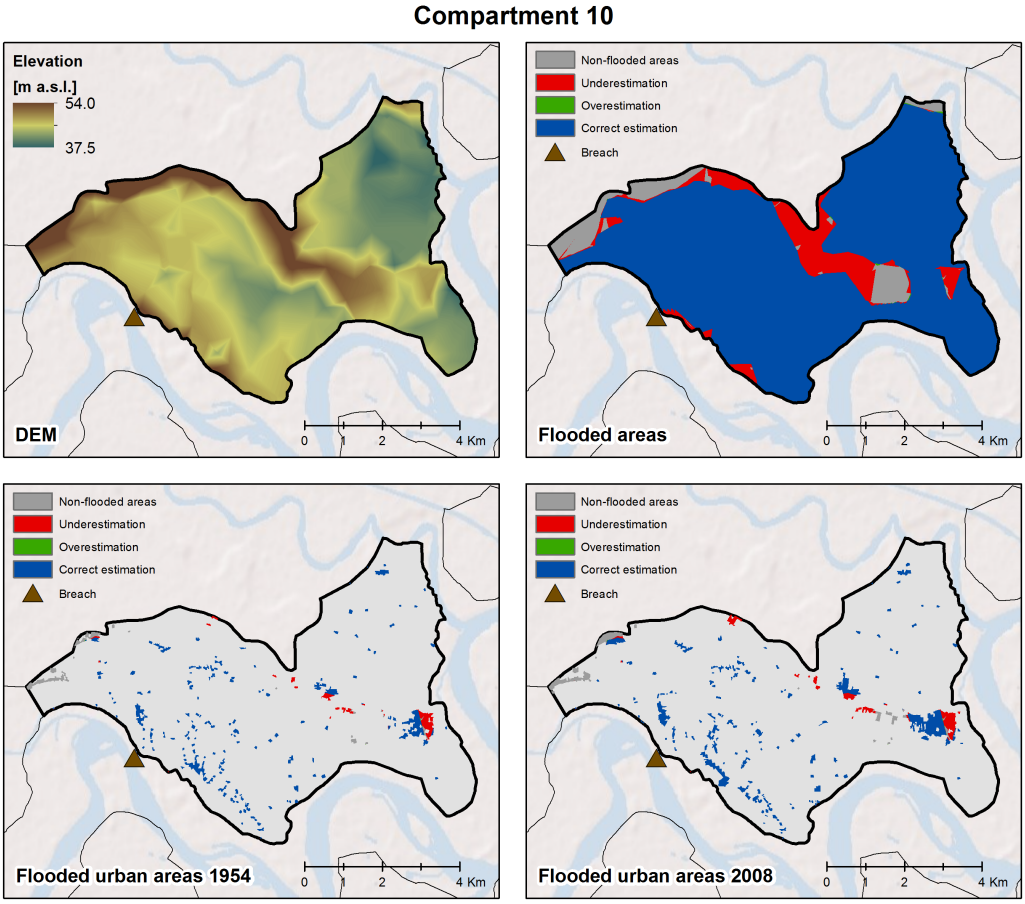

Figure 4.9: Compartment 10: DEM (top-left panel) and comparison between the Hec-Ras 5.0 and the Telemac-2D models in terms of total flooded areas (top-right panel) and flooded urban areas in 1954 and 2008 (bottom panels).

A further step was the estimation of the total direct damages in each compartment for both years by referring to a similar methodology to the one described in Sec. 4.6.2. Among the available depth-damage curves, for the sake of coherence, we referred to the one implemented in the MCM (see Fig. 4.3 at page 77), but we quantified the direct flood losses in urban areas starting from water depth directly, instead of HVCs. This means that we studied the enveloping surface of the simulated water surface elevations resulting from the fully-2D models, considering the maximum water-depth in each 100 km^2 urban area that resulted flooded (because of the 10 m horizontal resolution of

the used DEM). Figure 4.10 represents an example of this analyses showing in red the urban areas' cells in which the maximum water depth exceeds 3 m (h_{100} value, beyond which the percentage of damage is constant and equals 100%, i.e. equal to the overall economic value of the flooded buildings; see Fig. 4.3) and in blended-blue the urban areas flooded by the water depth lower than 3 m (characterized by the variable percentage of flood damage).

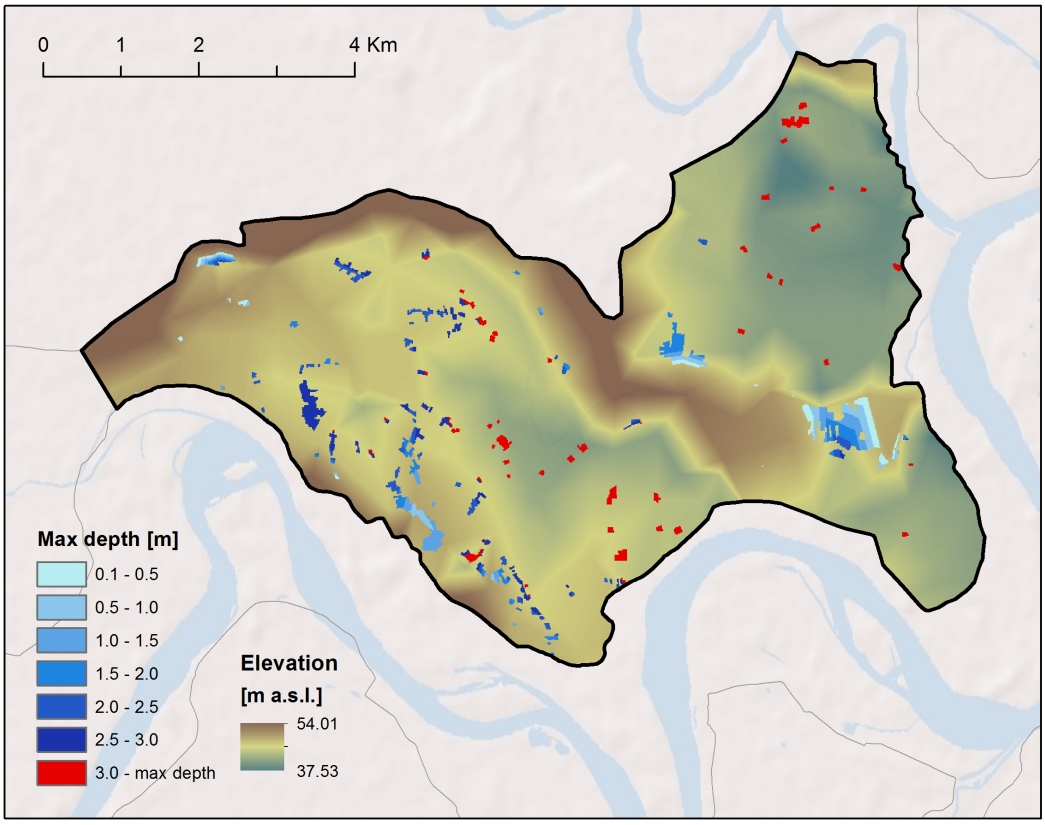

Figure 4.10: Compartment 10: schematic representation of the combination of the results in terms of maximum water depth obtained by each inundation scenario for estimating potential flood damages in urban areas.

Similarly to the methodology described in Sec. 4.6.2, constant damages in the urban zones where the inundation depth exceeds 3 m in Fig. 4.10 (A_{100}, with simulated inundation water depths higher than h_{100}, i.e. red areas), D_{100}, can be computed as:

$$D_{100} = E \cdot A_{100} \tag{4.7.2}$$

where E [€/m^2] indicates the mean economic value of residential buildings in the

compartment.

For the remaining portion of the flooded urban areas in the compartment (A_{tot} - A_{100}, represented by the blended-blue areas in Fig. 4.10) the flood damage D_h is related to the local water depth and can be calculated as:

$$D_h = \int_{A_{100}}^{A_{tot}} E \cdot d[h(A)]dA \tag{4.7.3}$$

where A_{tot} represents the total amount of flooded urban areas (sum of red and blended-blue areas in Fig. 4.10), $d[\cdot]$ the depth-damage curve as a function of the simulated water depth associated with $A \in [A_{100}, A_{tot}]$. According to Eq. 4.7.2 and Eq. 4.7.3, we calculated the total direct damage in the compartment, D, as:

$$D = D_{100} + D_h \tag{4.7.4}$$

Once the flood damages for both years was estimated, we compared the percentage difference between the total direct damages calculated with the water surface elevations resulting from the Telemac-2D model (reference model) and those resulting from the Hec-Ras 5.0 model for 1954 and 2008.

In relation to the Telemac-2D model, Table 4.3 reports the maximum water depth simulated through this fully-2D model for each flooded compartment of interest, together with the estimation of the extent of urban areas flooded in 1954 and 2008 and of the economic damages associated with the considered inundation scenario. Maximum water depth, urban areas extent and estimated damage with regard to the Hec-Ras 5.0 model are shown in Table 4.4.

Table 4.3: Flooded C-Buffer compartments according to the Telemac-2D model.

Compartment	Maximum water depth [m]	Flooded urban area 1954 [ha]	Flooded urban area 2008 [ha]	Estimated economic damages 1954 [billion €]	Estimated economic damages 2008 [billion €]
6	6.75	23.65	34.25	0.18	0.24
8	8.20	122.04	249.27	1.01	2.08
10	6.61	149.19	201.13	0.81	1.08
18	3.94	50.84	115.36	0.30	0.76
4 Compartments	**-**	**∼345**	**∼600**	**∼2.30**	**∼4.16**

Table 4.4: Flooded C-Buffer compartments according to the Hec-Ras 5.0 model.

Compartment	Maximum water depth [m]	Flooded urban area 1954 [ha]	Flooded urban area 2008 [ha]	Estimated economic damages 1954 [billion €]	Estimated economic damages 2008 [billion €]
6	6.81	21.98	30.72	0.18	0.23
8	8.38	112.19	226.40	1.00	2.04
10	6.94	120.85	165.49	0.79	1.05
18	3.94	45.43	112.08	0.31	0.74
4 Compartments	**-**	**∼300**	**∼535**	**∼2.28**	**∼4.07**

In particular, we observed that the overall urban extent affected by the inundation was equal to ∼345 ha in 1954 and ∼600 ha in 2008 with regard to the Telemac-2D model (see Table 4.3), and ∼300 ha and ∼535 ha respectively for 1954 and 2008 with reference to the Hec-Ras 5.0 model (see Table 4.4). Consequently, we calculated the overall damage associated with urban buildings equal to ∼2.30 billion € in 1954, that rose to ∼4.16 billion € in 2008 in relation to the first model (i.e. Telemac-2D; see Table 4.3), whereas the overall damage with regard to the second model (i.e. Hec-Ras 5.0; see Table 4.4) was estimated respectively for 1954 and 2008 equal to ∼2.28 billion € and ∼4.07 billion €. In both economic damage estimations we noticed that damages associated with urban buildings almost doubled during the last five decades.

Table 4.5 reports for each compartment of interest the FAI relative to the total flooded areas and to urban areas inundated in 1954 and 2008, showing also the percentage difference in terms of damage calculation for both years.

Table 4.5: Comparison between the Hec-Ras 5.0 and Telemac-2D models for the flooded compartments of interest.

Compartment	**FAI for flooded urban areas 1954** [-]	**FAI for flooded urban areas 2008** [-]	**Difference in damage calculation 1954** [%]	**Difference in damage calculation 2008** [%]
6	0.91	0.89	0.63	2.61
8	0.91	0.91	0.82	1.97
10	0.82	0.82	3.15	2.68
18	0.90	0.97	-3.42	1.95

The FAI resulted in all cases very close to 1 (i.e. almost a perfect agreement between the inundation extents provided by Hec-Ras and Telemac-2D models) for all compartments. The differences in damage calculations mirrored the results in terms of FAI, with minimum percentage difference of ∼0.6% for Compartment 6 and maximum percentage difference of ∼-3.4% for Compartment 18, both in 1954.

From the point of view of the comparison between the two fully-2D hydrodynamic models, the study showed that Hec-Ras 5.0 is able of simulating the flooded areas in the compartments of interest with a high accuracy.

As far as what the dependence of flood risk assessment on the considered fully-2D hydrodynamic model is concerned, our analysis observed that, under equal conditions, the difference in hydrodynamic scheme can affect the results only by up to 3.5% on estimate potential damages.

Quasi-2D vs. fully-2D approach

Practically, the difference between 2D models with respect to the quasi-2D models consists of the flooding dynamics of the compartments: while in a fully-2D method the inundation front represents more realistic evolution, following the elevation profile of the area combined with other information (e.g. roughness coefficients), the simulated water level in the quasi-2D model is computed as a function of the water volume exchanged with the main river and/or adjacent storage areas (i.e. the model floods at the same time all points with the same elevation, independently from their distance from the breach). In order to validate the simplified approach we proposed, in a large-scale perspective, the inundation extents simulated by Telemac-2D (considered as the reference model) was then to be compared with the corresponding extents retrieved from the quasi-2D schematization.

Firstly, we quantified the agreement between flooded urban areas in 1954 and 2008 by means of the FAI, described by the Eq. 4.7.1 in the previous section (see Sec. 4.7.3). In this case, A is the extent of the areas simulated as flooded by both fully-2D and quasi-2D models (blue areas in Fig. 4.11, lower panels), B is the extent of the urban area that is flooded in the quasi-2D schematization and dry according to the fully-2D one (i.e. the simplified model overestimates the flooded areas simulated by the fully-2D model; green areas in Fig. 4.11), while C is the opposite of B (i.e. the quasi-2D model underestimates the flood extent simulated by the fully-2D model; red areas in Fig. 4.11).

Table 4.6 reports the FAI for flooded urban areas in 1954 and 2008 and for each compartment of interest in the second and third columns, while the difference in terms of damage calculation for both years is indicated in the last two columns. The FAI value for flooded urban areas in 1954 and 2008 was very close to 1 (i.e. perfect agreement between simplified and traditional flood risk assessment) for two out of four

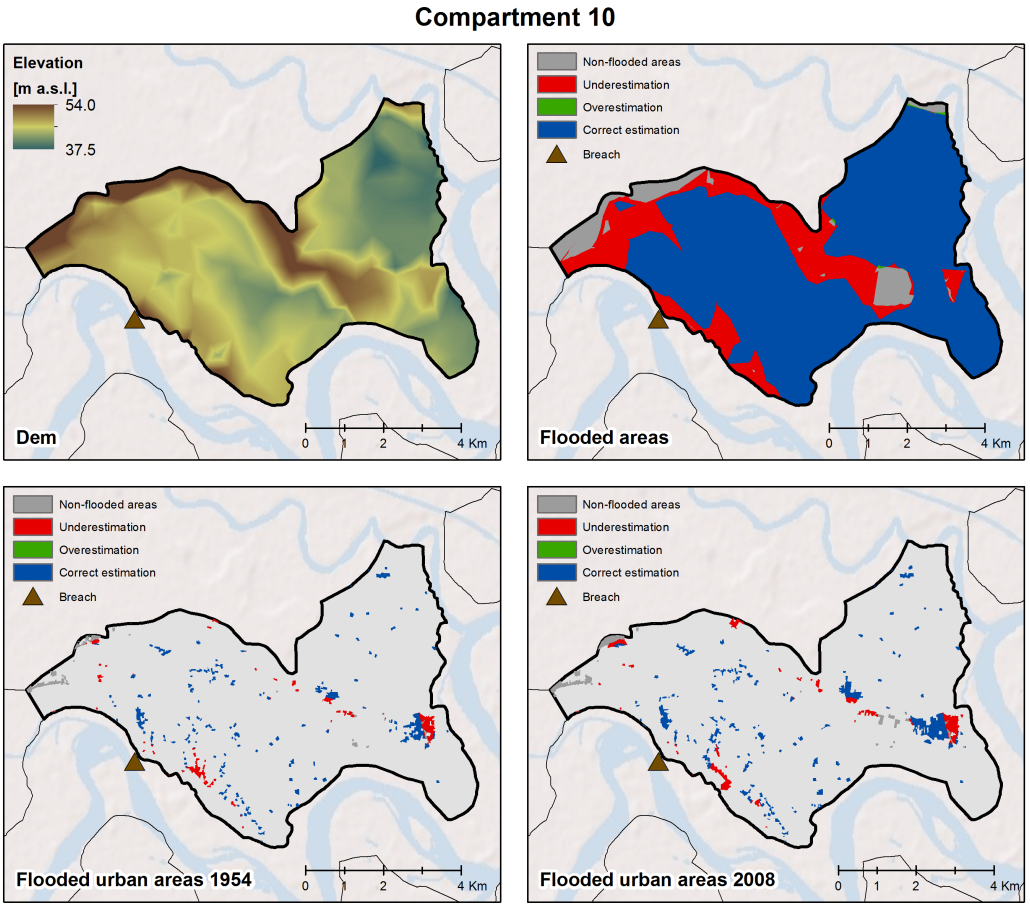

Figure 4.11: Compartment 10: DEM and comparison between the quasi-2D and the fully-2D model in terms of flooded areas (top panels) and flooded urban areas in 1954 and 2008 (bottom panels).

compartments (No. 6 and 8), whereas the agreement was poorer for the remaining two compartments (No. 10 and 18). The differences of losses estimated with the traditional and the simplified approaches followed the results in terms of FAI: both in 1954 and 2008, compartment 8 showed the minimum percentage difference (∼2%), while compartment 10 pointed out the maximum percentage difference, higher than 40% (see Fig. 4.11).

The analysis showed that the simplified approach is capable of simulating the flooded areas in the compartments of interest with a reasonable accuracy. However, in two out of four study compartments we observed a significant difference in terms of simulated flood extent and flood-related damages. Looking at Fig. 4.11, one can

Table 4.6: Comparison between the quasi-2D and fully-2D models for the flooded compartments of interest.

Compartment	FAI for flooded urban areas 1954 [-]	FAI for flooded urban areas 2008 [-]	Difference in damage calculation 1954 [%]	Difference in damage calculation 2008 [%]
6	0.91	0.89	2.90	3.44
8	0.92	0.91	2.03	2.88
10	0.70	0.71	42.92	40.47
18	0.58	0.68	33.71	32.16

observe that this inaccuracy resulted from inappropriate compartment delineation. In the specific case of compartment 10, the simplified quasi-2D model could not correctly reproduce the flooding dynamics, since the inundation developed from the lowland portion of the compartment, regardless the position of the levee breach. On the contrary, the fully-2D model ensured a correct reproduction of the flood dynamics given the topography of the study compartment. According to findings of other recent studies (see e.g. Papaioannou et al., 2016), we expect that the more precise delineation of the compartments would lead to a higher accuracy of our procedure, which can thus be considered to be a valid simplified approach to assess the flood risk and its evolution in time over large geographical areas.

4.8 Main assumptions and limitations of the proposed simplified approach for flood damages computation

Despite the potential of the methodology, there are some limitations that have to be considered given the assumptions adopted in our study, in addition to the need of a better and proper compartment delineation, highlighted in Sec. 4.7.3.

First, the spatial distribution of different building types (e.g. commercial, stores, offices, etc.) over the area of interest cannot be inferred from land use maps that are

typically adopted for large scale analysis (e.g. CORINE). The lack of accurate information concerning the location of specific building categories constrains the possibility to evaluate their exposure to floods through specific HVCs (i.e. different HVCs defined for civil or detached houses, garages or other buildings categories).

Second, the adoption of AE estimates (see Table 4.1) inevitably undervalues the overall losses for urban areas, and in particular for residential buildings, since a series of other direct (e.g. chattel, furniture, stocks, etc.) and indirect (e.g. economic losses indirectly related to the loss of private houses) costs are not considered and economically quantified. The estimates provided by AE represents the real estate market values at a given time of a given building type, that is more an expression of the overall economic well-being of a specific area rather than the actual economic loss in case of a flood event. This bias is expected to be more significant for the productive infrastructures (i.e. industries), where a number of different variables (such as for example the type of production, the technology level of the industries, the amount of stocks, the day of work interruption, etc.) strongly influence the overall damages associated with inundation events.

Finally, using an averaged economic value for all urban assets within a given compartment may introduce biases in the economic assessment of the flood impacts. The expansion and development of urban areas at higher elevations in the compartment (and thus in *safer* locations) may increase the overall economic value use of urban settlements within the compartment. Consequently, averaging the economic value over all residential areas in the compartment would increase the economic value also of rural residential areas situated in the lowland portion of the compartment, with the paradox that a correct land-use development policy may increase the risk in the flood-prone areas. This limitation can be easily overcome by constructing different HVCs for different municipalities (or economically different residential areas) within each compartment and by using them in parallel. Furthermore, when using a single HVC for all urban settlements within a given compartment, as in this study, bias can be effectively reduced by referring to a single economic value, as we did (i.e. 2014), for all considered historical land-use scenarios (i.e. 1954 and 2008 in this study). Under this hypothesis, the analysis of the urban development over the period of interest was considered exclusively in terms of elevation, that is considering in which part of the compartment the urban area expanded (i.e. in areas that are more or less prone-to-floods), without considering its

economic development during the last half century.

Despite these limitations, the proposed methodology appeared appropriate for the purpose of the analysis, that was not aimed at providing a comprehensive and exhaustive quantification of the flood risk or of the overall flood losses expected in case of an extreme flood event, but rather to propose a tool which enables the inferring of factors that mainly drove the evolution of the residual flood risk in a specific area, or for investigating alternative flood risk mitigation strategies at basin scale.

4.9 The *levee paradox* along the Po river

Following the concept of the *levee effect* (see e.g. Tobin, 1995), the feeling of safety ensured by levee systems may encourage the economic and social growth on the floodplain areas, leading to the potential condition for a faster development of human settlements (see Fig. 2.1 at page 33). However, considering our study area, we already stated that while during the last fifty years we observe an increase of the total economic losses associated with a given inundation scenario (see Fig. 4.5), the *levee effect* paradigm is not supported by the associate population dynamics. Considering Fig. 4.7, the population growth on the area closer to the river appears comparable with the one measured in the remaining part of the basin (i.e. Emilia-Romagna and Lombardy) until 1950. Starting from the 1950s, people moved from the floodplains toward the major cities and settled far away from the main river, causing a significant decrease of number of people exposed to floods. The shock induced by the flood disaster occurred in the 1951 to the floodplain socioeconomic system (see e.g. Amadio et al., 2013; Di Baldassarre et al., 2013) is clearly visible in Fig. 4.7. Together with an increased flood risk awareness resulted from the 1951 inundation event, the rapid industrial and economic growth that characterized the aftermath of the World War II is undoubtedly another important driver that attracted people from rural areas towards richer and more industrialized areas, such as large cities.

Figure 4.12 further investigates the *levee paradox* in the study area. Left panel, in particular, compares the growth rate of the urban settlements in the C-Buffer with the one observed in the Emilia-Romagna and Lombardy districts during the last half-century. Urban extent in the C-Buffer doubled in the last fifty years (increase of about 180%), while the growth rate observed in Emilia-Romagna and Lombardy districts is

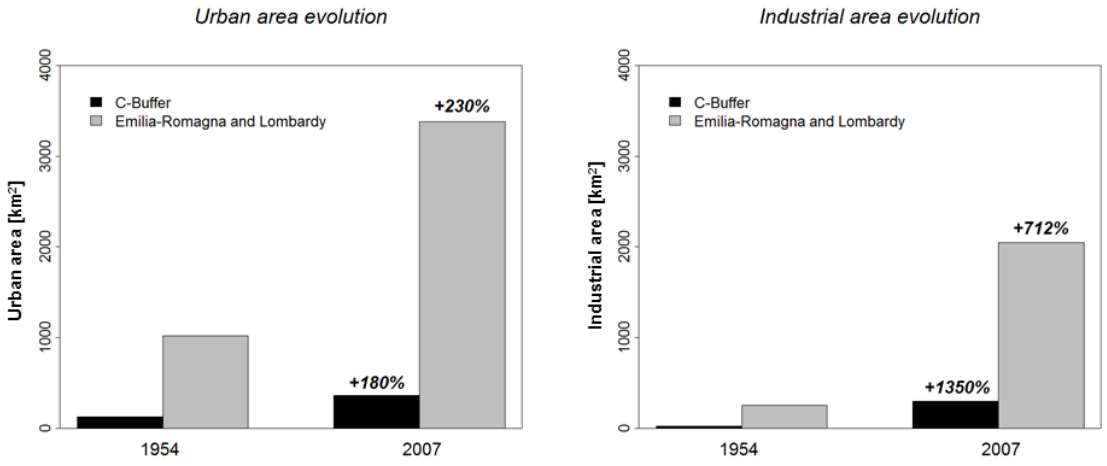

Figure 4.12: Evolution over the last half-century of the overall extent of urban (left panel) and industrial (right panel) areas in the C-Buffer (black bars) and in Emilia-Romagna plus Lombardy regions (grey bars).

higher than or equal to 230%. Even though the urban development in the flood-prone area is evident and representative of the *levee-effect*, it appears to be less pronounced than in other parts of the basin. These findings seem to support the idea that the expansion of residential areas is related mainly to social and economic drivers, than to the proximity to the water, that no longer represents a peculiarity of favourable development conditions in developed society (Di Baldassarre et al., 2013). A different behaviour could otherwise be expected considering the industrial sector, where the availability of a large amount of fresh water still represents a key element for developing productive activities. Right panel of Fig. 4.12 confirms these considerations for the study area. Referring to the results of a preliminary investigation, right panel of Fig. 4.12 compares the extent and growth rate of industries in the C-Buffer and in the Emilia-Romagna and Lombardy districts, showing an opposite trend relative to what can be observed for residential areas. Even though industrial areas grew over 712% in Emilia-Romagna and Lombardy, the industrial activities experienced a higher grow-rate (1350%) in the areas closer to the river (i.e. C-Buffer). The presence of a levee system, together with the proximity to abundance of fresh water, is evidently an incentive to the development of industries, which is also encouraged by the lower costs of formerly rural areas. The dynamic of the industrial asset strongly impacts the evolution of the residual flood risk and will be the objective of specific future analyses.

4.10 Concluding remarks

Our study considered the middle-lower portion of the Po river and analysed the evolution of the residual flood risk during the last half century for residential areas in the Pianura Padana, large and socio-economically very important dyke-protected flood-prone area located in the Northern Italy, by investigating changes in flood frequency (i.e. flood hazard) and exposure to floods.

Consistently with previous investigations performed for the Po river (see e.g. Montanari, 2012; Zanchettini et al., 2008), the results of trend detection analyses performed by Domeneghetti et al. (2015) along the study reach pointed out the absence of statistically significant temporal trends, aside from a slight increase of the annual variability of daily streamflows recorded at the Pontelagoscuro. Therefore the flood hazard evolution along the middle and lower portion of Po river in the last five decades did not seem to play any significant role on the flood risk dynamics over the same time span. Changes in the residual flood risk, if any, could be mainly ascribed to the evolution of the exposure to floods (see e.g. previous studies sustaining this findings, as De Moel et al., 2011): this consideration supported our assessment of residual flood risk changes on the basis of a 500 year inundation scenario identified referring to streamflow data collected along the study reach (see Castellarin et al., 2011a), which we considered for representing the residual flood hazard for the study area (i.e. the C-Buffer, or dyke-protected flood prone area along the middle lower portion of the Po river).

We analysed the possible alteration of exposure to floods in the study area, looking in particular at the number of inhabitants and extension of residential areas. We proposed the use of simplified graphical tools (i.e. HVCs and HICs) for a quantitative, yet approximate, large-scale assessment of the direct tangible economic losses to private residential buildings and of the number of people affected by a given inundation scenario. HVCs and HICs can be constructed using a minimal set of information (i.e. a digital elevation model, land-use map, census data) for any given flood-prone compartment represented in a quasi two-dimensional numerical schematization as a storage area. Despite the usefulness and ease of the proposed methodology it is worth noting that its application in our study relies on a number of simplifying assumptions that need to be acknowledged in order not to misinterpret the results (see also Sec. 4.6.2):

- the flood hazard assessment was performed by means of a simplified quasi-2D

model (see Castellarin et al., 2011b) in which the flood-prone compartments are reproduced as storage areas regulated by means of volume-water level defined on a DEM with the resolution of 10 m (see Sec. 4.6.1); however, supporting previous assumption and findings by Falter et al. (2013) and references therein, the validation of our simplified methodology showed that less complex approaches like the use of a quasi-2D model are often sufficient to provide satisfying results in terms of accuracy, when compared to more complex simulations);

- aggregation classes adopted by land-use maps do not enable the identification of specific building typology, such as for example detached house, garages, office, stores, etc.; as a result, the economic estimates consider a single (average) building typology for each compartment;
- the economic estimates provided by AE represent the market value of the urban buildings in a given municipality and are not representative of the actual potential damages expected in case of inundations (e.g. damages to inventory are not considered);
- the population density adopted for the HICs was assumed to be uniform within a given municipality neglecting differences between rural and central urban areas.

These limitations notwithstanding, our preliminary application demonstrated the efficiency of HVCs and HICs and their potential for flood vulnerability and flood risk assessment. The accuracy of the proposed methodology can be easily increased by referring to more accurate data (e.g. finer land-use discretization, advanced economic estimate; etc.), different HVCs defined for each municipality or land use type, or to detailed simulation of the inundation characteristics (e.g. flood dynamics simulated by means of 2D hydraulic models).

The analysis pointed out a significant growth of the extension of residential areas over the study region, with a consequent increase in the expected damage that is almost doubled relatively to the considered inundation scenario (recurrence interval $\sim$500 years). On the contrary, the number of exposed inhabitants showed only marginal modifications during the study period. These findings offer important elements to further the discussion on the existence and importance of the *levee effect* (or *call-effect*, Tobin, 1995) along the middle-lower portion of the Po river. The study outcome also fosters some general considerations on the arguable applicability

of the *call-effect* for developed and technologically advanced countries, where the physical proximity to fresh water may not represent the predominant factor of the development of residential settlements (Di Baldassarre et al., 2013). Despite our study focused on the development of urban settlements only, different evidences seem to arise from preliminary analysis performed relatively to the industrial asset. In fact, we have noticed in the C-Buffer a greater industrial growth rate than the one occurred in the rest of Emilia-Romagna and Lombardy districts. However, further investigations are needed to address this specific point for getting a more definite answer concerning the existence and entity of a call-effect related to industrial activities in the study area during the last fifty years. Further analyses are also required to enable the assessment of flood losses that are potentially expected in commercial and industrial areas, for which the economic values provided by the AE appear far from being useful as indicators of the expected losses (see also Sec. 4.6.2).

Over the past two decades the flood risk management experienced a shift from a hazard-driven view to a risk-based perspective, in which the risk management policies are increasingly identified and evaluated in the light of system susceptibility and resilience, thus focusing on the capacity of the system to coexist with, and recover from, inundations (see e.g. Merz et al., 2010a). The FD 2007/60/EC further promotes this process requiring the MS to identify flood risk mitigation plans in order to reduce the adverse consequences (e.g. number of people affected, damages, etc.) of a given inundation event. In this context, keeping in mind all the assumptions that were previously highlighted, the combination of HVCs (and HICs) with inundation scenarios computed through simplified hydraulic models can be a viable strategy for quantitative large-scale assessments of the residual flood risk. The proposed methodology may be useful for decision-makers in charge of the definition of large scale flood risk mitigation strategies, as the resort to HVCs can provide stakeholders with a preliminary estimation of the impact of a given inundation event and enables them to easily compare the effectiveness of alternative flood risk mitigation strategies (e.g. controlled flooding vs. strengthening of the existing levee system, see e.g. Castellarin et al., 2011a; Merz et al., 2010a; Vis et al., 2003).

Chapter 5

Flood losses estimation with uni- and multi-variate models (case study 3: the Secchia River flood-prone area, Italy)

5.1 Introduction

The third considered case study focused on a real inundation event occurred in Italy in January 2014 and caused by a breach in the right embankment of the Secchia river during an intense flood event. The overflowing volume was estimated to be between $36.3 \cdot 10^6$ and $38.7 \cdot 10^6$ m^3, flooding an area of about 52 km^2 (see Fig. 5.1). The total estimated flooding damage was about 500 million € (about 16 million € considering only residential properties). The aim of this study was to assess the importance of vulnerability as one component of flood risk, based on a large database of observed losses. We defined empirical uni- and multi-variate damage models and tested their efficiency relatively to the performance of some literature damage functions in estimating real estate and movable properties losses.

Figure 5.1: Inundation event of January 2014: pictures of the flooded municipalities of Modena, Bastiglia and Bomporto (sources: *www.youreporter.it*; *www.gazzettadimodena.gelocal.it*; *www.sulpanaro.net*; *www.modena24.net*; *www.meteoweb.eu*).

5.2 Study area and flood event

The right levee collapse occurred on 19^{th} January 2014 in San Matteo, in the Northern part of the Modena municipality (see yellow dot in Fig. 5.2), and let the flood to inundate the neighbouring municipalities of Bastiglia, Bomporto and Modena (green, red and blue polygons in Fig. 5.2, respectively) in less than 30 hours. Towns and surrounding countryside remained flooded for more than 48 hours, until a water volume in excess of 20 million cubic metres was finally pumped out of the inundated area.

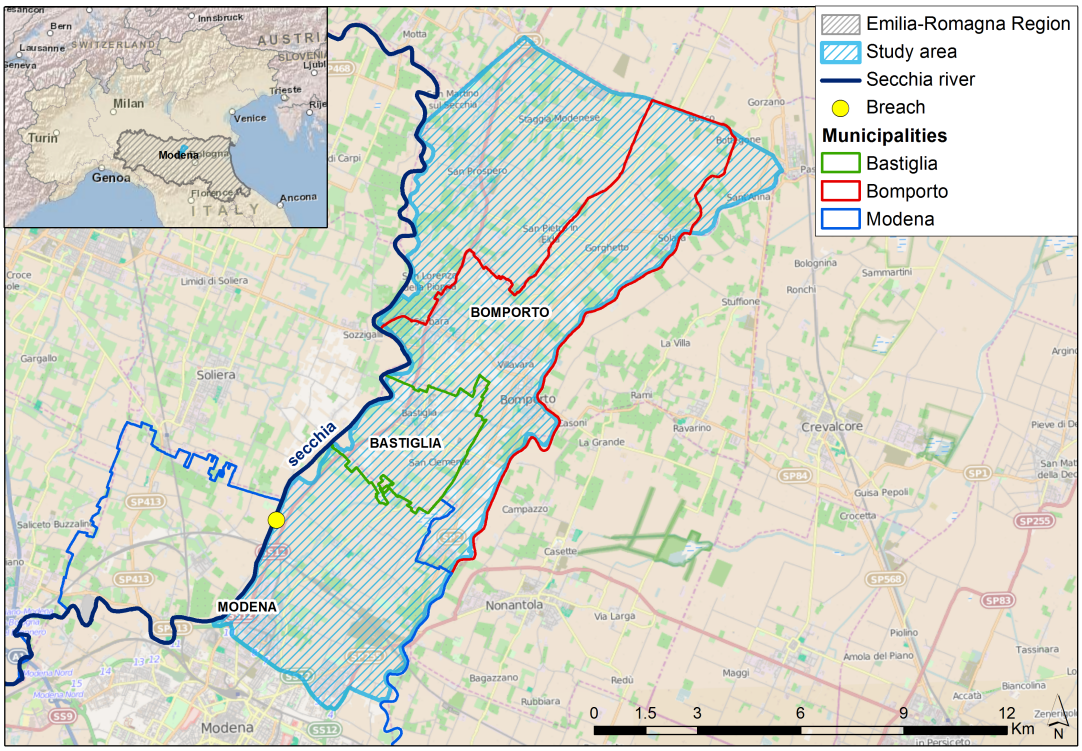

Figure 5.2: Study area: Secchia river with breach point (yellow dot) and municipalities of interest (Bastiglia, Bomporto and Modena).

The study area of this analysis includes the entire towns of Bomporto and Bastiglia and the Northern part of the Municipality of Modena. It is located on the downriver right side and extends for approximately 112 km^2. The only remarkable relieves consist of roads or railways embankments and minor river levees. The small main slope is oriented in a North-Eastern direction: it decreases from the maximum elevation (30 m a.s.l.) in the Southern territories to the minimum elevation (18 m a.s.l.) about 20

km Northwards.

The determination of the study area boundaries was due in particular to different topographic features. Figure 5.2 shows that the Secchia river represents the Western boundary, while the Eastern boundary consists of the Panaro river in its left embankment and flows to the North-East, almost parallel to the Secchia river. The Northern boundary is represented by roads embankments and drainage channels, which turned out to be especially important in the delimitation of the liquid front, preventing urban areas further North from being flooded (this fact confirmed the findings of Ch. 3, showing the role of road and railways embankment and channels in influencing the flooding dynamics).

The breach (see Fig. 5.3) occurred in the 2.5 km-long artificial straightening of the river, indicating a pronounced human intervention that has significantly impacted the morphological evolution of the study stretch between the city of Modena and the town of Bastiglia.

The breach was first detected at 6:30 a.m. (Orlandini et al., 2015). A trapezoidal part of the embankment, with a base width of about 10 m, was removed and the embankment's top elevation became immediately 1 m lower than the river water surface. The breach reached maximum bottom width of about 80 m and the embankment's top elevation became equal to the ground level within 9 hours (3:00 p.m. of 19^{th} January 2014). Given the advanced state of the development of the breach when it was first discovered, no repair of the breached levee was attempted.

Figure 5.3: Pictures of the breaching point on the right embankment of the Secchia river (sources: *www.emiliaromagnameteo.com*; *www.nimbus.it*).

In order to identify causes and consequences of the Secchia river flood event, the committee of scientists designed by the Italian Civil Protection Agency collected all

available information, field surveys, statistical analyses and numerical models outcomes to reconstruct the event (see D'Alpaos et al., 2014; DICAM-PCREM, 2015). In situ measures and lab works were performed to identify the terrain properties of the levee and its foundation. Analyses of water depth and embankment's top elevation at the breaching moment enabled the Scientific Committee to exclude the possibility that the levee breach occurred due to the overtopping of the embankment. According to the scientific committee, the levee breach, suddenly lowering of the embankment crest and subsequently overflowing water from the river at high velocity, can be explained by two different circumstances, which could also have happened in combination:

- progressive internal erosion due to the presence of animal burrows inside the embankment, characterized by very wet conditions due to antecedent intense rainfall events;
- progressive geomechanical instability of the embankment, locally undermined by the presence of burrows and favoured by the partial saturation induced by the flood and direct precipitations on the ground.

Both circumstances, considering modelling uncertainties, showed a satisfying consistency between obtained results and available observations. They were also supported by the study of Orlandini et al. (2015). They observed the early stage of a levee failure along the Panaro river under similar hydroclimatic conditions during the afternoon of the same day, with a failure mechanism that can realistically assumed to be similar to the one occurred along the Secchia river and then performed a detailed numerical modelling of rainfall, river flow, and variably saturated flow occurring in disturbed levees in response to complex hydroclimatic forcing. Outcomes of these analyses confirmed that the Secchia levee breach may have been triggered either by direct river inflow into the den system or by the collapse of a hypothetical den, which was separated by a 1 m earthen wall from the levee riverside and saturated during the hydroclimatic event.

Figure 5.4 represents three different hydrographs. The blue one describes the discharge in a river cross-section upstream of the breach and the black one represents the streamflow downstream the breach. The red curve shows the water outflowing from the breach during the flood. Considering the levee breach upstream and downstream hydrographs, it was possible to identify the overflow volume from the breach, which was estimated between $36.3 \cdot 10^6$ and $38.7 \cdot 10^6$ m^3.

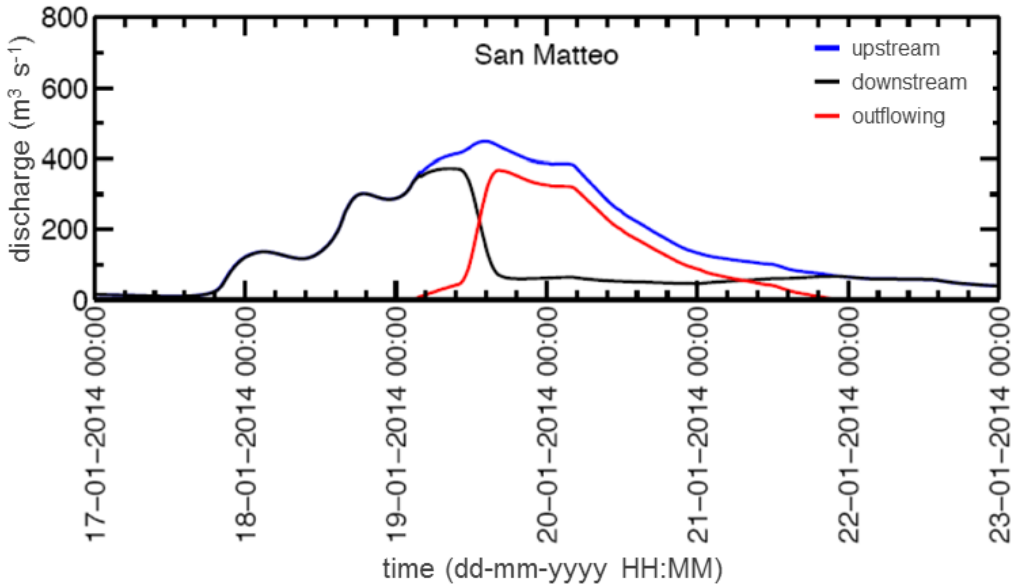

Figure 5.4: Hydrographs describing the water flow in the upstream and downstream the breach and at the breach point, in different days (D'Alpaos et al., 2014; DICAM-PCREM, 2015).

Thanks to several eyewitness accounts, video footage and studies conducted by the scientific committee (D'Alpaos et al., 2014; DICAM-PCREM, 2015), it was possible to identify the flood event propagation dynamics, shown in Fig. 5.5. This data was used, together with local testimonies, pictures and videos of the flooded municipalities, to reconstruct the event by means of a fully-2D hydrodynamic model (see Sec. 5.3).

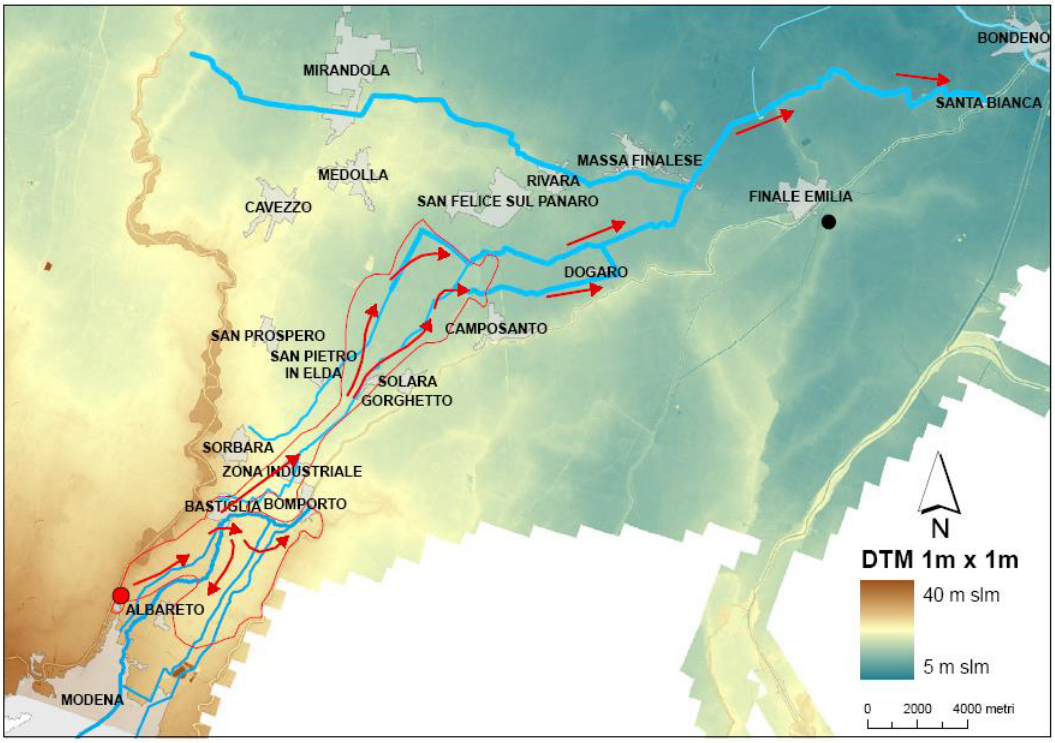

Figure 5.5: Flooding wave propagation (D'Alpaos et al., 2014).

5.3 Reconstruction of the inundation event

The reconstruction of the flood event was performed by means of a 2D finite element numerical model, Telemac-2D, briefly described in Sec. 1.3 and already used in Ch. 3 and 4 because of its high reliability and diffusion in the scientific field for the simulation of flooding scenarios (Galland et al., 1991; Hervouet and Bates, 2000).

As noted during the flooding phase, and confirmed later by the scientific committee (D'Alpaos et al., 2014), the progress dynamics of the liquid front in the study area were strongly influenced by the presence of topographic singularity (e.g. road embankments, land reclamation channels, etc.). For this reason, with the aim to implement a realistic reproduction of the events, a detailed LiDAR with spatial resolution of 1 m was used to identify each discontinuity elements on the flat plain (e.g. embankment, roads, etc.), as well as drainage canals or natural waterways that, in the presence or absence of banks, could intercept the flooding water. In order to reproduce the plain elevation and the discontinuities in the model, an unstructured triangular finite element mesh of the study area was generated. The mesh is composed of 34 082 nodes connecting 66 596 elements with variable size from 1 to 200 m in the flat zones, covering the total

112 km^2 area. This accurate mesh ensures that the slope breaks at these locations are captured. The channels of the drainage system where the mesh was refined were chosen based on their depth. Only channels with a minimal depth of 0.5 m were considered (see Maatar, 2015). Figure 5.6 represents the unstructured mesh implemented in the model. The two small panels show zooms to special topographic elements such as roads and minor rivers, covered by a more accurate mesh.

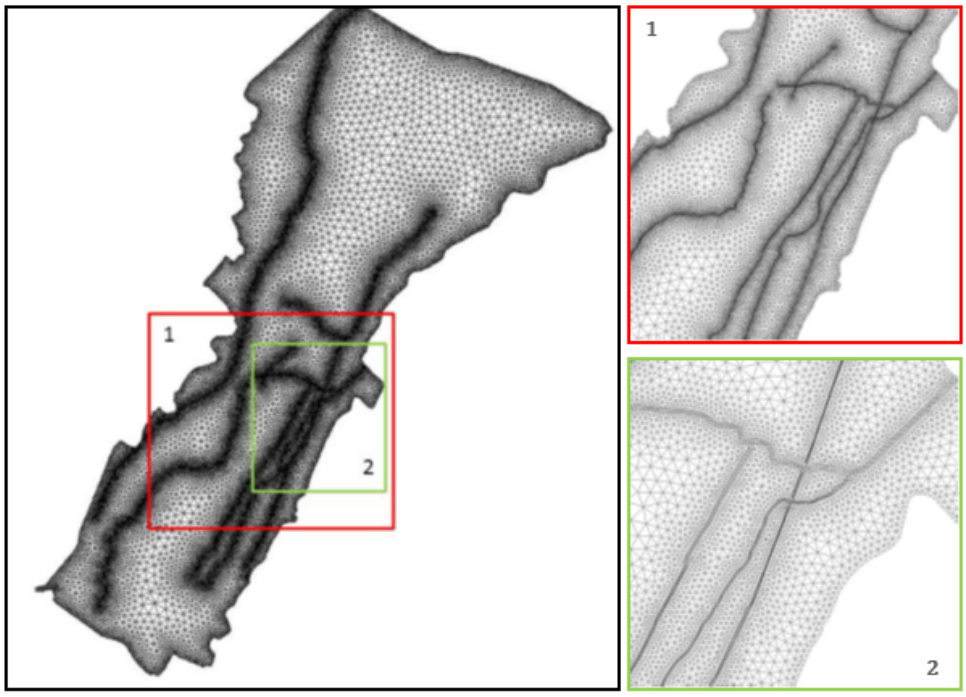

Figure 5.6: Unstructured mesh used for the 2D model, showing different mesh sizes in order to reproduce topographic singularities (DICAM-PCREM, 2015).

An upstream boundary condition was implemented, represented by the flow hydrograph of the water outflowing from the levee breach (see Fig. 5.7), suitably reconstructed by the scientific committee which studied the event (D'Alpaos et al., 2014).

The calibration of the 2D model was performed by varying the roughness coefficients used for flood plains. Specifically, the Gauckler Strickler's values were identified by distinguishing between agricultural areas and urban areas. For the latter, since the construction of the computational mesh did not take into account buildings' footprints or other obstacles in the urban context, as well as the possible storage capacity of flooded buildings, the adopted roughness coefficient was equal to

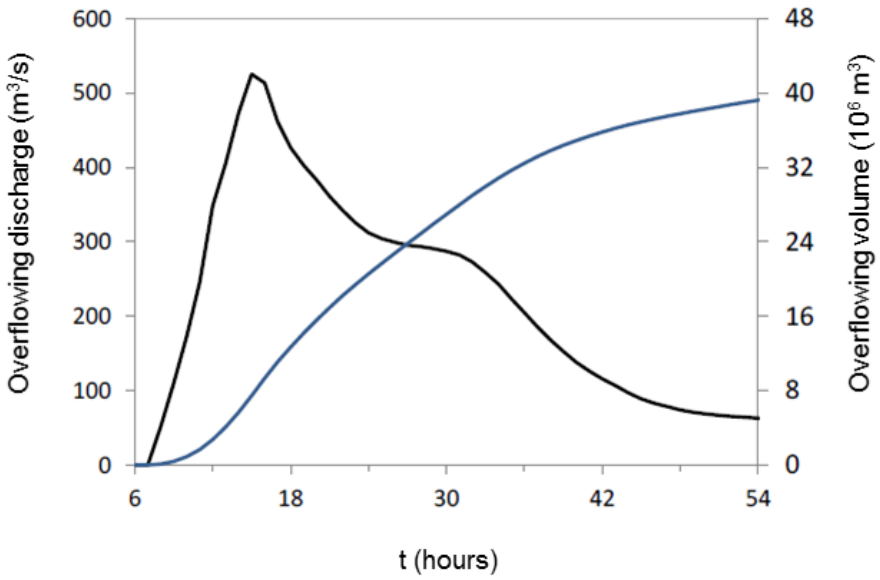

Figure 5.7: Hydrograph (black line) and total volume (blue line) flooded from Secchia river during the study event (DICAM-PCREM, 2015).

10 $m^{1/3}/s$ and considered constant during the calibration phase. The calibration phase has therefore concerned the identification of Gauckler-Strickler's value for agricultural areas, resulted as a value of 30 $m^{1/3}/s$, in line with the roughness values usually adopted in the literature for this type of soil use (see e.g. Domeneghetti et al., 2013; Vorogushyn, 2008).

The calibration phase was conducted referring to the available information about the flooding dynamics at different time steps, to the information obtained by the scientific committee in the analysis and reconstruction of the event, and to pictures and maps made available by competent authorities.

The outputs of the simulation with the Telemac-2D model, in terms of maximum water depth and maximum water velocity, are shown in Fig. 5.8, top and bottom panel, respectively.

This 2D model was used here as the reference tool for the detailed analysis of the hydraulic hazard in study area. In fact, despite the significant and wide data collection activities implemented by the competent authorities to monitor the damages caused by the flood in the post-event period, official available data about hydraulic variables (i.e., water depth, flow velocity, flood duration, etc.) in the flooded area are very limited. The few available data provided by the municipal authorities were collected together with pictures, videos and reports made available on the Internet sites some

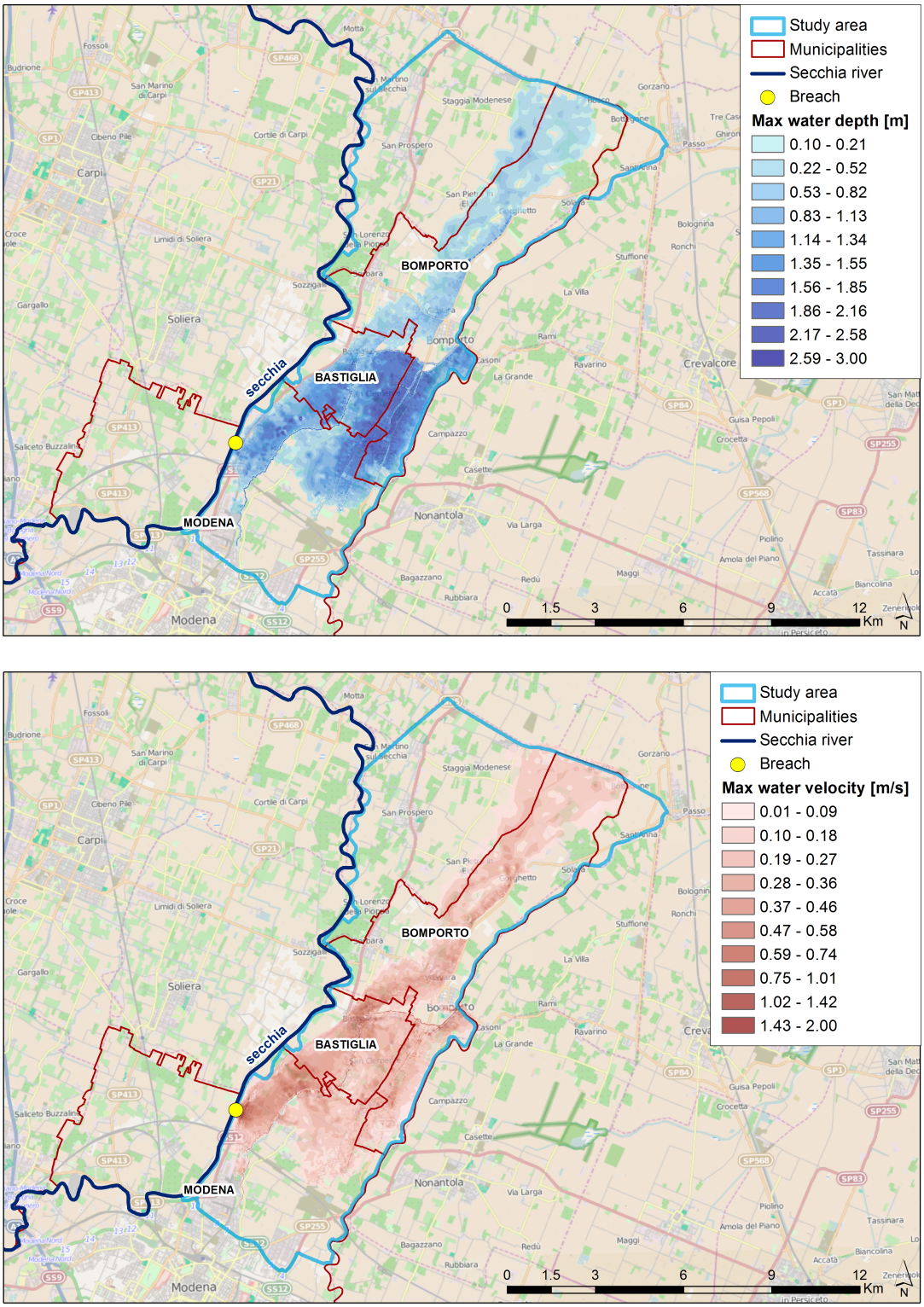

Figure 5.8: Maximum water depths (top panel) and maximum water velocity (bottom panel), simulated by the 2D model.

months after the event, as well as in situ interviews. They were used to compare model outcomes with data representing the real water depths in the flooded municipalities. This analyses represented the validation of the model, whose results showed that the flooding dynamics are simulated really good, except in some areas, in which simulated and observed water depth are slightly different. Areas where observed and simulated water depths differ more than 20 cm were not taken into account in the following analyses.

5.4 Available data

In the immediate post-event period, authorities of Emilia-Romagna Region, Modena Province and affected municipalities started a data collection campaign to get as much information as possible on the damages caused by the flood event. The aim of the survey was, according to Regional Decree n. 8 of 24^{th} January 2014, to *"quantify the financial needs for the restoration of damaged public buildings, infrastructure network, hydraulic and hydrogeological works, as well as private properties for residential use, private movable properties, private registered goods and real estates and goods related to the productive sector"*.

In order to get these data, citizens and property owners were asked to fill the following forms:

- Form A - public properties damages;
- Form B - private properties, furniture and registered goods damages;
- Form C - economic and productive activities damages;
- Form D - agriculture and agro-industrial sector damages.

In the present analysis, damage assessment focuses exclusively on private properties (Form B). Preliminary studies on industrial and agricultural damages are still in progress and will be discussed in a future paper.

Authorities collected in total 2448 forms, divided as per the affected municipalities. In order to geocode the position of every damaged property, the complete database was filtered, considering only records for which the complete address was available (see Table 5.1, second column). This database regarded private properties affected by different kinds of potential damages: structural real estate damages, movable properties damages, common structural damages and registered

goods damages. Our analyses focused only on properties affected at least by structural real estate damages. The total amount of considered forms is therefore 1330 (see Table 5.1, third column).

Table 5.1: Number of forms filled by private owners, divided as per municipality.

Municipality	**Affected private properties**	**Affected private properties (available address)**	**Affected private properties (available address and at least structural damages to real estate)**
Bastiglia	1728	1349	887
Bomporto	624	577	392
Modena	76	73	51
Total	2448	1999	1330

Even though the number of available data is not particularly high compared to similar analyses performed in other European contexts (see e.g. Merz et al., 2013), this data set is one of the most complete in Italy so far and it represents an important opportunity to perform such assessments at Italian scale.

1330 records of damaged real estate were geocoded with a GIS procedure, followed by a careful control activity using pictures, Google Street View and Google Earth, in order to check and solve errors due to a possible inaccurate geocode, mainly in the countryside, where distances between civic numbers are higher. In fact, an inaccurate real estate location causes a wrong assignment of the variables of interest (maximum water depth, maximum water velocity and flood duration, in our case).

Points in Fig. 5.9 indicate the geocoded locations of the damaged private properties, divided as per municipalities (see legend). It is worth noting that all points are included in the flooded area, as a further confirmation of the reliability of the 2D model.

Combining the 2D model outcomes and the geocoded point shapefile, it was possible to extract in each point shown in Fig. 5.9 the corresponding maximum water depth, the maximum flow velocity and the duration of the flood, to compensate for the unavailability of these data.

Among all the information reported in the forms we considered the building surface and the structural typology (masonry, reinforced concrete, etc.) as important

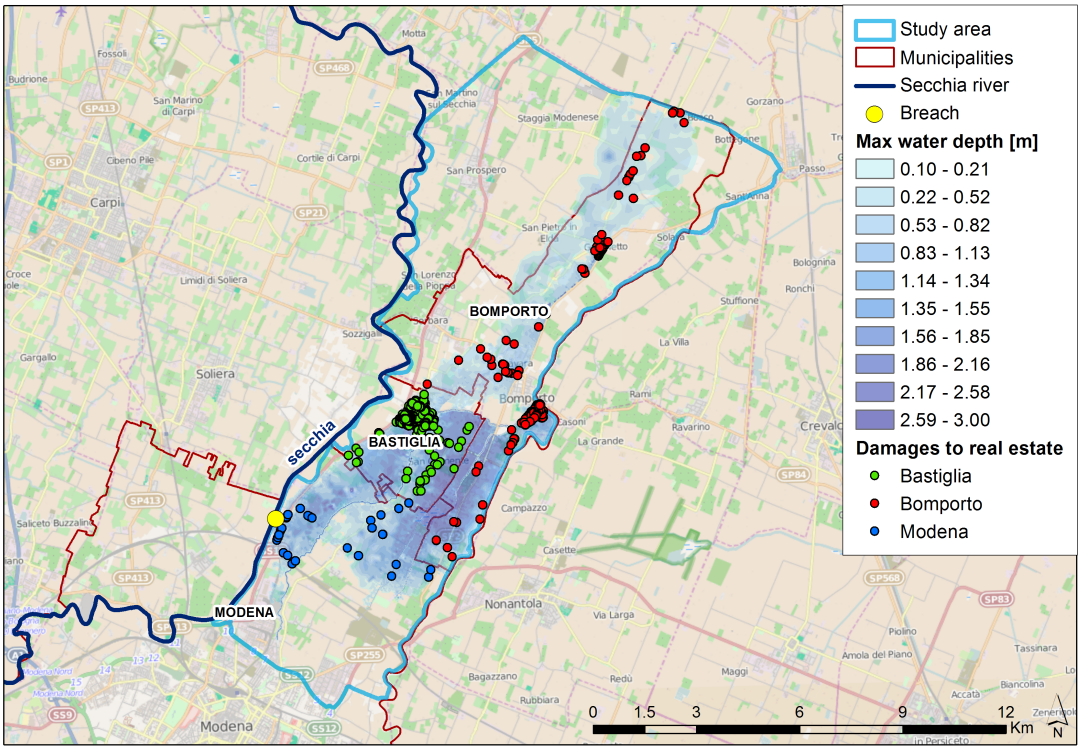

Figure 5.9: Geocoded damaged real estate, divided as per municipalities.

information for our analyses, because these variables have a potential impact on the damage process (see Sec. 2.3).

Another important variable that can significantly impact the damage process is building value, which in this study was retrieved for each property by means of the economic estimate provided by the AE. Every six months AE provides the open-market values [€/m^2] for different assets (e.g. civil houses, offices, stores, etc.) in each Italian administrative district (spatial scale of municipality), taking into account different classes of residential and industrial buildings and the overall economic well-being of the region (see Sec. 4.3). These values are different for each homogeneous geographical area (OMI zone) and determine a market value range per unit area. Focusing on residential buildings, we defined the real estate's economic values [€/m^2] as the average of the values provided for each property in the same OMI zone. It is important to notice that these values do not consider possible fall in price due to catastrophic events.

The forms filled by citizens were collected from municipalities authorities, which

divided the refund requests into different assets typologies: real estate damages, movable properties damages, structural damages to common parts and registered goods (e.g. cars, motorcycles, etc.). Table 5.2 shows in details the different assets which could be refunded, as far as what real estate and movable properties damages are concerned (we neglected structural losses to common parts and registered goods in our analyses because of their limited amount of data collected).

Table 5.2: Refundable assets in accordance to Ordinance No. 2 of 5^{th} June 2014 and Law No. 93 of 26^{th} June 2014.

Typology	**Description**	
Real estate damages	- Structural parts:	roofs, foundations, supporting structures, interior or exterior stairs, retaining walls for the stability of the building;
	- Non-structural parts:	walls or delimitation fence, interior flooring, plastering, interior and exterior painting, interior and exterior fixtures;
	- Installations:	electrical, heating, water, TV antenna, lifts, stair lifts for disabled or elderly people.
Movable properties damages	- Furniture and household appliances: refrigerator, dishwasher, oven, sink, stove, washer, dryer, TV and personal computers.	

Authorities verified the authenticity of the declarations (e.g. by means of experts evaluation in case of damages higher than 15 000 €) and defined the final compensation granted to owners in accordance to Ordinance No. 2 of 5^{th} June 2014 and Law No. 93 of 26^{th} June 2014, which specifies the refund criteria. For instance, the maximum coverage for each damaged to real estate was established equal to 85 000 €, while each owner could receive up to 15 000 € for movable properties damages, divided as follows:

- up to 5000 € for the kitchen or, alternatively, 6000 € for the living room with kitchenette;
- up to 2000 € for each room and the living room (for a maximum of 3 refundable

rooms);

- up to 1000 € for each bath (for a maximum of 2 refundable baths);
- up to 2000 € for a maximum of 1 appliance (e.g. garage, cellar, laundry;

It is understandable, therefore, that the need to find an objective criterion for all the affected properties led, in many cases, the reduction of the amount of damages refundable to the owners. In fact, the refundable assets are only a percentage of the assets that can be found in a property and, in addition, the suffered damages could be higher than the maximum coverage established by authorities. The difference, in terms of total absolute real estate damages, between refunded and required damages is equal to about 2.1 million € (16.3 million € of declared real estate losses vs. 14.1 million € of refunded real estate losses). Focusing on the movable properties, this difference is even more evident (because of the stricter refund criterion) and is equal to about 6 million € (11 million € of total declared losses to movable properties vs. 5 million € of total refunded movable properties losses). In order to maintain the representativeness of the losses data and considering the strict criteria that regulate the damages refund, we chose to perform all the following analyses considering the damages declared by citizens in the Form B as observed losses.

Summing up, Table 5.3 reports all the variables considered in our analysis for each record, providing information about the their original sources: they are divided as per observed (i.e. declared by owners in the official forms), simulated by the hydrodynamic model and retrieved from external sources (e.g. AE).

Table 5.3: Summary of the considered variables and their sources.

Variable	Description	Observed	Simulated	External sources
max_w_depth	Maximum water depth [m]		•	
max_vel	Maximum water velocity [m/s]		•	
fl_dur	Flood duration [h]		•	
area	Building area [m^2]	•		
build_val	Building value [€/m^2]			•
str_type	Structural typology [-]	•		
abs_dam_real_est	Absolute damages to real estate [€]	•		
rel_dam_real_est	Relative damages to real estate [-]	•		
abs_dam_mov_prop	Absolute damages to movable properties [€]	•		

5.5 Considered damage models

5.5.1 Uni-variate damage models

As already discussed in Sec. 2.3, damage models return the amount of losses potentially suffered by certain elements (population, buildings, economic activities, ecosystem, etc.) as a result of a specific flood event, thus providing an estimate of the assets susceptibility. These models relate relative (or absolute) losses to different input variables. The most frequently used models in Europe are uni-variate damage models, i.e. they estimate the amount of relative damages as a function of a single input variable (Jongman et al., 2012; Merz et al., 2010b; Messner et al., 2007), differentiated by building use, type, etc. (Gerl et al., 2016). Since 1945, when White (1945) linked the water level to relative (i.e., the loss ratio) or total (i.e., in monetary values) damage, most uni-variate models use this parameter to assess relative losses (see e.g. Apel et al., 2009; Kreibich et al., 2009; Merz et al., 2013; Penning-Rowsell et al., 2005; Smith, 1994), although this assumption leads a big source of uncertainty in the damages estimation. In fact, it implies a generalisation of the real situation and other factors, such as flood duration and flow velocity, which can have an important influence on damage processes, are excluded from the damage assessment (De Moel and Aerts, 2011; Merz et al., 2013).

In addition, it is worth noting that the most known literature depth-damage models are often internationally used as standard methodologies of estimating flood damages (Merz et al., 2010b, 2007; Smith, 1994), but in most of the cases they are neither tested nor calibrated for the specific study area (Amadio et al., 2016). Estimating losses by means of models for different elements at risk, geographical areas and flood events from the ones for which they are derived could provide large errors (Merz et al., 2010b, 2004; Schröter et al., 2016), most of them avoidable with the development of models derived from a comprehensive local data set.

In this section, the most used depth-damage models (also called "stage-damage models") are briefly described and they are used in the following sections to estimate relative losses to real estate, comparing them to the observed losses during the flood event of the Secchia river. Literature damage models can be graphically represented by damage curves, as shown in Fig. 5.10.

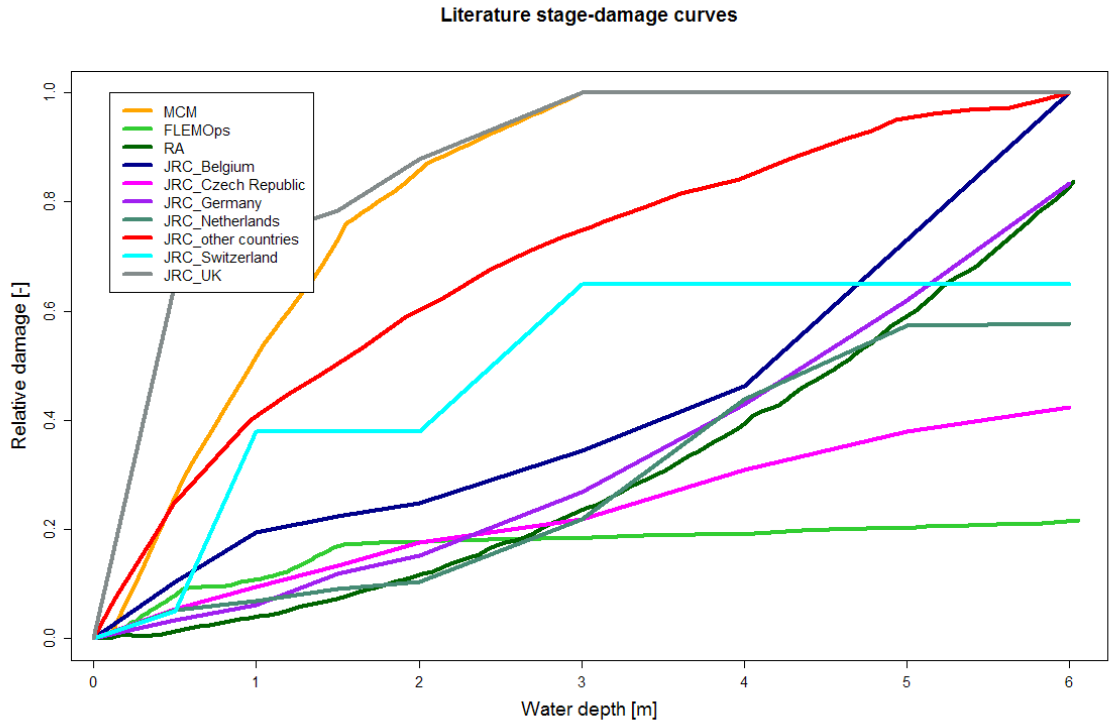

Figure 5.10: Considered literature stage-damage models.

MCM

The damage curve implemented in the Multi-Colored Manual (MCM) (Penning-Rowsell et al., 2005) is the one used in Ch. 4 to evaluate estimated residential losses in the Po plain. It is considered as one of the most advanced models for flood damage estimation in Europe and is used as a support for water management policy and quantitative assessment of the effect of investment decisions (Jongman et al., 2012; Penning-Rowsell et al., 2010). It represents a viable tool for the estimation of the losses related to floods. It estimates different kinds of expected losses (losses to building structure, equipment, immobile inventory, mobile inventory, stock; see Kreibich et al., 2010) as a function of the local water depth, like other analysed stage-damage functions. Contrary to most other damage models, the MCM model estimates real estate damages using absolute depth-damage curves, i.e. it defines monetary potential losses related to water depth, rather than providing damages percentage (Bubeck and Kreibich, 2011; Jongman et al., 2012; Penning-Rowsell et al., 2005). This stage-damage model estimates losses for a wide

variety of residential, commercial and industrial buildings, based almost exclusively on synthetic analysis and expert judgement from the insurance industry or engineers estimating the amount of damages that would occur to a specific element at risk under certain flood conditions (Bubeck and Kreibich, 2011; Penning-Rowsell et al., 2005). In order to represent national economic losses, all damage values are based on the pre-flood depreciated value of the affected properties. For matter of homogeneity with other damage models used in this study, the MCM absolute damage function was converted into a relative curve, trying to respect the maximum damage level and the proportional increase of losses with water depth and keeping the model outcomes unchanged.

FLEMOps

The Flood Loss Estimation MOdel for private sector (FLEMOps) is an empirical model developed based on comprehensive data of up to 2158 private households that were affected by flood events in 2002, 2005 and 2006 in Germany and which caused significant damages. The model was developed by the German Research Centre for Geosciences (GFZ), an advanced center for flood risk scientific analysis from local to national scale. According to Thieken et al. (2008), the database used for the damage model definition was obtained through computerized telephone interviews with a sample of people affected by this serious event. These interviews consisted of 180 questions conceived to reconstruct the flood details, both from the hydraulic point of view and regarding the type of the damage suffered. As result, the FLEMOps model assesses relative flood damages for private households referring to several factors:

- inundation depth (h) (five classes: $h \leq 20$ cm, $h = 21 \div 60$ cm, $h = 61 \div 100$ cm, $h = 101 \div 150$ cm, $h > 150$ cm);
- building types (three classes, in order to capture differences between building values: one-family homes, (semi-)detached houses, multifamily houses);
- building quality (two classes, representative of the state of conservation of a building, that can influence both the economic asset value and the building resistance to the water flow: low/medium quality, high quality);
- water contamination (three classes in order to represent the degree of water pollution of the flood current: none, medium, heavy (i.e. oil or multiple) contamination);

- private precaution (three classes reporting the existence of preventive measures for flood risk mitigation: none, good, very good precaution).

In this study, FLEMOps model was reduced to its decisive parameter, i.e. the water depth. As for the quality and types of residential properties, average values are used, while no information was available about water contamination and precaution. The FLEMOps model was later developed for different flood types (Elmer et al., 2010; Kreibich et al., 2011; Kreibich and Thieken, 2008), but these specific versions were not used in this study.

RA

The Rhine Atlas (RA) model was designed for the hydraulic risk assessment in the catchment area of the Rhine river, which originates in the Swiss Alps and flows through Switzerland, Lichtenstein, Austria, France and Germany up to the Netherlands, where it branches in the North Sea and in the Ijssel lake. In order to facilitate transportation and distribution industries, the Rhine river underwent significant changes due to human intervention; this caused serious impact on the fauna and flora, as well as on the flood regime (Bubeck et al., 2011). To date, over 10 million people live in area with a very high flood risk.

In 1993 and in 1995 two severe floods caused a large amount of economic damage in Germany and the evacuation of 250 000 people in the Netherlands (Bubeck et al., 2011). After these floods, in 1998 the International Commission for the Protection of the Rhine (ICPR) worked to identify and reduce flood risk in the Rhine river basin (Jongman et al., 2012) and in 2001 developed the RA damage model, in which the damage intensity and the maximum damage values were established on the basis of collected empirical data, combined with a synthetic approach (Bubeck and Kreibich, 2011). This model includes five different stage-damage functions, each of them related to a different land-use class derived from the reclassification of the standardized classes adopted by the CORINE project (European Environment Agency, 2007). Figure 5.10 shows the RA damage model used in this analysis, i.e. the stage-damage curve related to the residential sector.

JRCs

These curves were developed by the European Commission's Joint Research Centre - Institute for Environment and Sustainability (JRC-IES) (Huizinga, 2007) as

part of a project to estimate trends in European flood risk under climate change (Ciscar et al., 2011; Feyen et al., 2012). The curves group consists of different depth-damage functions and maximum damage values which can be used by all EU countries. On the basis of the land-use data retrieved from the CORINE project (European Environment Agency, 2007), five damage classes were established: residential, commercial, industrial, roads and agriculture. For eleven countries it was possible to acquire stage-damage functions from existing studies and to apply them to the corresponding damage classes. For countries where stage-damage curves were not available, among which Italy (Manciola et al., 2003; Molinari et al., 2012), an average of all available functions for the specific class was assigned ("Joint Research Centre (JRC) other countries" model). Maximum damage values were acquired from the EU countries for which this information was available and damage models were known. For the other countries the average of these values was calculated for each of the damage classes and applied, proportioning it to the GDP per capita. For example, depth-damage models based on Penning-Rowsell et al. (2005) and van der Sande (2001) were used to develop a stage-damage model for the United Kingdom and, regarding Germany, depth-damage functions were chosen using a combination of many existing models (see Jongman et al., 2012).

Besides estimating flood losses by means of the most used literature curves, we developed two empirical damage curves starting from study event data set. The performance of these two models in estimating flood damages were then compared with the ones of the literature existing models.

SE

What we called "Secchia Empirical (SE) damage model" is the first stage-damage curve derived from the observed relative losses for the Secchia river flood event of 2014. It was obtained combining the points which represent the median value for the observed data for considering water depth classes of 25 cm. This curve is obviously limited to the maximum water depth observed in the 2D simulation (see blue curve in Fig. 5.11).

SSRRs

These uni-variate damage models were also empirically obtained, simply performing a root square regression on the observed relative losses in the study flood event, related to maximum water depth (SSRR_wd), maximum water velocity (SSRR_wv) and building area (SSRR_ba) recorded for every real estate, respectively. Testing linear, logarithmic and square root regressions of the observed data, the latter ones resulted the best curves to estimate Secchia observed damages relatively to water depth, water velocity and building area. In fact, in all cases they presented the highest value of Nash-Sutcliffe Efficiency (NSE), defined by Eq. 5.5.1:

$$NSE = 1 - \frac{\sum_{i=1}^{n}(O_i - P_i)^2}{\sum_{i=1}^{n}(O_i - \bar{O})^2} \tag{5.5.1}$$

with O observed and P predicted values.

The resulting SSRR_wd, SSRR_wv and SSRR_ba curves are therefore defined by Eq. 5.5.2, 5.5.3 and 5.5.4, respectively:

$$y = 0.052\sqrt{x} + 0.059 \tag{5.5.2}$$

$$y = 0.027\sqrt{x} + 0.093 \tag{5.5.3}$$

$$y = -0.003\sqrt{x} + 0.135 \tag{5.5.4}$$

The developed SSRR_wd curve is represented by the dark red line in Fig. 5.11.

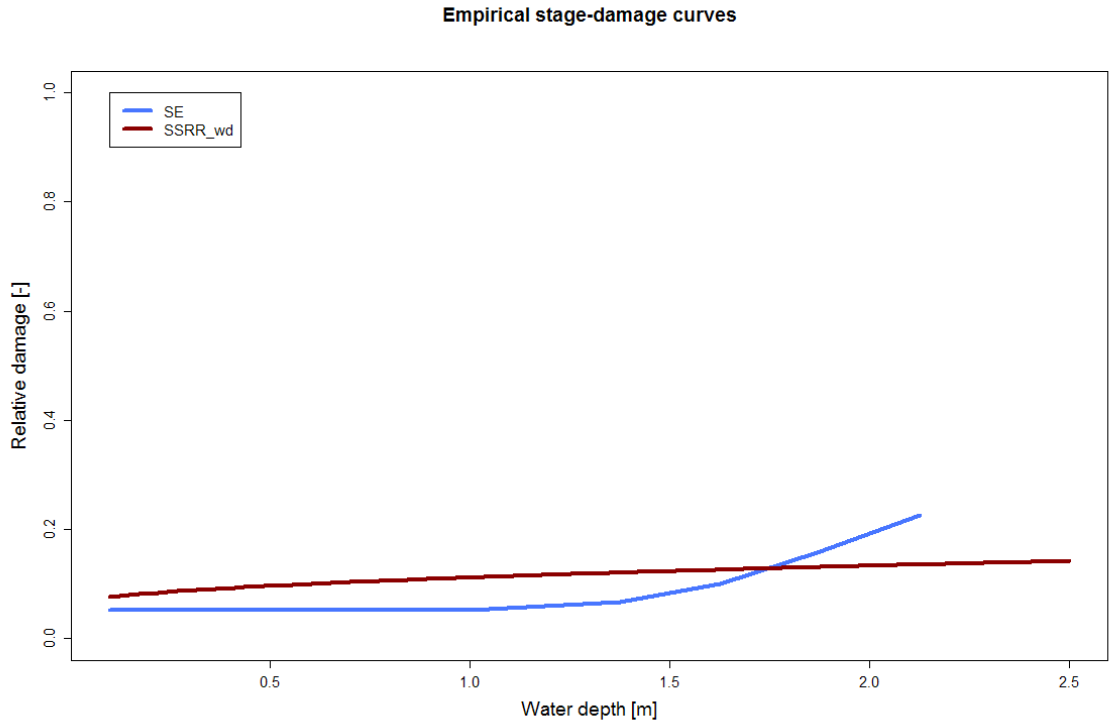

Figure 5.11: Stage-damage models empirically developed on the basis of the Secchia flood event collected data.

5.5.2 Multi-variate damage model - SBTs

The analyses of the estimation of relative flood losses for the Secchia river flood event was performed also thanks to an innovative approach, i.e. considering a multi-variate model in order to take into account multiple factors that can have an important role in the damaging process and are not independent from each other (e.g. water depth, flow velocity, duration of inundation, contamination of flood water, quality of external response in a flood situation, early warning, flood experience and precautionary measures; see Merz et al., 2013, 2010b; Meyer et al., 2013). In fact, although water depth seems to be the most important parameter in damage analyses (see e.g. Apel et al., 2009; Kreibich et al., 2009; Merz et al., 2013; Penning-Rowsell et al., 2005; Smith, 1994), many studies demonstrated that the consideration of multiple factors in the damage assessment leads to better results in terms of losses estimation, compared to the observed losses values (see e.g. Apel et al., 2009; Kreibich et al., 2009; Merz et al., 2013).

The multi-variate model used in this study, called "Secchia Bagging Decision Trees (SBTs)" is an adaptation of a model developed and validate at the German Research Centre for Geosciences (GFZ), on the basis of the available data for our flood event.

Similar version of the model was also used by Wang et al. (2015) for flood hazard risk assessment in China and consists of many regression trees, which are tree-building algorithms for predicting continuous dependent variables. The procedure of growing each tree consists of the approximation of a non-linear regression structure, recursively repeating a sub-division of the given data set into smaller parts, in order to maximize the predictive accuracy. The classification and regression tree (CART) methodology (Breiman et al., 1984) is used to select and split variables (splitting criterion) and to identify leaf nodes (stop criterion). It uses an exhaustive search method on a randomly chosen set of variables to identify the variable with the best split based on a measure of node impurity (in our case the Root Mean Square Error (RMSE) of the response values in the respective parts). The splitting is stopped either if a certain threshold of node impurity is reached or if no further splitting is possible. These steps create a tree structure with several nodes, whereby the beginning node is called root node and the last nodes are called leaf nodes and each resulting node of the tree represents the answer to the partition question asked in the previous interior nodes. The prediction for an input x_1, x_2, ..., x_k is the average of the response variable of all the parts of the original data set that belong to this terminal node (Merz et al., 2013). A possible problem of regression trees is overfitting, i.e. the fact of having too large trees with many leaves whereas the sample size of the leaves is small. The consequence is that the model works well with the training data but have a large uncertainty on the validation with independent data. In order to avoid this problem and reduce the uncertainty associated with the selection of a single tree, Breiman (2001) proposed the so-called Random Forest (RF) algorithm, in which multiple data set samples are created using the resampling bootstrap method and classification and regression trees develop corresponding to each bootstrap sample. This methodology is used also by Merz et al. (2013) as well, who then combine all the trees together and take as reliable response the average over the responses of a combination of individual regression trees. All the regression trees develop by replicating the data set many times, i.e. randomly sampling the subset of the input data set (see Fig. 5.12).

The RF algorithm has the useful ability to provide estimates regarding the hierarchy of variables in the classification (Wang et al., 2015), and thus, in our case,

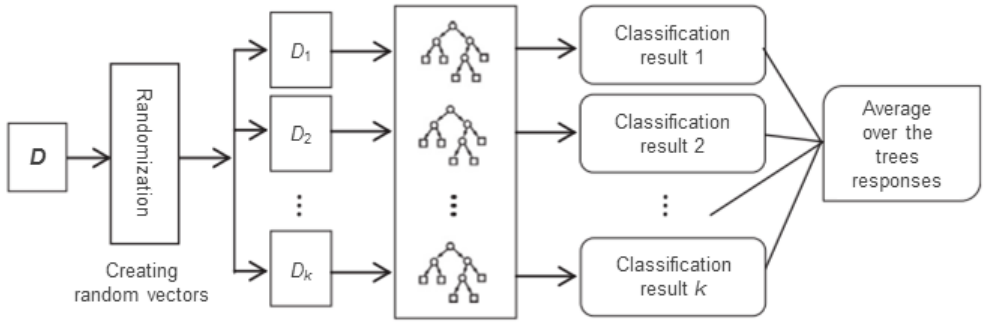

Figure 5.12: RF method (Wang et al., 2015).

to evaluate the importance of the contribution of the variables in the damage process: randomly permuting the values of the predictor variables, the algorithm simulates the absence of a particular variable and calculates the difference of the prediction error with and without the permutation. The variables being randomly permuted presenting a low accuracy are the most important ones in the damage prediction, as their influence in the prediction process is very high.

The RF algorithm was used in many different scientific fields: earthquake-induced damage classification (Solomon and Liu, 2010), prediction of rock burst classification (Dong et al., 2013), genomic data analysis (Chen and Ishwaran, 2012), tree species classification (Immitzer et al., 2012), gene selection (Deng and Runge, 2013), computer-aided diagnosis (Mihailescu et al., 2013) and others. All these applications show the numerous advantages of using the RF method, including high forecast accuracy, acceptable tolerance to outliers and noise, and easy avoidance of overfitting problems. Except the cited studies by Merz et al. (2013) and Wang et al. (2015), few applications of this method to flood risk were performed (Meyer et al., 2013; Wang et al., 2015). Nevertheless, Merz et al. (2013) demonstrated that tree based models are able to improve the performance of existing models like stage-damage functions and to better identify the most important damage influencing variables and their interactions (e.g., they can identify different importance levels of a same variable, depending on the value of another variable). Other important advantages of this learning machine are the possibility to include both continuous, e.g. water depth, and categorical predictors, e.g. building type, and the ability of the model to handle incomplete data: if data is missing, the model considers prediction only for the leaves that can be reached given the available data. On the other hand, Bagging Decision

Trees models present some disadvantages: for example, they only reflect relationships contained within the available data and a large amount of data are needed in order to correctly identify complex connections between variables, especially in geographically large areas. This is one of the reasons why this kind of models is scarcely used in regions where comprehensive, multi-dimensional databases are not available (Merz et al., 2013).

5.6 Results and discussion

5.6.1 Relative losses to real estate

First preliminary analysis regarded the correlation test between the values of relative losses to real estate and six predictive variables: maximum water depth, maximum water velocity, flood duration, building value, building area and structural typology. Being the latter a categorical variable, it was converted to dummy variable encoding in order to calculate the correlation of continuous and categorical data together. Figure 5.13 shows the results in terms of Spearman correlation coefficient.

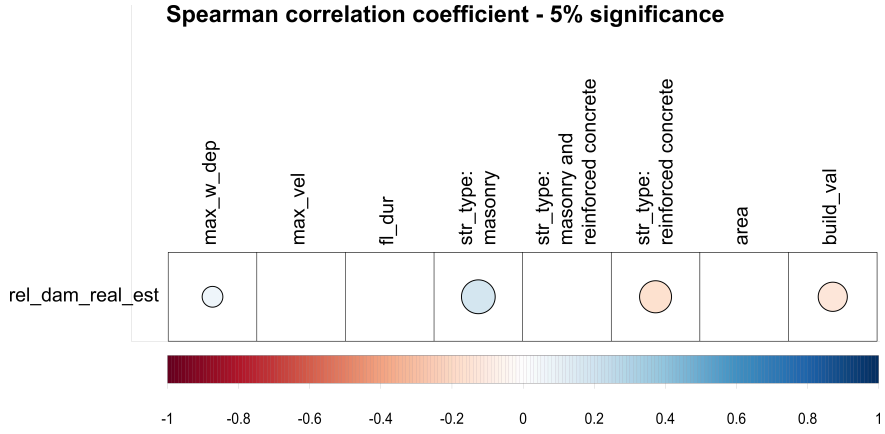

Figure 5.13: Spearman correlation of the relative losses to real estate (rel_dam_real_est) and the predictive variables (max_w_dep = maximum water depth; max_vel = maximum water velocity; fl_dur = flood duration; str_type = structural type - masonry, masonry and reinforced concrete or reinforced concrete; area = building surface; build_val = building value). White boxes represent statistically insignificant correlation (lower than 5% significance level).

White boxes represent statistically insignificant correlations (lower than 5% significance level). The only variables that resulted significantly correlated with the relative losses to real estate were the the maximum water depth, the building value

and the structural typology. However, correlations coefficients between these variables and relative damages to real estate were visibly low, precisely lower than ±0.18. Pearson correlation was also calculated and the resulting coefficients were similar to the Spearman's ones. They are not reported for the matter of brevity.

Figure 5.14 shows the relative damage data to real estate collected in the three municipalities (green, red and blue dots for Bastiglia, Bomporto and Modena, respectively) related to the maximum water depth. Despite the statistically significant correlation, the low correlation coefficient between the two quantities was confirmed by the high noise in the points cloud, which means that the water depth alone is not really able to explain the damage process.

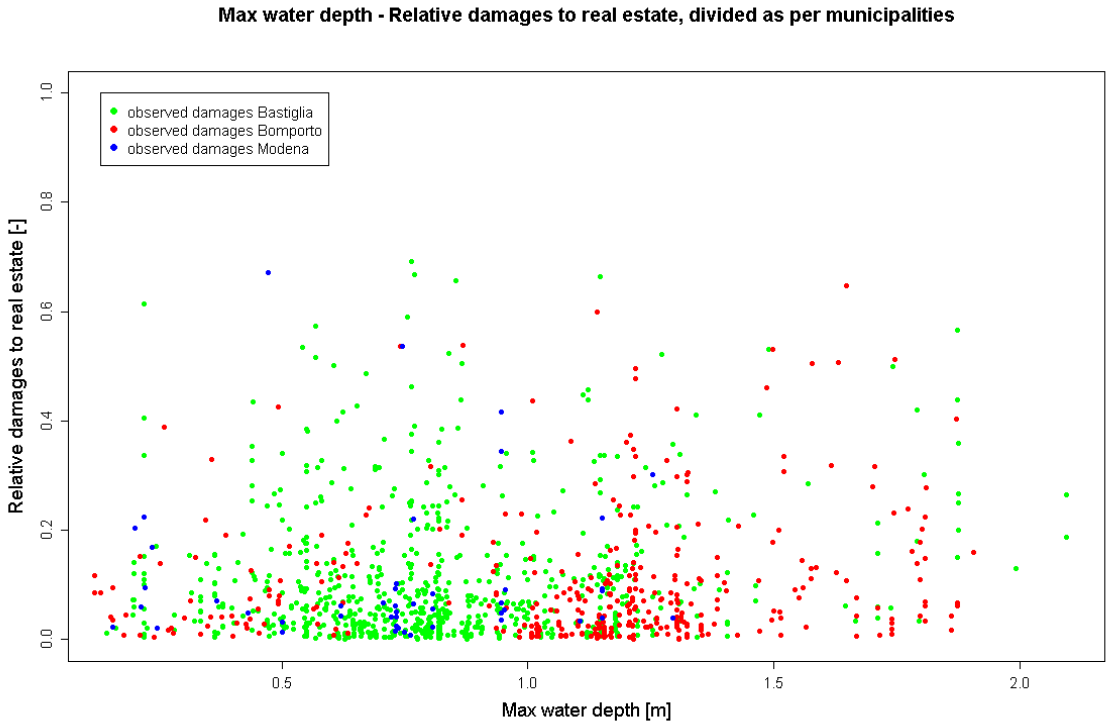

Figure 5.14: Scatter plot of the link between maximum water depth [m] and relative damages to real estate [-]. Municipalities are represented in different colors.

Being the water depth the most used variable in uni-variate flood models in the literature (see Merz et al., 2010b), the first analysis in the study focused on the estimations of relative losses to real estate thanks to the stage-damage models described in Sec. 5.5.1 and shown in Fig. 5.10, which use maximum water depth as

the only predictive parameter. Figure 5.15 shows the outcomes of this assessment (for argument's sake, the considered maximum x-axis value is the maximum water depth reached in the hydrodynamic simulation for the study area). Coloured dots represent the estimated relative losses to real estate using literature and empirically obtained damage curves. With respect to Fig. 5.10, grey points indicating the observed relative losses to real estate were added in the background, in order to allow an immediate comparison between damage curves and observed losses values.

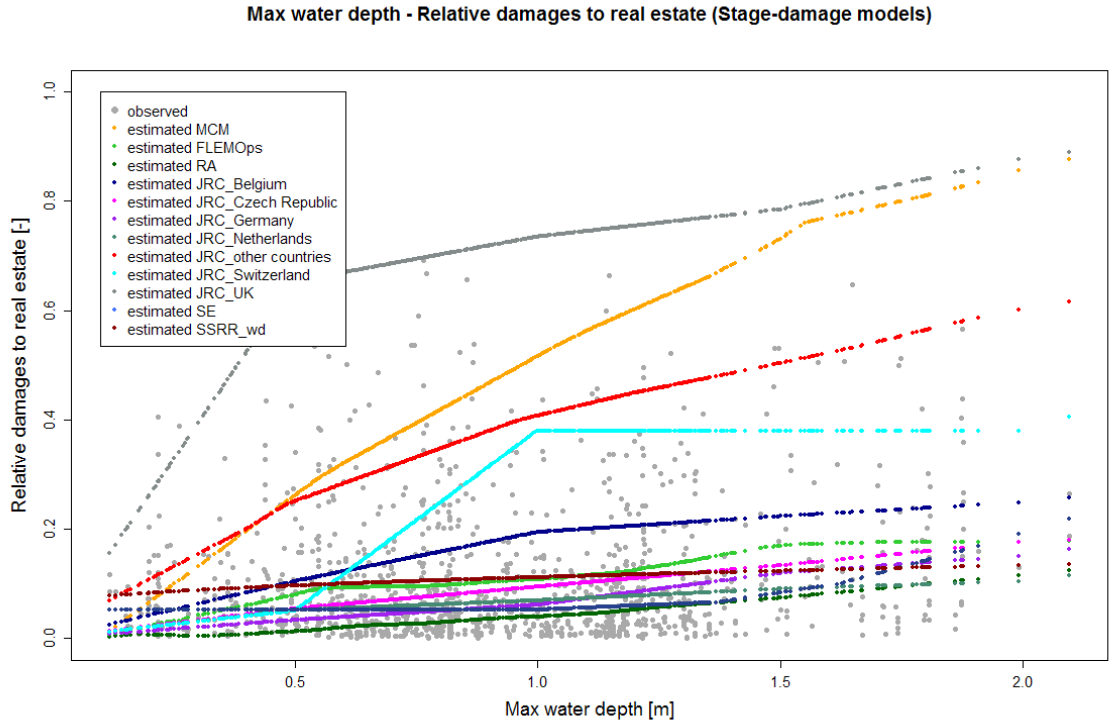

Figure 5.15: Relative damages to real estate estimated with different literature and empirical stage-damage models.

The discrepancy between the observed and estimated values in terms of Mean Bias Error (MBE), Mean Absolute Error (MAE) and RMSE is reported in Table 5.4. MBE, MAE and RMSE are defined by Eq. 5.6.1, 5.6.2 and 5.6.3, respectively:

$$MBE = \frac{1}{n}\sum_{i=1}^{n}(O_i - P_i) \tag{5.6.1}$$

$$MAE = \frac{1}{n}\sum_{i=1}^{n}|O_i - P_i| \tag{5.6.2}$$

$$RMSE = \sqrt{\frac{1}{n}\sum_{i=1}^{n}(O_i - P_i)^2} \tag{5.6.3}$$

with O observed and P predicted values.

The next step consisted of the estimation of the relative losses to real estate by means of the innovative multi-variate model, the so-called Secchia Bagging Decision Trees (SBTs) model, which considered other predictive variables besides the maximum water depth (see Sec. 5.5.2). Results of this analyses are shown in Fig. 5.16, 5.17 and 5.18, where relative damages to real estate are functions of maximum water depth, maximum water velocity and building area, respectively. In each of these three graphs grey points represent the observed data, black points indicate estimated losses by means of the SBTs and dark red points represent estimated damages thanks to the uni-variate square root regression models, retrieved by the relation of observed damage data with maximum water depth (SSRR_wd), maximum water velocity (SSRR_wv) and building area (SSRR_ba), respectively.

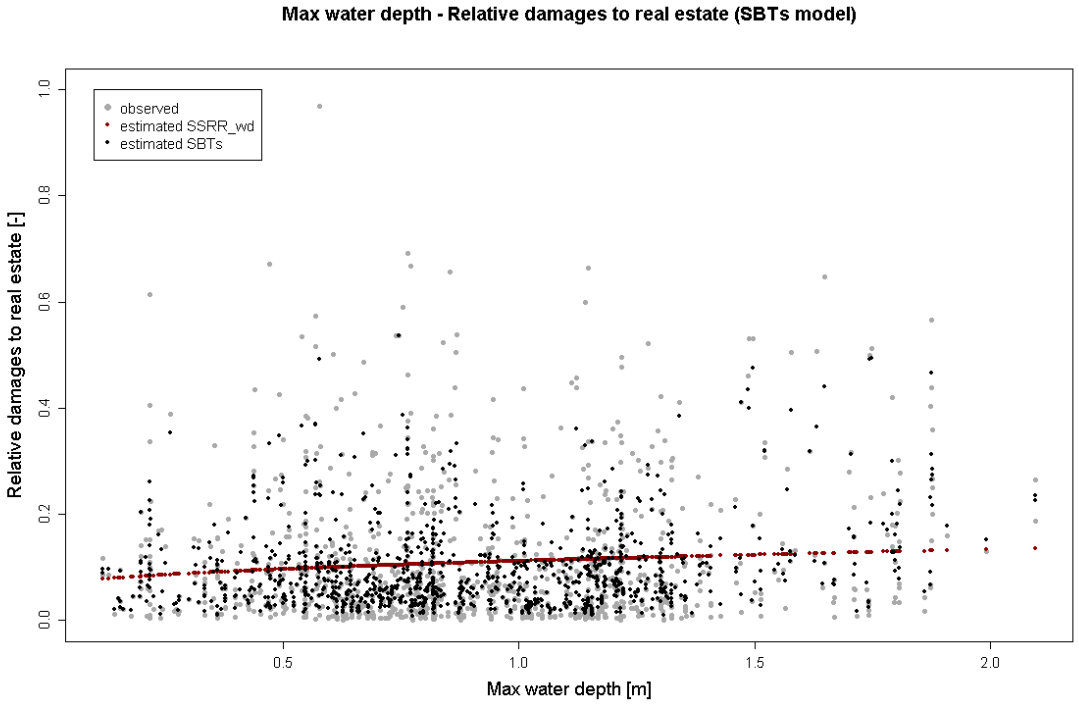

Figure 5.16: Relative damages to real estate estimated with the SSRR_wd model (dark red dots) and the SBTs model (black dots).

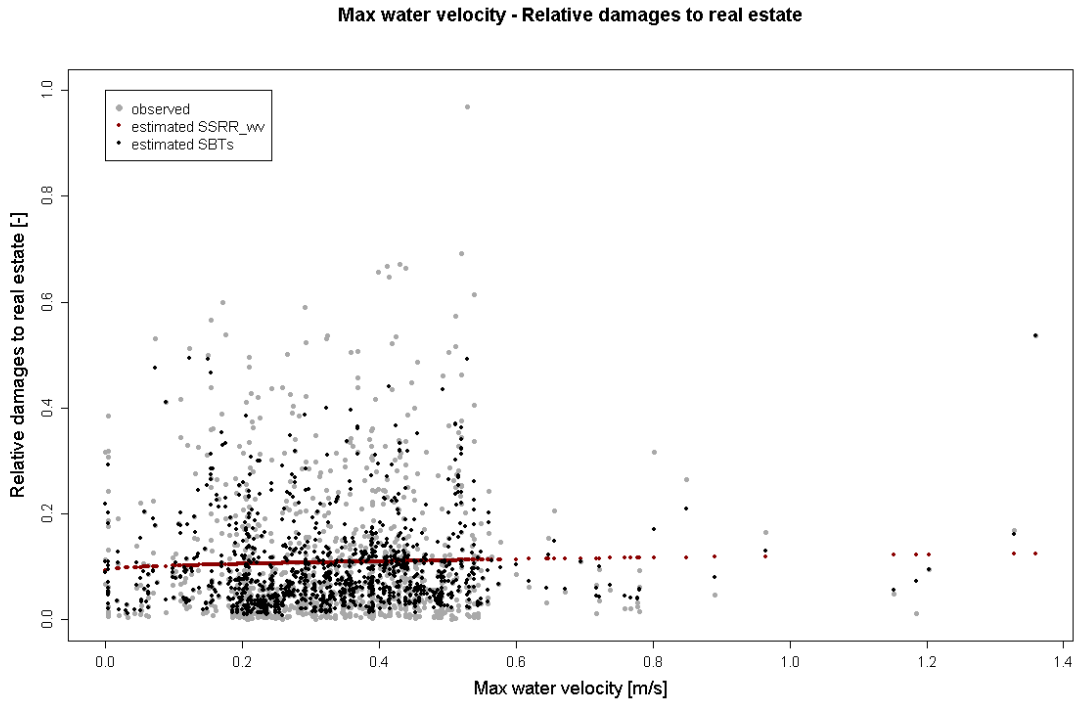

Figure 5.17: Relative damages to real estate estimated with the SSRR_wv model (dark red dots) and the SBTs model (black dots).

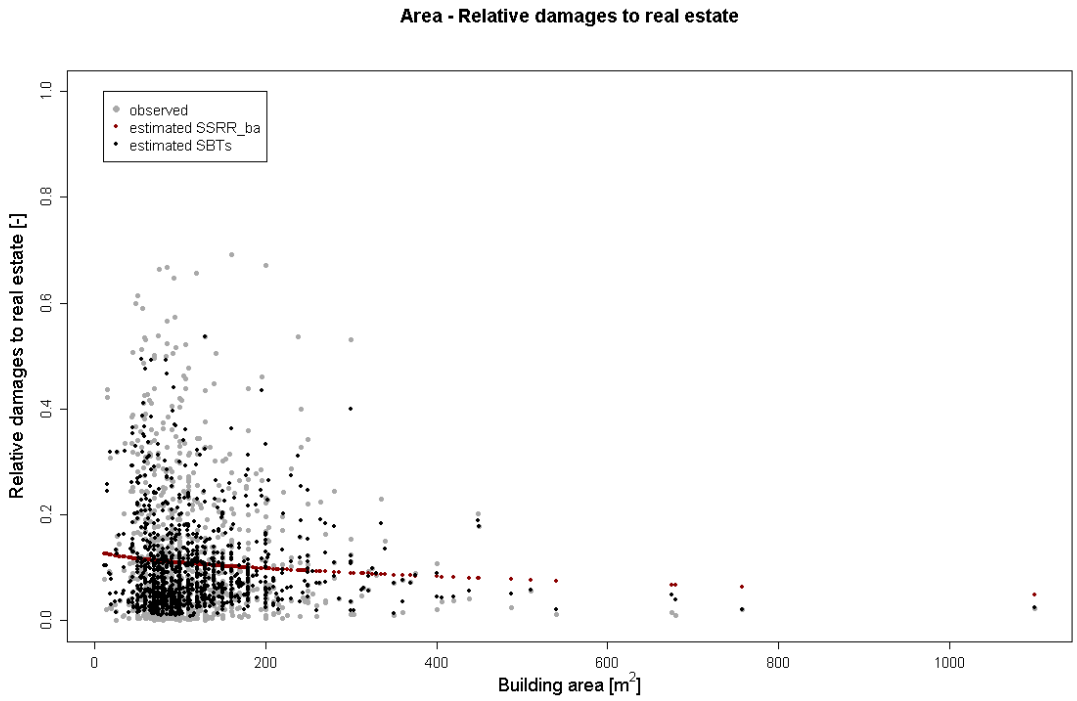

Figure 5.18: Relative damages to real estate estimated with the SSRR_ba model (dark red dots) and the SBTs model (black dots).

The better correspondence between observed and estimated damages with SBTs model, compared to estimated losses shown by other uni-variate curves, is already visible in four mentioned graphs (Fig. 5.15, 5.16, 5.17 and 5.18), but it is even better described by Table 5.4, that reports the performance of all used models in terms of the different errors mentioned above.

SBTs turned out to be the model that presents the lowest value of RMSE (0.062), equal to the half of the second best model, i.e. the empirical curve SSRR_wd (RMSE=0.124), retrieved by performing a square root regression on the available observed Secchia data set, related to the maximum water depth. Secchia Square Root Regression (SSRR) models based on maximum water velocity (SSRR_wv) and building area (SSRR_ba) also provided relative losses estimation with almost identical results, followed by FLEMOps and JRC_Czech Republic models which present satisfying values of RMSE, equal to 0.125 and 0.127, respectively. RMSE values derived from the relative losses estimation with JRC_Netherland, SE, JRC_Germany, JRC_Belgium and RA are between 0.13 and 0.15, while the worse performance in terms of RMSE resulted by JRC_Switzerland, JRC_other countries, MCM and JRC_UK models. These outcomes reflect the fact that the damage curves

Table 5.4: Performance of different uni- and multi-variate models in estimating relative damages to real estate, compared to the observed ones. Models are sorted in terms of increasing RMSE.

	MBE [-]	**MAE** [-]	**RMSE** [-]	**Differences between total observed and total estimated damages to real estate [million €]**
SBTs	-0.012	0.034	0.062	1.5
SSRR_wd	0.000	0.089	0.124	-0.8
SSRR_ba	0.000	0.089	0.124	-0.2
SSRR_wv	0.000	0.090	0.124	-0.9
FLEMOps	-0.003	0.089	0.125	-0.3
JRC_Czech Republic	-0.022	0.085	0.127	2.5
JRC_Netherlands	-0.043	0.082	0.131	5.7
SE	-0.048	0.080	0.132	6.3
JRC_Germany	-0.046	0.082	0.133	6.1
JRC_Belgium	0.056	0.119	0.142	-8.8
RA	-0.071	0.087	0.143	9.8
JRC_Switzerland	0.149	0.196	0.232	-22.5
JRC_other countries	0.256	0.272	0.300	-38.4
MCM	0.350	0.364	0.406	-52.1
JRC_UK	0.585	0.586	0.607	-86.8

related to these last models are positioned in the upper part of the graph, away form the other curves, which are very close together (see Fig. 5.15). In terms of MBE and MAE, outcomes reflect the ones as regards RMSE quite proportionally, with some differences regarding the SSRR models, which present a MBE value that is slightly lower than the one derived from the SBTs model estimation.

The same results can be observed in terms of absolute losses to real estate, calculated multiplying the relative ones times the real building values [€]. The last column of Table 5.4 report the differences between the total observed absolute damages to real estate (15.2 million €) and the total absolute losses to real estate estimated by means of the different uni- and multi-variate models. These values are

proportional to the results in terms of errors: SBTs seems to have slightly worse performance than SSRR_wd, SSRR_wv and SSRR_ba (and FLEMOps, regarding these specific outcomes).

It is also worth noting that six out of fifteen tested models provided an underestimation of the total absolute losses to real estate, while the remaining nine models tended to overestimate them. In this consideration, one should take into account the uncertainty derived from the fact that the considered building values were not depreciated ones because of the flood event (see Sec. 2.3).

One of the advantages of Bagging Decision Trees models, as discussed in Sec. 5.5.2, is the possibility to understand the importance of the variables taken into account in the losses estimation, and then their influence on the damage process for this specific context. Figure 5.19 shows the output of this assessment performed by the SBTs on the basis of the six used variables (building area, building value, flood duration, maximum water velocity, maximum water depth and structural typology). The absence of a parameter that could be considered more important than the others, is evident, contrary to what happens in other similar studies (see Merz et al., 2013). Water depth appears to be a slightly stronger loss predictor than the other ones, immediately followed by water velocity and building area, while the other variables show very small importance. These outcomes are in line with those linked to variables correlation and shown in Fig. 5.13.

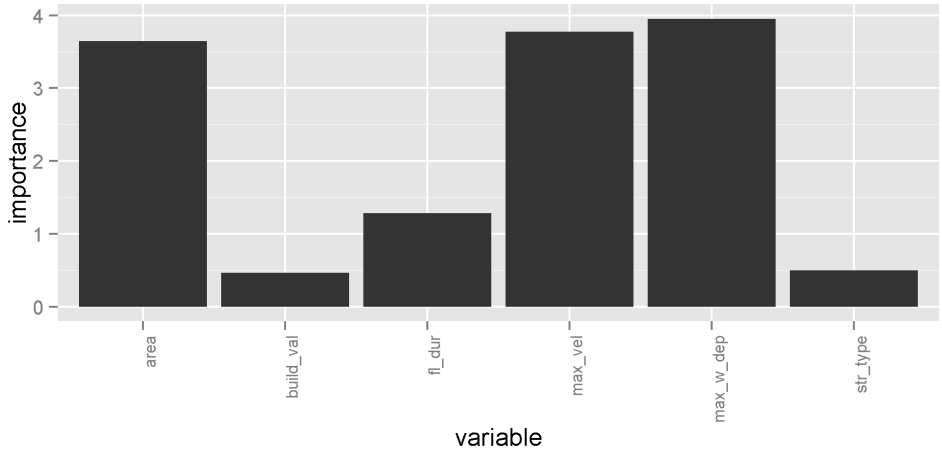

Figure 5.19: Importance of predictive variables considered in the BTs model (area = building surface; build_val = building value; fl_dur = flood duration; max_vel = maximum water velocity; max_w_dep = maximum water depth; str_type = structural type).

5.6.2 Losses to movable properties

The last important observed data taken into account in this analysis was absolute movable properties data (e.g. furniture and household appliances: refrigerator, dishwasher, oven, sink, stove, washer, dryer, TV and personal computers). For each building, given the absence of specific data on what the term "movable properties" refers to, it is impossible to identify the movable properties values and consequently relative losses data to movable goods. Because of the variability of the assets, no reliable damage curve for movable properties is available in the literature. Thus, we assessed if there was a relation between observed absolute losses to real estate and observed absolute losses to movable properties (see the bilogarithmic graph in Fig. 5.20).

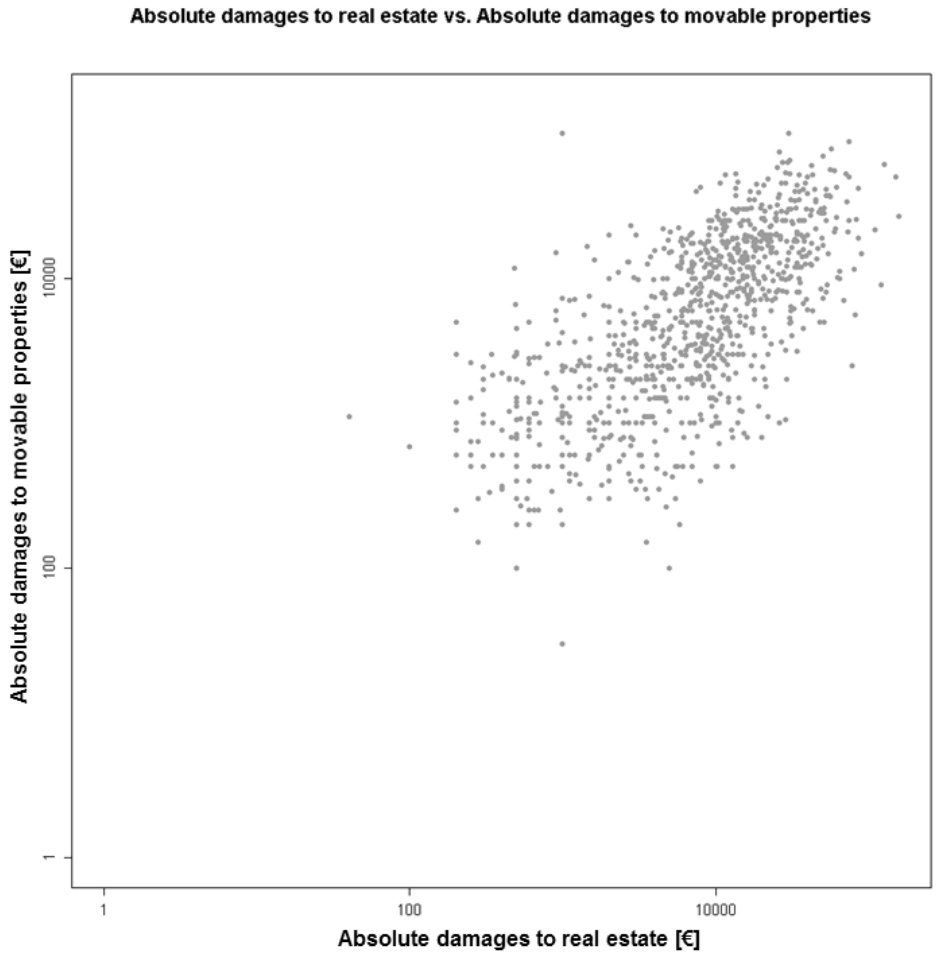

Figure 5.20: Scatter plot of the relation between damages to real estate [€] and damages to movable properties [€].

Different types of regression were tested (linear, square root, logarithmic and bilogarithmic) and the square root regression resulted the one with the highest value of NSE (see Eq. 5.5.1), i.e. the one that at best relates real estate with movable properties losses values. Therefore it was applied to estimate absolute damages to movable properties starting from the absolute damages to real estate estimated thanks to the uni- and multi-variate damage models analysed in the previous sections. The function is defined by Eq. 5.6.4:

$$y = 125\sqrt{x} - 1966 \tag{5.6.4}$$

Table 5.5 reports the output of this assessment in terms of MBE, MAE, RMSE, and differences between total observed absolute damages to movable properties and total estimated absolute damages (10.4 million €).

The outcomes reflected the results of the estimation of relative losses to real estate, especially regarding the models that showed worse performance in estimating relative damages to real estate (see Sec. 5.6.1): JRC_Switzerland, JRC_other countries, MCM and JRC_UK models present the higher values for all the performance indicators. The ranking of the remaining models in terms of RMSE is JRC_Netherlands (12 702 €), JRC_Germany, SE, JRC_Czech Republic, RA, SSRR_wv, FLEMOps, SSRR_ba, SSRR_wd, JRC_Belgium and SBTs (15 292 €). The performance of all considered models, with the exception of the last four, is still more than acceptable, as difference values between total observed and total estimated losses to movable properties do not exceed ±4 million € (except for JRC_Belgium that presents a difference value of 7.2 million €). JRC_Netherlands, SE, JRC_Germany, SBTs and JRC_Czech Republic show difference values lower than ± 2 million €. Unlike the results of the real estate damages analysis, most of damage models seemed to overestimate movable properties losses, while JRC_Netherlands, SE, JRC_Germany and RA slightly underestimated them.

Table 5.5: Performance of different uni- and multi-variate models in estimating movable properties damages, compared to the observed ones. For the sake of homogeneity, the order of the models is the same of Table 5.4.

	MBE [€]	**MAE [€]**	**RMSE [€]**	**Differences between total observed and total estimated damages to movable properties [million €]**
SBTs	8 520	13 246	15 292	-1.6
SSRR_wd	3 445	10 324	13 157	-3.8
SSRR_ba	3 362	10 283	13 136	-3.6
SSRR_wv	2 903	1 0066	13 026	-3.8
FLEMOps	3 121	10 167	13 076	-3.3
JRC_Czech Republic	2 051	9 684	12 863	-1.7
JRC_Netherlands	299	8 993	12 702	0.1
SE	-1 038	8 549	12 741	0.6
JRC_Germany	-491	8 722	12 708	0.6
JRC_Belgium	7 671	12 705	14 836	-7.2
RA	-2 528	8 174	12 948	3.6
JRC_Switzerland	14 481	17 634	19 260	-11.4
JRC_other countries	16 260	19 051	20 631	-17.1
MCM	19 365	21 659	23 157	-20.3
JRC_UK	25 996	27 527	28 931	-28.7

5.6.3 Transferability of the empirically developed models

Based on the output in Secs. 5.6.1 and 5.6.2, it is worth noting that the application to the Secchia case study of the JRC_other countries model, in which Italy should be included, provided poor results in terms of both real estate and movable properties losses. This confirms how challenging it is to identify a generalised regional or large scale model that could be applied to a specific locality (see also Sec. 2.3 and Amadio et al., 2016; Cammerer et al., 2013).

At national level, besides some models developed elsewhere and neither tested nor calibrated for the specific study area in which they are used (Amadio et al., 2016), one can found many examples supporting the assumption about transferability difficulties. Molinari et al. (2014b), for example, tried to export in other contexts some models developed on the basis of specific flood event data (Freni et al., 2010; Luino et al., 2006), with disappointing results due to various reasons. Firstly, it is important to cite the extreme variability of geographical and geomorphological contexts as well as of urban patterns and building typologies typical of Italy. Secondly, a general lack of data of acceptable quality is evident, as well as the small size of the usually available data set relating to flood events on small catchment areas, compared to other European case studies (see also Molinari et al., 2012).

In this study we assessed the transferability on similar contexts of empirical models, calibrated against quite large amount of observed data (1330 records). SSRR and SBTs models, developed on the basis of the entire data set, demonstrate good performance in the estimation of relative damages to real estate in the study area; therefore, we tried to derive similar models on the basis of a single municipality's data and to apply them to the estimation of relative losses in another adjacent municipality. In particular, starting from Bomporto's data set (392 records), we calibrated the Bomporto Square Root Regression (Bo_SRR) models (considering maximum water, maximum water velocity and building area as single predictor variables) and the Bomporto Bagging Decision Trees (Bo_BTs) model, and applied them for the estimation of Bastiglia's losses and vice versa (887 records as starting data set to derive Bastiglia Square Root Regression (Ba_SRR) and Bastiglia Bagging Decision Trees (Ba_BTs) models). We neglected Modena's municipality because of its exiguous number of damaged real estate (51 records).

Figures 5.21, 5.22 and 5.23 show the results of the transferability assessment: top panels refer to Bastiglia's relative damages to real estate related to maximum water

depth, maximum water velocity and building area (respectively), estimated by means of Bomporto's calibrated models, while, on the contrary, bottom panels indicate Bomporto's damages estimated by means of Bastiglia's models; in each graph grey dots represent observed losses, red dots indicate relative damages to real estate estimated with Square Root Regression (SRR) models and finally blue dots show the estimation of relative losses using the BTs models. Red dots seem to have a quite similar trend in all figures, while better performance of the Ba_BTs model is evident compared to those of Bo_BTs model: blue dots in bottom panels overlap more evenly the observed damage clouds, while in the upper panels they seem to overestimate the relative losses to real estate.

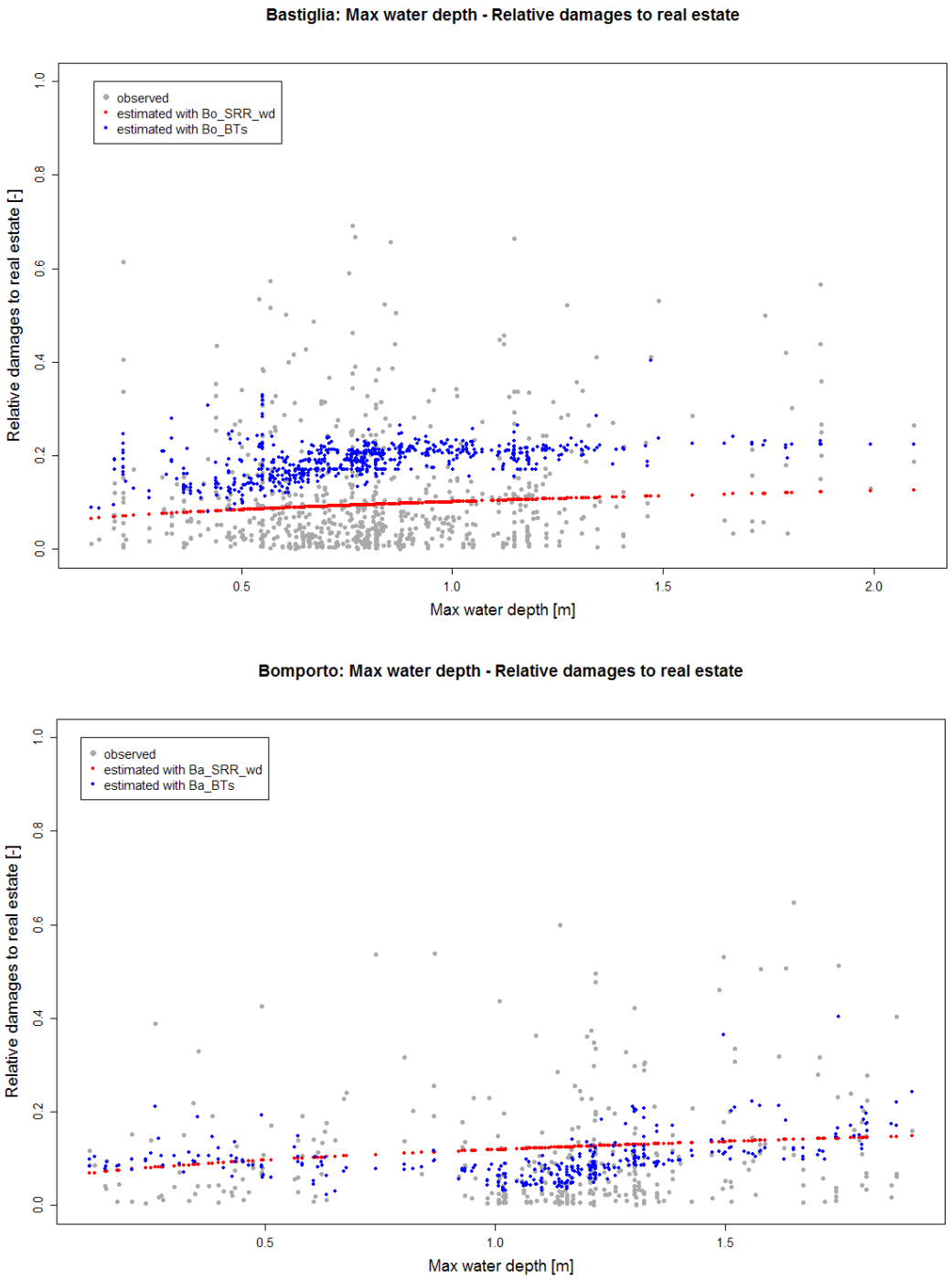

Figure 5.21: Top panel: Bastiglia relative damages to real estate estimated with SRR_wd model (red dots) and the BTs model (blue dots), both calibrated on Bomporto's data set; Bottom panel: Bomporto relative damages to real estate estimated with SRR_wd model (red dots) and the BTs model (blue dots), both calibrated on Bastiglia's data set. In both panels, grey points represent the observed data.

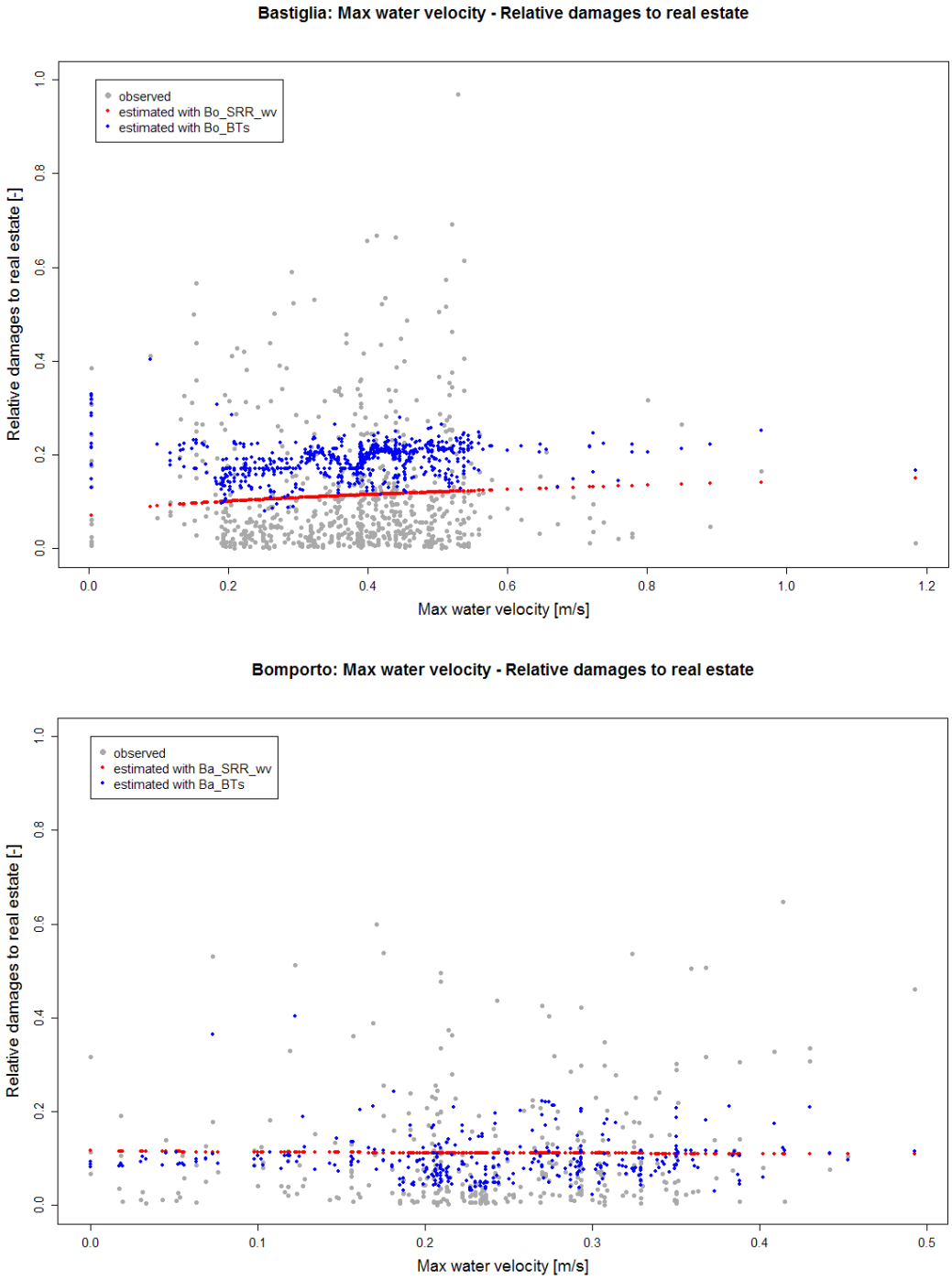

Figure 5.22: Top panel: Bastiglia relative damages to real estate estimated with SRR_wv model (red dots) and the BTs model (blue dots), both calibrated on Bomporto's data set; Bottom panel: Bomporto relative damages to real estate estimated with SRR_wv model (red dots) and the BTs model (blue dots), both calibrated on Bastiglia's data set. In both panels, grey points represent the observed data.

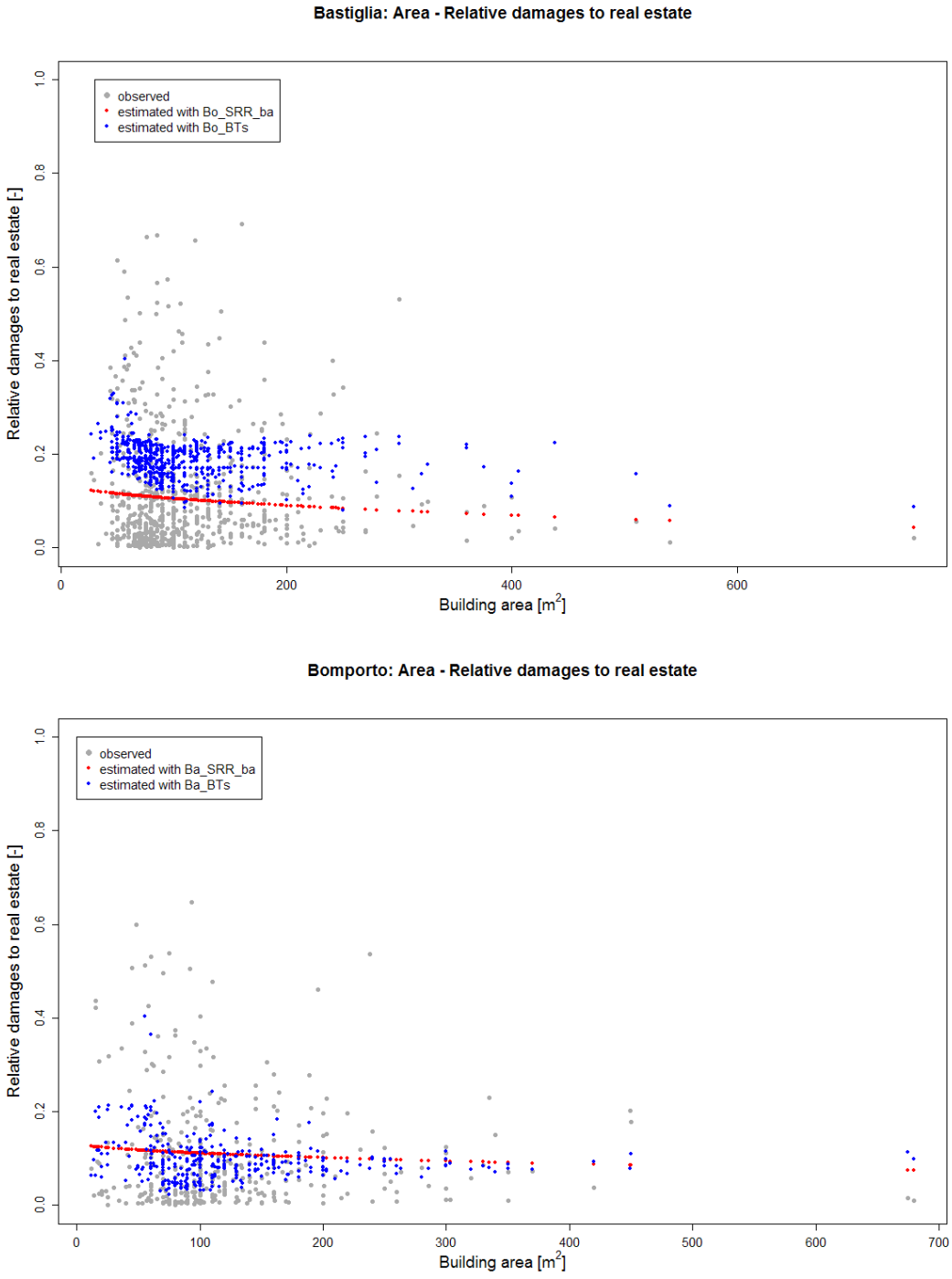

Figure 5.23: Top panel: Bastiglia relative damages to real estate estimated with SRR_ba model (red dots) and the BTs model (blue dots), both calibrated on Bomporto's data set; Bottom panel: Bomporto relative damages to real estate estimated with SRR_ba model (red dots) and the BTs model (blue dots), both calibrated on Bastiglia's data set. In both panels, grey points represent the observed data.

This impression is confirmed by Table 5.6, which presents the results of this analysis in terms of MBE, MAE and RMSE between estimated and observed damages in both cases.

Table 5.6: Performance of different uni- and multi-variate models in estimating relative damages to real estate, compared to the observed ones. In the top part of the table, the models were calibrated on Bomporto's data set (392 records) and used to estimate damages in Bastiglia, while in the bottom part of the table the models were calibrated on Bastiglia's data set (887 records) and used to estimated damages in Bomporto.

Calibration on Bomporto's data set and application to Bastiglia			
	MBE [-]	**MAE** [-]	**RMSE** [-]
Bo_BTs	0.089	0.136	0.155
Bo_SRR_wd	0.000	0.085	0.118
Bo_SRR_wv	0.000	0.085	0.118
Bo_SRR_ba	0.000	0.085	0.118
Calibration on Bastiglia's data set and application to Bomporto			
	MBE [-]	**MAE** [-]	**RMSE** [-]
Ba_BTs	-0.006	0.080	0.115
Ba_SRR_wd	0.000	0.091	0.126
Ba_SRR_wv	0.000	0.091	0.126
Ba_SRR_ba	0.000	0.091	0.126

While uni- and multi-variate models calibrated on Bastiglia's data and applied to Bomporto's damages do not differ much, with a slight preference for the BTs model compared to the SRR ones, the multi-variate model derived from Bomporto's data set presents a much higher error estimating losses in Bastiglia (uni-variate SRR models' results also for Bastiglia case are comparable with those for Bomporto's municipalities). The worst performance of the multi-variate model in the Bastiglia's

damages evaluation can be explained by the smaller size of the Bomporto data set (less than a half of the Bastiglia's one): as outlined in Sec. 5.5.2, in order to have satisfying results from this kind of models, it is necessary to have a large amount of data available. In addition, this study showed the importance to have a data set size proportional to the surface that it refers to. This allow to better represent the relationship between the considered variables and to explain different local characteristic of the study area (Schröter et al., 2014). Being Bastiglia flooded area equal to less than half the one in Bomporto (see Fig. 5.2) and having Bastiglia data set more than twice the records of the Bomporto one, it is easy to understand that a BTs model calibrated on its data provides more reliable results.

5.7 Concluding remarks

This case study focused on the estimation of flood losses starting from a quite large database of observed damage data (1330 records), collected after a recent flood event occurred in January 2014 caused by a breach in the right embankment of the Secchia river, in the Northern part of Modena's municipality. This important flood event caused the inundation of more than 50 km^2 of the adjacent plain (Bastiglia, Bomporto and Modena were the more affected municipalities) and more than 500 million € of total damages. Being this data set one of the largest and most comprehensive in Italy, it was used to derive empirically uni- and multi-variate damage models, whose performance has been compared with the one of some existing literature stage-damage functions (MCM, FLEMOps, RA and JRC models for different countries). Empirically uni-variate models consist of three curves obtained performing a square root regression on the observed values of maximum water depth (SSRR_wd), maximum water velocity (SSRR_wv) and building area (SSRR_ba), respectively, and one model, called Secchia Empirical (SE), representing, each 25cm step of maximum water depth, the median values of the observed relative damage data. The multi-variate SBTs is the adaptation of a similar model developed by Merz et al. (2013), whose output are the estimated losses obtained by a large number of classification and regression trees grown considering all available variables and splitting the data set in order to maximize the accuracy of the prediction.

Outcomes showed that the tested models are positioned according to the following ranking (considering as the best one the model that provides the minimum value of RMSE between estimated and observed losses): SBTs, SSRR_wd, SSRR_wv,

SSRR_ba, FLEMOps, JRC_Czech Republic, JRC_Netherland, SE, JRC_Germany, JRC_Belgium, RA, JRC_Switzerland, JRC_other countries, MCM and JRC_UK. Consistently with outcomes by Dottori et al. (2016a) and Scorzini and Frank (2015), to cite some, empirically obtained models (except the SE model) provide better estimation of relative damages to real estate also in terms of MBE, MAE and differences between estimated and observed absolute damages to real estate. This result showed the difficulty and the higher uncertainties deriving from the application of literature models to context other than from the one in which they are developed (this problem has been already discussed by many authors, see e.g. Cammerer et al., 2013; Green et al., 2011; Jongman et al., 2012; Molinari et al., 2014b, and Sec. 2.3). In addition, though the performance of some literature curves is not very different from the one of the empirical models based on local data, it is difficult to predict a priori which are the best ones, among all possible damage curves. Practically, this consideration limits and affects the use of these curves for predictive purposes, i.e. to estimate the expected damages in not flooded areas.

Among the four best models concerning the estimation of relative losses to real estate, the multi-variate SBTs model demonstrated slightly better performance in terms of error indicators (except differences between estimated and observed data) than the other three models. This outcome, however, is not confirmed by the output of the analyses on movable properties damages, where the opposite situation occurred.

Although it did not seem to provide real important improvements in the estimation of flood losses in this case study, regression trees composing the BTs forest have the important advantage to avoid the need to find a parametric function that works with all the data. Also, BTs provide useful information about the relationship among the variables and to exploit the local relevance of predictors (Merz et al., 2013). These can be very useful information for authorities and stakeholders to define preventive measures and/or mitigation strategies. It is also worth noting that the improvement of the BTs model could be increased using a larger number of common variables with the ones taken into account in the original Bagging Decision Trees model by Merz et al. (2013): Gerl et al. (2016) showed how the smaller the number of common variables, the lower the explanatory power of sophisticated multi-variable or probabilistic models, and consequently the larger the loss estimations uncertainties.

According to Elmer et al. (2010), Schröter et al. (2014) and Schröter et al. (2016), it is true that using additional explanatory variables (larger databases and more

complex models compared to the uni-variate ones) leads to additional knowledge, especially if the interdependencies of the parameters are considered, but, on the other hand, it also introduces additional uncertainties, especially if the additional parameters are not collected specifically aiming at this kind of analysis. Secchia's database, in fact, was collected in order to give authorities a quantification of damages to be refunded to citizens and did not include data about hydraulic parameters provided by hydrodynamic models. In addition, further uncertainties came from the records' geocoding (see Sec. 5.4), which sometimes did not match perfectly with the real building location and can influence the assignment of right hydraulic parameters (some of them, e.g. water velocity, can dramatically vary with short distances; see Merz et al., 2010b). Moreover, it is worth considering that the building values provided by AE represent the real estate market values at a given time of given building typologies, that is more an expression of the overall economic well-being of a specific area rather than real depreciated economic real estate values in case of a flood event.

However, as the outcomes of the models transferability clearly highlighted and in order to lead to satisfying results, the use of this kind of multi-variate models requires a sufficient amount of data (Merz et al., 2013; Schröter et al., 2014). With the aim of defining a model that can be exported in other contexts, a detailed and structured acquisition of explanatory variables is necessary (Schröter et al., 2016), both in the definition context and in the application one, in order to adapt the model in the best way, or at least to quantify and communicate the relative uncertainties. According to Amadio et al. (2016), Molinari et al. (2012), Molinari et al. (2014b), and Scorzini and Frank (2015), to cite some similar studies, the most urgent need in Italy, as far as losses estimation is concerned, is exactly to identify guidelines, valid for the whole country, to collect consistent and comparable data even if they relate to different contexts. This data should include a large amount of useful information (in addition to those commonly collected), like those described item by item by Merz et al. (2010b), i.e. observed water depths, flood duration, presence of sediments, contamination rate, early warning or precautionary measures adopted, as well as other indication about the buildings composition (numbers of floors, type of movable properties, presence of basements, building condition, etc.), preferably collected in the immediate post-event. In this regard, even more importance assume studies on the potential of social media as a support tool to collect parameters useful both for flooded areas mapping and

for improving emergency management and financial compensation and reconstruction planning (see e.g. Fohringer et al., 2015; Herfort et al., 2014).

As a more general observation, it is worth noting that the empirically uni-variate models derived in this case study, with the available data provided by authorities, still represent a good compromise between model complexity and reliable damages estimation results. Unlike other literature models developed for site-specific application and rarely tested for transferability, this study demonstrates that models can be export in similar contexts with satisfying results. If creating one unique model is almost impossible because of the already cited extreme variability of geographical and geomorphological contexts as well as urban patterns and building typologies typical of Italy, the definition of various damage models for different standardized Italian contexts could be very important for future flood risk analyses.

Conclusions

The present Dissertation focuses on several aspects of flood hazard and flood risk assessment and management, where the term flood risk refers in this context to the damage expected for a given element due to a flood event characterized by a specific intensity at a given time period. From the analytical point of view, flood risk is the combination of hydraulic hazard (i.e. the probability with which a flood event with a certain intensity can occur in a specific area and in a specific time period) and vulnerability (or damage, which provides information concerning which and how many elements can be affected by risk, and if and how much they are able to withstand a certain flood event). Flood vulnerability, in turn, is a function of exposure (which indicates the quantification and qualification of the elements exposed to risk) and flood susceptibility (i.e. the attribution of a loss value to the given element, as a function of one or more hydraulic parameters).

During the last decade, due to the steadily increasing impact of floods in Europe and worldwide and the promulgation of the FD 2007/60/EC, important efforts were made by investing research efforts, resources and money to shift from the flood defence paradigm to the flood management one. Moreover, recent analyses about the relationship between floods and other factors as climate variability, population growth and socio-economic changes assumed higher significance.

Nevertheless, there is still a large number of uncertainties and open problems that need to be investigated in order to better assess flood risk and its evolution in time and space, in one word its dynamics. Focusing on the Italian context, the present Dissertation addresses several key issues, on which indications reported by the scientific literature are still sparse. In particular, we focussed on three different elements and associated open problems, each one of which is associated with a specific component of flood risk and investigated thoroughly by means of a real world case study. The conclusions about the addressed aspects of flood risk management are briefly summarised below, answering the Thesis' research questions in order to

draw some general conclusions on the investigated issue.

Does anthropogenic land-subsidence provide changes in flood hazard dynamics and, in case it does, how relevant are they?

Concerning the drivers of hazard component of flood risk, we investigated the influence of human-induced (or human-accelerated) land-subsidence in altering the riverine inundation dynamics. To assess this issue, we considered a case study in the flood-prone areas near the city of Ravenna. The area is the most prominent case of anthropogenic land-subsidence in Italy due to the intense extraction of underground water and natural gas after World War II. By means of a fully-2D model, four different breaches in the left embankment of Montone river were considered. The flooding dynamics in the riverine flood-prone areas were first simulated by considering two topographic configurations, i.e. the current DEM and the reconstruction of the ground elevation before the acceleration of land-subsidence, at the end of XIX century. Second, the most important topographic discontinuities, i.e. railways and roads embankment and land reclamation channels, which were not captured by the 5 m resolution DEM, were added to both topographic configurations and new hydrodynamic simulations were performed. Results in terms of extent and distribution of flooded area and distribution of water depth, current velocity and intensity, show that human-induced land-subsidence may induce some changes in the flooding dynamics in the riverine flood-prone areas. Although differences between scenarios are limited, the outcomes showed that the areas near Ravenna city centre get inundated in the current terrain configuration, while they are not inundated for the pre-subsidence configuration. This observation is quite relevant, because high damages are expected in these areas due to the presence of residential areas and industrial activities. Nevertheless, the magnitude of these changes are negligible if compared to those resulting from the construction of roads, railways and channels. This consideration highlights the importance of an accurate assessment and mapping of the major topographic discontinuities when simulating flood dynamics. Furthermore, even though anthropogenic land-subsidence may not be seen as a significant potential driver of riverine flood hazard and risk changes, further analyses need to be performed aiming at studying land-subsidence effect in terms of ground-lowering gradients, which could alter the hydraulic behaviour of rivers embankments, and ultimately flood hazard.

Can simplified and easy-to-use approaches for assessing flood risk evolution over large scale areas be developed? To what extent changes in exposure influence flood risk dynamics?

This second issue dealt with the assessment of the historical evolution of exposure to flood over the floodplains of large European rivers from the aftermath of the II World War until present. We addressed this problem by focusing on entire floodplain of the middle-lower portion of the Po river (∼350 km). In particular, we performed a quasi-2D numerical simulation of the middle-lower stretch of the Po river for 1954 and 2008 and we evaluated the potential damages by means of simplified tools, developed for each zone of interest by combining information retrieved from high-resolution DEMs with land-use and land-coverage digital layers. If coupled with the results of a the numerical simulation in terms of water level, they enable one to define the amount of flooded area, for a certain land-use class. Combining this information with a specific depth- damage curve (which provides the percentage of damage suffered by the element at risk if this latter is flooded with a certain water depth), it is possible to estimate the expected direct economic losses in case of a flood event for both years and each area of interest. Outcomes pointed out a significant growth of the exposure of private real estate sector over the study area during the last 50 years, with a consequent increase in the expected direct losses that is almost doubled relatively to the considered inundation scenario (return period of ∼500 years). Nevertheless, the number of potentially affected inhabitants, evaluated by means of similar simplified tools, showed only marginal modifications during the study period. The developed procedure, despite the assumptions and limitations with the large-scale generalisations adopted in our study, proved to be a useful and efficient simplified tool for flood vulnerability and flood risk assessment. The methodology need to be further tested in other case studies, for instance by means of more accurate data, more elaborate hydrodynamic simulations or better delineation of flooded areas boundaries. The procedure demonstrated to be an appropriate tool for investigating alternative flood risk mitigation strategies at basin scale.

Are the literature uni- and multi-variate models capable of accurately reproducing flood losses in contexts that differ geographically and socio-economically from those for which the models were originally developed?

In other words, what is the value of uncritically exporting flood damage models

to different contexts? Because of the scarcity of reliable literature damage models in the Italian context, the third and last topic addressed in the Dissertation concerned the estimation of economic flood damages with the main aim of analysing post-event losses data collected from a real case study (flood event of the Secchia river in January 2014) and developing empirical damage models for the area of interest. Performance of these models was compared with the one of different literature models for flood losses evaluation. The models tested in our analysis are mostly uni-variate damage models, which relate the water depth to the relative or absolute amount of damages, as far as real estate and movable properties are concerned. One of the model, instead, is the adaptation of a multi-variate model available in the literature, which considers other damage influencing factors besides water depth, such as water velocity, flood duration, structural building type, economic building value and building area. Results confirmed previous findings by other authors (Cammerer et al., 2013; Green et al., 2011; Jongman et al., 2012; Molinari et al., 2014b) which affirm the difficulty to export literature damage models to contexts that differ from the one in which they were developed. Empirical uni- and multi-variate models, obtained from the basis of observed data in the same context, provided better performances in estimating potential damages. Furthermore, despite the multi-variate model used showed lower errors in terms of estimated losses compared with the uni-variate ones, the analysis underlined the need for large and comprehensive observed data sets to correctly derive it. The main open issue in this context regards the necessity to collect observed flood data, in order to validate existing models and to develop new reliable ones for different contexts.

Although having addressed the issues described in the Thesis can bring a significant contribution on flood risk assessment concerning these very aspects (i.e. hazard, exposure, susceptibility and vulnerability), there are also other relevant topics which need to be further investigated in the future researches.

First of all, in addition to the detailed assessment of the interactions between floods, climate and socio-economic factors, further studies about flood risk drivers and their evolution over time need to be carried out, aiming at providing realistic risk estimates over long periods of time, which can be used to assess sustainability of flood risk policies.

Regarding flood vulnerability, a potential interesting future assessment could focus, for instance, on the evolution of the industrial flood exposure (Domeneghetti et al., 2015): industrial sector experimented a significant growth in the last half century in

many part of the world and the literature with respect to this topic, however, is still scarce in terms of both industrial areas exposure and industrial sector damage models.

The limited availability of validation studies about flood risk assessment is another key point which needs to be improved (see e.g. Amadio et al., 2016; De Moel et al., 2015; Merz et al., 2010b; Molinari et al., 2012, 2014b; Scorzini and Frank, 2015), for instance through a more detailed and standardized post-disaster data collection for improving calibration, validation and thus performance of flood risk models.

Furthermore, several authors (see e.g. Carrera et al., 2015; De Moel et al., 2015) pointed out that considering only direct economic damages does not provide an exhaustive estimation of the consequences of floods. Instead, including indirect damages should become a standard approach in flood risk management in order to give a better indication of the total propagation effects of catastrophic floods.

Finally, scarce studies concerning non-structural protection measures are still provided by the literature. These measures include organization and communication schemes, content and planning of information campaigns, procedures in case of emergency, and recommendations. They have an irreplaceable role in the flood risk management and deserve to be thoroughly investigated in order to reduce flood risk (Escuder-Bueno et al., 2012).

Improvements in all these fields are needed in order to reach a holistic view of flood risk management. The system approach should include innovative weather generators coupled with hydrological catchment models, serving as boundary conditions for river-levee-floodplain hydraulic and geotechnical models, which consider the evolution of direct, indirect, tangible and intangible flood losses over long temporal scales. The ultimate aim should be the development of comprehensive methodologies that, with the necessary simplifications associated with the scale of the problem and the study area at hand, are capable to assess and compare different flood risk reduction strategies with the least possible uncertainty.

List of Acronyms

1D one-dimensional

2D two-dimensional

3D three-dimensional

AE Agenzia delle Entrate (Italian Revenue Agency)

AMS Annual Maximum Series

Ba_BTs Bastiglia Bagging Decision Trees

Ba_SRR Bastiglia Square Root Regression

Ba_SRR_ba Bastiglia Square Root Regression - building area

Ba_SRR_wd Bastiglia Square Root Regression - water depth

Ba_SRR_wv Bastiglia Square Root Regression - water velocity

Bo_BTs Bomporto Bagging Decision Trees

Bo_SRR Bomporto Square Root Regression

Bo_SRR_ba Bomporto Square Root Regression - building area

Bo_SRR_wd Bomporto Square Root Regression - water depth

Bo_SRR_wv Bomporto Square Root Regression - water velocity

BTs Bagging Decision Trees

CORINE COoRdinated INformation on the Environment

Curr current morphology

Curr_Infr current morphology with infrastructures

DEM Digital Elevation Model

FAI Flood Area Index

FLEMOps Flood Loss Estimation MOdel for private sector

FD Flood Directive

GIS Geographic Information System

HIC Hypsometric Inhabitants Curve

HVC Hypsometric Vulnerability Curve

JRC Joint Research Centre

MAE Mean Absolute Error

MBE Mean Bias Error

MCM Multi-Colored Manual

MS Member States

NSE Nash-Sutcliffe Efficiency

Past past morphology

Past_Infr past morphology with infrastructures

RA Rhine Atlas

RF Random Forest

RMSE Root Mean Square Error

SBTs Secchia Bagging Decision Trees

SD Standard Deviation

SE Secchia Empirical

SRR Square Root Regression

SRR_ba Square Root Regression - building area

SRR_wd Square Root Regression - water depth

SRR_wv Square Root Regression - water velocity

SSRR Secchia Square Root Regression

SSRR_ba Secchia Square Root Regression - building area

SSRR_wd Secchia Square Root Regression - water depth

SSRR_wv Secchia Square Root Regression - water velocity

SV Saint Venant

List of Figures

List of Tables

Bibliography

AdB-Po (1999). Progetto di Piano stralcio per lAssetto Idro-geologico (PAI) Interventi sulla rete idrografica e sui versanti. Technical report, AdB-Po, Parma, Italy.

AdB-Po (2006). Caratteristiche del bacino del fiume Po e primo esame dell'impatto ambientale delle attività umane sulle risorse idriche. Technical report, AdB-Po, Parma, Italy.

AdB-Reno, AdB-RR, AdB-Marecchia-Conca (2016). Piano di gestione del rischio alluvioni. Technical report, AdB-Reno, AdB-Regionali Romagnoli, AdB-Marecchia-Conca, Florence, Italy.

AdB-RR (2011). Piano Stralcio per il Rischio Idrogeologico Variante al Titolo II Assetto della rete idrografica. Technical report, Regione Emilia-Romagna.

Aerts, J. C. J. H., Botzen, W. J. W., de Moel, H., and Bowman, M. (2013). Cost estimates for flood resilience and protection strategies in New York City. *Annals of the New York Academy of Sciences*, 1294(1):1–104.

Alfieri, L., Feyen, L., Dottori, F., and Bianchi, A. (2015). Ensemble flood risk assessment in Europe under high end climate scenarios. *Global Environmental Change*, 35:199–212.

Amadio, M., Mysiak, J., Carrera, L., and Koks, E. (2016). Improving flood damage assessment models in Italy. *Natural Hazards*, 82(3):2075–2088.

Amadio, M., Mysiak, J., Pecora, S., and Agnetti, A. (2013). *Looking Forward from the Past: Assessing the Potential Flood Hazard and Damage in Polesine Region by Revisiting the 1950 Flood Event.* Fondazione eni enrico mattei working papers. paper 852. edition.

Apel, H., Aronica, G. T., Kreibich, H., and Thieken, A. H. (2009). Flood risk analyses - How detailed do we need to be? *Natural Hazards*, 49(1):79–98.

Aronica, G. T., Apel, H., Baldassarre, G. D., and Schumann, G. J.-P. (2013). HP - Special Issue on Flood Risk and Uncertainty. *Hydrological Processes*, 27(9):1291–1291.

Aronica, G. T., Franza, F., Bates, P. D., and Neal, J. C. (2012). Probabilistic evaluation of flood hazard in urban areas using Monte Carlo simulation. *Hydrological Processes*, 26(26):3962–3972.

Baldi, P., Casula, G., Cenni, N., Loddo, F., and Pesci, A. (2009). GPS-based monitoring of land subsidence in the Po Plain (Northern Italy). *Earth and Planetary Science Letters*, 288(1-2):204–212.

Barredo, J. I. (2009). Normalised flood losses in Europe: 19702006. *Natural Hazards and Earth System Sciences*, 9(1):97–104.

Bates, P. D. (2012). Integrating remote sensing data with flood inundation models: How far have we got? *Hydrological Processes*, 26(16):2515–2521.

Bates, P. D. and De Roo, A. P. J. (2000). A simple raster-based model for flood inundation simulation. *Journal of Hydrology*, 236(1-2):54–77.

Bates, P. D., Horritt, M. S., Aronica, G., and Beven, K. (2004). Bayesian updating of flood inundation likelihoods conditioned on flood extent data. *Hydrological Processes*, 18(17):3347–3370.

Bhatta, B., Saraswati, S., and Bandyopadhyay, D. (2010). Urban sprawl measurement from remote sensing data. *Applied Geography*, 30(4):731–740.

Bitelli, G., Bonsignore, F., and Unguendoli, M. (2000). Levelling and GPS networks to monitor ground subsidence in the Southern Po Valley. *Journal of Geodynamics*, 30(3):355–369.

Bouwer, L. M., Bubeck, P., and Aerts, J. C. (2010). Changes in future flood risk due to climate and development in a Dutch polder area. *Global Environmental Change*, 20(3):463–471.

Breiman, L. (2001). Random forests. *Machine Learning*, 45(1):5–32.

Breiman, L., Friedman, J., Olshen, R. A., and Stone, C. J. (1984). *CART: Classification and Regression Trees*. Wadsworth, belmont (ca) edition.

Brière, C., Abadie, S., Bretel, P., and Lang, P. (2007). Assessment of TELEMAC system performances, a hydrodynamic case study of Anglet, France. *Coastal Engineering*, 54(4):345–356.

Brown, S. and Nicholls, R. J. (2015). Subsidence and human influences in mega deltas: The case of the Ganges-Brahmaputra-Meghna. *Science of the Total Environment*, 527-528:362–374.

Bubeck, P., De Moel, H., Bouwer, L. M., and H. Aerts, J. C. J. (2011). How reliable are projections of future flood damage? *Natural Hazards and Earth System Science*, 11(12):3293–3306.

Bubeck, P. and Kreibich, H. (2011). Natural Hazards: direct costs and losses due to the disruption of production pro- esses - CONHAZ (Costs of Natural Hazards) Report. Technical report.

Büchele, B., Kreibich, H., Kron, A., Thieken, A., Ihringer, J., Oberle, P., Merz, B., and Nestmann, F. (2006). Flood-risk mapping: Contributions towards an enhanced assessment of extreme events and associated risks. *Natural Hazards and Earth System Sciences*, 6(4):483–503.

Büttner, G., Soukup, T., and Kosztra, B. (2014). CLC2012. Addendum to CLC2006 Technical Guidelines. Technical report, European Environment Agency, Malaga, Spain.

Cammerer, H., Thieken, A. H., and Lammel, J. (2013). Adaptability and transferability of flood loss functions in residential areas. *Natural Hazards and Earth System Sciences*, 13(11):3063–3081.

Carminati, E. and Martinelli, G. (2002). Subsidence rates in the Po Plain, northern Italy: the relative impact of natural and anthropogenic causation. *Engineering Geology*, 66:241–255.

Carrera, L., Standardi, G., Bosello, F., and Mysiak, J. (2015). Assessing direct and indirect economic impacts of a flood event through the integration of spatial and computable general equilibrium modelling. *Environmental Modelling & Software*, 63:109–122.

Castellarin, A., Di Baldassarre, G., Bates, P. D., and Brath, A. (2009). Optimal Cross-Sectional Spacing in Preissmann Scheme 1D Hydrodynamic Models. *Journal of Hydraulic Engineering*, 135(2):96–105.

Castellarin, A., Di Baldassarre, G., and Brath, A. (2011a). Floodplain management strategies for flood attenuation in the river Po. *River Research and Applications*, 27:1037–1047.

Castellarin, A., Domeneghetti, A., and Brath, A. (2011b). Identifying robust large-scale flood risk mitigation strategies: A quasi-2D hydraulic model as a tool for the Po river. *Physics and Chemistry of the Earth*, 36(7-8):299–308.

Ceola, S., Laio, F., and Montanari, A. (2014). Satellite nighttime lights reveal increasing human exposure to floods worldwide. *Geophysical Research Letters*, 41(20):7184–7190.

Chen, X. and Ishwaran, H. (2012). Random forests for genomic data analysis. *Genomics*, 99(6):323–329.

Ciscar, J.-C., Iglesias, A., Feyen, L., Szab o, L., Van Regemorter, D., Amelung, B., Nicholls, R., Watkiss, P., Christensen, O. B., Dankers, R., Garrote, L., Goodess, C. M., Hunt, A., Moreno, A., Richards, J., and Soria, A. (2011). Physical and economic consequences of climate change in Europe. *Proceedings of the National Academy of Sciences, USA*, (108):2678–2683.

Ciullo, A., Viglione, A., Castellarin, A., Crisci, M., and Di Baldassarre, G. (2017). Socio-hydrological modelling of flood-risk dynamics: comparing the resilience of green and technological systems. *Hydrological Sciences Journal*.

Coratza, L. (2005). Aggiornamento del catasto delle arginature maestre di Po. Technical report, AdB-Po, Parma, Italy.

Costabile, P., Macchione, F., Natale, L., and Petaccia, G. (2015). Flood mapping using LIDAR DEM. Limitations of the 1-D modeling highlighted by the 2-D approach. *Natural Hazards*, 77(1):181–204.

Crichton, D. (1999). *The risk triangle*. Tudor Rose, Leicester, UK.

D'Addabbo, A., Refice, A., Pasquariello, G., Lovergine, F., and Manfreda, S. (2016a). Sar/Optical Data Fusion for Flood Detection. In *2016 IEEE Workshop on Environmental, Energy, and Structural Monitoring Systems (EESMS)*, number 1, pages 7631–7634. IEEE.

D'Addabbo, A., Refice, A., Pasquariello, G., Lovergine, F. P., Capolongo, D., and Manfreda, S. (2016b). A Bayesian Network for Flood Detection Combining SAR Imagery and Ancillary Data. *IEEE Transactions on Geoscience and Remote Sensing*, 54(6):3612–3625.

Daito, K. and Galloway, D. L. (2015). Preface: Prevention and mitigation of natural and anthoropogenic hazards due to land subsidence. *Proceedings of the International Association of Hydrological Sciences*, 372(1):555–557.

D'Alpaos, L., Brath, A., Fioravante, V., Gottardi, G., Mignosa, P., and Orlandini, S. (2014). Relazione tecnico-scientifica sulle cause del collasso dell ' argine del fiume Secchia avvenuto il giorno 19 gennaio 2014 presso la frazione San Matteo. Technical report, Bologna, Italy.

De Moel, H. and Aerts, J. C. J. H. (2011). Effect of uncertainty in land use, damage models and inundation depth on flood damage estimates. *Natural Hazards*, 58(1):407–425.

De Moel, H., Aerts, J. C. J. H., and Koomen, E. (2011). Development of flood exposure in the Netherlands during the 20th and 21st century. *Global Environmental Change*, 21(2):620–627.

De Moel, H., Asselman, N. E. M., and H. Aerts, J. C. J. (2012). Uncertainty and sensitivity analysis of coastal flood damage estimates in the west of the Netherlands. *Natural Hazards and Earth System Science*, 12(4):1045–1058.

De Moel, H., Bouwer, L. M., and Aerts, J. C. J. H. (2014). Uncertainty and sensitivity of flood risk calculations for a dike ring in the south of the Netherlands. *Science of the Total Environment*, 473-474:224–234.

De Moel, H., Jongman, B., Kreibich, H., Merz, B., Penning-Rowsell, E., and Ward, P. J. (2015). Flood risk assessments at different spatial scales. *Mitigation and Adaptation Strategies for Global Change*, 20:865–890.

Deng, H. and Runge, G. (2013). Gene selection with guided regularized random forest. *Pattern Recognition*, 46(12):3483–3489.

Di Baldassarre, G., Castellarin, A., and Brath, A. (2009a). Analysis of the effects of levee heightening on flood propagation: example of the River Po, Italy. *Hydrological Sciences Journal*, 54(6):1007–1017.

Di Baldassarre, G., Castellarin, A., Montanari, A., and Brath, A. (2009b). Probability-weighted hazard maps for comparing different flood risk management strategies: A case study. *Natural Hazards*, 50(3):479–496.

Di Baldassarre, G., Kooy, M., Kemerink, J. S., and Brandimarte, L. (2013). Towards understanding the dynamic behaviour of floodplains as human-water systems. *Hydrology and Earth System Sciences*, 17(8):3235–3244.

Di Baldassarre, G., Schumann, G., and Bates, P. (2009c). Near real time satellite imagery to support and verify timely flood modelling. *Hydrological Processes*, 23:799–803.

Di Baldassarre, G., Schumann, G., Bates, P. D., Freer, J. E., and Beven, K. J. (2010). Flood-plain mapping: a critical discussion of deterministic and probabilistic approaches. *Hydrological Sciences Journal*, 55(3):364–376.

Di Baldassarre, G., Viglione, A., Carr, G., Kuil, L., Yan, K., Brandimarte, L., and Blöschl, G. (2015). Debates - Perspectives on socio-hydrology: Capturing feedbacks between physical and social processes. *Water Resources Research*, 51(6):4770–4781.

DICAM-PCREM (2015). Convenzione-quadro quinquennale di ricerca tra Agenzia di Protezione Civile della Regione Emilia-Romagna e il Dipartimento di Ingegneria Civile, Chimica, Ambientale e dei Materiali ALMA MATER STUDIORUM, Università di Bologna - Relazione conclusiva quarta . Technical report.

Dimitriadis, P., Tegos, A., Oikonomou, A., Pagana, V., Koukouvinos, A., Mamassis, N., Koutsoyiannis, D., and Efstratiadis, A. (2016). Comparative evaluation of 1D and quasi-2D hydraulic models based on benchmark and real-world applications for uncertainty assessment in flood mapping. *Journal of Hydrology*, 534:478–492.

Domeneghetti, A. (2014). Effects of minor drainage networks on flood hazard evaluation. *Proceedings of the International Association of Hydrological Sciences*, 364(June):192–197.

Domeneghetti, A., Carisi, F., Castellarin, A., and Brath, A. (2015). Evolution of Flood Risk Over Large Areas: Quantitative Assessment for The Po River. *Journal of Hydrology*, 527:809–823.

Domeneghetti, A., Vorogushyn, S., Castellarin, A., Merz, B., and Brath, A. (2013). Probabilistic flood hazard mapping: Effects of uncertain boundary conditions. *Hydrology and Earth System Sciences*, 17(8):3127–3140.

Dong, L. J., Li, X. B., and Peng, K. (2013). Prediction of rockburst classification using Random Forest. *Transactions of Nonferrous Metals Society of China*, 23(2):472–477.

Dottori, F., Di Baldassarre, G., and Todini, E. (2013). Detailed data is welcome, but with a pinch of salt: Accuracy, precision, and uncertainty in flood inundation modeling. *Water Resources Research*, 49(9):6079–6085.

Dottori, F., Figueiredo, R., Martina, M., Molinari, D., and Scorzini, A. R. (2016a). INSYDE: a synthetic, probabilistic flood damage model based on explicit cost analysis. *Natural Hazards and Earth System Sciences*, 16:2577–2591.

Dottori, F., Martina, M. L. V., and Figueiredo, R. (2016b). A methodology for flood susceptibility and vulnerability analysis in complex flood scenarios. *Journal of Flood Risk Management*, pages 1–14.

Elmer, F., Hoymann, J., Düthmann, D., Vorogushyn, S., and Kreibich, H. (2012). Drivers of flood risk change in residential areas. *Natural Hazards and Earth System Science*, 12(5):1641–1657.

Elmer, F., Thieken, A. H., Pech, I., and Kreibich, H. (2010). Influence of flood frequency on residential building losses. *Natural Hazards and Earth System Science*, 10(10):2145–2159.

Escuder-Bueno, I., Castillo-Rodriguez, J. T., Zechner, S., Jöbstl, C., Perales-Momparler, S., and Petaccia, G. (2012). A quantitative flood risk analysis methodology for urban areas with integration of social research data. *Natural Hazards and Earth System Science*, 12(9):2843–2863.

European Commission (2007). DIRECTIVE 2007/60/EC OF THE EUROPEAN PARLIAMENT AND OF THE COUNCIL of 23 October 2007 on the assessment and management of flood risks.

European Environment Agency (2005). Vulnerability and adaptation to climate change in Europe. Technical Report 7, Copenaghen, Denmark.

European Environment Agency (2007). CLC2006 technical guidelines. Technical Report 17, Copenhagen, Denmark.

European Environment Agency (2010). Mapping the impacts of recent natural disasters and technological accidents in Europe - An overview of the last decade. Technical Report 13, Copenhagen, Denmark.

EXCIMAP (2007). *Handbook on good practices for flood mapping in Europe.*

Falter, D., Schröter, K., Dung, N. V., Vorogushyn, S., Kreibich, H., Hundecha, Y., Apel, H., and Merz, B. (2015). Spatially coherent flood risk assessment based on long-term continuous simulation with a coupled model chain. *Journal of Hydrology*, 524.

Falter, D., Vorogushyn, S., Lhomme, J., Apel, H., Gouldby, B., and Merz, B. (2013). Hydraulic model evaluation for large-scale flood risk assessments. *Hydrological Processes*, 27(9):1331–1340.

Feyen, L., Dankers, R., Bodis, K., Salamon, P., and Barredo, J. I. (2012). Fluvial flood risk in Europe in present and future climates. *Climate Change*, 112:47–62.

Fohringer, J., Dransch, D., Kreibich, H., and Schröter, K. (2015). Social media as an information source for rapid flood inundation mapping. *Natural Hazards and Earth System Sciences*, 15(12):2725–2738.

Freni, g., La Loggia, G., and Notaro, V. (2010). Uncertainty in urban flood damage assessment due to urban drainage modelling and depth-damage curve estimation. *Water Science and Technology*, 61(12):2979–2993.

Galland, J. C., Goutal, N., and Hervouet, J. M. (1991). Telemac: a new numerical model for solving shallow water equations. *Advances in Water Resources*, 14(3):38–148.

Gambolati, G., Ricceri, G., Bertoni, W., Brighenti, G., and Vuillermin, E. (1991). Mathematical simulation of the subsidence of Ravenna. *Water resourches research*, 27:2899–2918.

Gerl, T., Kreibich, H., Franco, G., Marechal, D., and Schröter, K. (2016). A review of flood loss models as basis for harmonization and benchmarking. *PLOS ONE*, 11(7):1–22.

Giambastiani, B. M. S., Antonellini, M., Oude Essink, G. H. P., and Stuurman, R. J. (2007). Saltwater intrusion in the unconfined coastal aquifer of Ravenna (Italy): A numerical model. *Journal of Hydrology*, 340(1-2):91–104.

Gotoh, H., Takezawa, M., Maeno, Y., Oshiki, H., Nagashima, S., Nishimura, Y., and Ohta, M. (2009). *Development and restoration of the urban rivers: examples from old downtown Tokyo, Japan*, volume 124. Wit press edition.

Govi, M. and Turitto, O. (2000). Casistica storica sui processi diterazione delle correnti di piena del Po con arginature e con elementi morfotopografici del territorio adiacente (Historical documentations about the processes of dam breaks in the River Po, in Italian). Technical report, Istituto Lombardo Accademia di Scienza e Lettere, Milan, Italy.

Green, C., Viavattene, C., Thompson, P., and Green, C. (2011). Guidance for assessing flood losses - CONHAZ (Costs of Natural Hazards) Report. Technical report, Middlesex University.

Hailemariam, F. M., Brandimarte, L., and Dottori, F. (2014). Investigating the influence of minor hydraulic structures on modeling flood events in lowland areas. *Hydrological Processes*, 28(4):1742–1755.

Hall, J., Arheimer, B., Aronica, G. T., Bilibashi, A., Bohac, M., Bonacci, O., Borga, M., Burlando, P., Castellarin, A., Chirico, G. B., Claps, P., Fiala, K., Gaal, L., Gorbachova, L., Gül, A., Hannaford, J., Kiss, A., Kjeldsen, T., Kohnova, S., Koskela, J. J., MacDonald, N., Mavrova-Guirguinova, M., Ledvinka, O., Mediero, L., Merz, B., Merz, R., Molnar, P., Montanari, A., Osuch, M., Parajka, J., Perdigao, R. A. P., Radevski, I., Renard, B., Rogger, M., Salinas, J. L., Sauquet, E., Sraj, M., Szolgay, J., Viglione, A., Volpi, E., Wilson, D., Zaimi, K., and Blöschl, G. (2015). A European flood database: Facilitating comprehensive flood research beyond administrative boundaries. *Proceedings of the International Association of Hydrological Sciences*, 370:89–95.

Hall, J., Sayers, P., and Dawson, R. (2005). National-scale assessment of current and future flood risk in England and Wales. *Natural Hazards*, 36:147–164.

Hamed, K. H. (2008). Trend detection in hydrologic data: The Mann-Kendall trend test under the scaling hypothesis. *Journal of Hydrology*, 349(3-4):350–363.

Hammond, M. J., Chen, A. S., Djordjević, S., Butler, D., and Mark, O. (2013). Urban flood impact assessment: A state-of-the-art review. *Urban Water Journal*, 12(1):14–29.

Herfort, B., de Albuquerque, J. P., Schelhorn, S.-J., and Zipf, A. (2014). Exploring the geographical relations between social media and flood phenomena to improve situational awareness. In Huerta, J., Schade, S., and Granell, C., editors, *Lecture Notes in Geoinformation and Cartography*, chapter Connecting. Springer International Publishing.

Hervouet, J. M. and Bates, P. (2000). The Telemac modelling system, special issue. *Hydrological Processes*, 14(13):2207–2363.

Howladar, M. F. and Hasan, K. (2014). A study on the development of subsidence due to the extraction of 1203 slice with its associated factors around Barapukuria underground coal mining industrial area, Dinajpur, Bangladesh. *Environmental Earth Sciences*, 72(9):3699–3713.

Huizinga, H. J. (2007). Flood damage functions for EU member states, HKVConsultants, Implemented in the framework of the contract #382442-F1SC awarded by the European Commission. Technical report, European Commission - Joint Research Center.

Immitzer, M., Atzberger, C., and Koukal, T. (2012). Tree species classification with random forest using very high spatial resolution 8-band worldview-2 satellite data. *Remote Sensing*, 4:2661–2693.

IPCC (2001). Climate Change 2001 : Synthesis Report. Technical report, New York, NY, USA.

IPCC (2014). Climate Change 2014: Synthesis Report. Technical report, Geneva, Switzerland.

ISTAT (2009). Rapporto Annuale - La situazione del Paese nel 2008. Technical report, ISTAT, Rome, Italy.

Jongman, B., Kreibich, H., Apel, H., Barredo, J. I., Bates, P. D., Feyen, L., Gericke, A., Neal, J., Aerts, J. C. J. H., and Ward, P. J. (2012). Comparative flood damage model assessment: towards a European approach. *Natural Hazards and Earth System Science*, 12(12):3733–3752.

Jonkman, S. N. (2005). Global perspectives on loss of human life caused by floods. *Natural Hazards*, 34(2):151–175.

Koks, E. E., Jongman, B., Husby, T. G., and Botzen, W. J. W. (2015). Combining hazard, exposure and social vulnerability to provide lessons for flood risk management. *Environmental Science and Policy*, 47:42–52.

Koutsoyiannis, D. (2013). Hydrology and change. *Hydrological Sciences Journal*, 58(6):1177–1197.

Kreibich, H., Botto, A., Merz, B., and Schröter, K. (2016a). Probabilistic, Multivariable Flood Loss Modeling on the Mesoscale with BT-FLEMO. *Risk Analysis*.

Kreibich, H., Botto, A., Schröter, K., and Merz, B. (2016b). Probabilistic , meso-scale flood loss modelling. In *EGU General Assembly 2016*, volume 18, page 12957, Vienna, Austria.

Kreibich, H., Meyer, S., and Diekkrger, B. (2011). Weiterentwicklung von FLEMOps zur Modellierung von Grundhochwasserschden und Wohngebauden. *Hydrologie und Wasserbewirtschaftung*, (55):300–309.

Kreibich, H., Piroth, K., Seifert, I., Maiwald, H., Kunert, U., Schwarz, J., Merz, B., and Thieken, A. H. (2009). Is flow velocity a significant parameter in flood damage modelling? *Natural Hazards and Earth System Science*, 9(5):1679–1692.

Kreibich, H., Schröter, K., and Merz, B. (2016c). Up-scaling of multi-variable flood loss models from objects to land use units at the meso-scale. *Proceedings of the International Association of Hydrological Sciences*, 373:179–182.

Kreibich, H., Seifert, I., Merz, B., and Thieken, A. H. (2010). Development of FLEMOcs a new model for the estimation of flood losses in the commercial sector. *Hydrological Sciences Journal*, 55(8):1302–1314.

Kreibich, H. and Thieken, A. H. (2008). Assessment of damage caused by high groundwater inundation. *Water Resources Research*, 44(9):1–14.

Kundzewicz, W. Z., Graczyk, D., Maurer, T., Pinskwar, I., Radziejewski, M., Svensson, C., and Szwed, M. (2005). Trend detection in river flow series: 1. Annual maximum flow. *Hydrological Sciences Journal*, 50(5):797–810.

Kvocka, D., Falconer, R. A., and Bray, M. (2016). Flood hazard assessment for extreme flood events. *Natural Hazards*, 84:1569–1599.

Lim, N. J. (2011). *Performance and uncertainty estimation of 1-and 2-dimensional flood models*. PhD thesis, Gävle University College.

Ludy, J. and Kondolf, G. M. (2012). Flood risk perception in lands "protected" by 100-year levees. *Natural Hazards*, 61(2):829–842.

Luino, F., Chiarle, M., Nigrelli, G., Agangi, A., Bidoccu, M., Cirio, C. G., and Giulietto, W. (2006). A model for estimating flood damage in Italy: preliminary results, in: Environmental Economics and Investment Assessment. 98:1–10.

Luino, F., Turconi, L., Petrea, C., and Nigrelli, G. (2012). Uncorrected land-use planning highlighted by flooding: The Alba case study (Piedmont, Italy). *Natural Hazards and Earth System Science*, 12(7):2329–2346.

Maatar, F. E. (2015). *Numerical Hydraulic Models for Flood-Risk Assessment and Management*. PhD thesis, University of Cadiz; University of Bologna.

Manciola, P., Biscarini, C., and Cingolani, A. (2003). La mappatura delle aree inondabili. In *Proceedings of "Riqualificazione, Difesa Idraulica e Recupero Ambientale delle Sponde Fluviali", Perugia, Italy, 26-28 May 2003*, Perugia, Italy.

Manfreda, S., Di Leo, M., and Sole, A. (2011). Detection of Flood-Prone Areas Using Digital Elevation Models. *Journal of Hydrologic Engineering*, 16(10):781–790.

Manfreda, S., Samela, C., Gioia, A., Consoli, G. G., Iacobellis, V., Giuzio, L., Cantisani, A., and Sole, A. (2015). Flood-prone areas assessment using linear binary classifiers based on flood maps obtained from 1D and 2D hydraulic models. *Natural Hazards*, 79(2):735–754.

Manfreda, S., Samela, C., Sole, A., and Fiorentino, M. (2014). Flood-Prone Areas Assessment Using Linear Binary Classifiers based on Morphological Indices. *Vulnerability, Uncertainty, and Risk*, pages 1635–1644.

Manfreda, S., Sole, A., and Fiorentino, M. (2008). Can the basin morphology alone provide an insight into floodplain delineation. *WIT Transactions on Ecology and the Environment*, 118:47–56.

Mani, P., Chatterjee, C., and Kumar, R. (2014). Flood hazard assessment with multiparameter approach derived from coupled 1D and 2D hydrodynamic flow model. *Natural Hazards*, 70(2):1553–1574.

Markantonis, V., Meyer, V., and Schwarze, R. (2012). Valuating the intangible effects of natural hazards - Review and analysis of the costing methods. *Natural Hazards and Earth System Science*, 12(5):1633–1640.

Masoero, A., Claps, P., Asselman, N. E. M., Mosselman, E., and Di Baldassarre, G. (2013). Reconstruction and analysis of the Po River inundation of 1951. *Hydrological Processes*, 27(9):1341–1348.

Massari, C., Tarpanelli, A., and Moramarco, T. (2015). A fast simplified model for predicting river flood inundation probabilities in poorly gauged areas. *Hydrological Processes*, 29(10):2275–2289.

McMillan, H., Montanari, A., Cudennec, C., Savenije, H., Kreibich, H., Krueger, T., Liu, J., Mejia, A., Van Loon, A., Aksoy, H., Di Baldassarre, G., Huang, Y., Mazvimavi, D., Rogger, M., Sivakumar, B., Bibikova, T., Castellarin, A., Chen, Y., Finger, D., Gelfan, A., Hannah, D. M., Hoekstra, A. Y., Li, H., Maskey, S., Mathevet, T., Mijic, A., Pedrozo Acuña, A., Polo, M. J., Rosales, V., Smith, P., Viglione, A., Srinivasan, V., Toth, E., van Nooyen, R., and Xia, J. (2016). Panta Rhei 20132015: global perspectives on hydrology, society and change. *Hydrological Sciences Journal*, 6667(September):1–18.

Merz, B., Aerts, J., Arnbjerg-Nielsen, K., Baldi, M., Becker, A., Bichet, A., Blöschl, G., Bouwer, L. M., Brauer, A., Cioffi, F., Delgado, J. M., Gocht, M., Guzzetti, F., Harrigan, S., Hirschboeck, K., Kilsby, C., Kron, W., Kwon, H. H., Lall, U., Merz, R., Nissen, K., Salvatti, P., Swierczynski, T., Ulbrich, U., Viglione, A., Ward, P. J., Weiler, M., Wilhelm, B., and Nied, M. (2014). Floods and climate: Emerging perspectives for flood risk assessment and management. *Natural Hazards and Earth System Sciences*, 14(7):1921–1942.

Merz, B., Elmer, F., and Thieken, A. H. (2009). Significance of high probability/low damage versus low probability/high damage flood events. *Natural Hazards and Earth System Sciences*, 9(3):1033–1046.

Merz, B., Hall, J., Disse, M., and Schumann, A. (2010a). Fluvial flood risk management in a changing world. *Natural Hazards and Earth System Sciences*, 10(1):509–527.

Merz, B., Kreibich, H., and Lall, U. (2013). Multi-variate flood damage assessment: A tree-based data-mining approach. *Natural Hazards and Earth System Science*, 13(1):53–64.

Merz, B., Kreibich, H., Schwarze, R., and Thieken, A. (2010b). Review article "assessment of economic flood damage". *Natural Hazards and Earth System Science*, 10(8):1697–1724.

Merz, B., Kreibich, H., Thieken, a., and Schmidtke, R. (2004). Estimation uncertainty of direct monetary flood damage to buildings. *Natural Hazards and Earth System Science*, 4(1):153–163.

Merz, B. and Thieken, A. H. (2004). Flood risk analysis: concepts and challenges. *sterreichische Wasser-und Abfallwirtschaft*, 56(3–4):27–34.

Merz, B., Thieken, A. H., and Gocht, M. (2007). *Flood Risk Mapping At The Local Scale: Concepts and Challenges*. Springer Netherlands, Dordrecht, Netherlands.

Messner, F., Penning-Rowsell, E., Green, C., Meyer, V., Tunstall, S., and van der Veen, A. (2007). Evaluating flood damages: guidance and recommendations on principles and methods. Technical report, HR Wallingford, UK.

Meyer, V., Becker, N., Markantonis, V., Schwarze, R., Van Den Bergh, J. C. J. M., Bouwer, L. M., Bubeck, P., Ciavola, P., Genovese, E., Green, C., Hallegatte, S., Kreibich, H., Lequeux, Q., Logar, I., Papyrakis, E., Pfurtscheller, C., Poussin, J., Przyluski, V., Thieken, A. H., and Viavattene, C. (2013). Review article: Assessing the costs of natural hazards-state of the art and knowledge gaps. *Natural Hazards and Earth System Science*, 13(5):1351–1373.

Mihailescu, D. M., Gui, V., Toma, C. I., Popescu, A., and Sporea, I. (2013). Computer aided diagnosis method for steatosis rating in ultrasound images using random forests. *Medical Ultrasonography*, 15(3):184–190.

Molinari, D., Aronica, G., Ballio, F., Berni, N., and Pandolfo, C. (2012). Le curve di danno quale strumento a supporto della direttiva alluvioni: criticità dei dati italiani. In *XXXIII Convegno Nazionale di Idraulica e Costruzioni Idrauliche - Brescia, 10-15 settembre 2012*, Brescia, Italy.

Molinari, D., Ballio, F., Handmer, J., and Menoni, S. (2014a). On the modeling of significance for flood damage assessment. *International Journal of Disaster Risk Reduction*, 10:381–391.

Molinari, D., Menoni, S., Aronica, G. T., Ballio, F., Berni, N., Pandolfo, C., Stelluti, M., and Minucci, G. (2014b). Ex post damage assessment: an Italian experience. *Natural Hazards and Earth System Science*, 14(4):901–916.

Montanari, A. (2012). Hydrology of the Po River: looking for changing patterns in river discharge. *Hydrology and Earth System Sciences*, 16(1):3739–3747.

Montanari, A., Young, G., Savenije, H., Hughes, D., Wagener, T., Ren, L., Koutsoyiannis, D., Cudennec, C., Toth, E., Grimaldi, S., Blöschl, G., Sivapalan, M., Beven, K., Gupta, H., Hipsey, M., Schaefli, B., Arheimer, B., Boegh, E., Schymanski, S., Di Baldassarre, G., Yu, B., Hubert, P., Huang, Y., Schumann, A., Post, D., Srinivasan, V., Harman, C., Thompson, S., Rogger, M., Viglione, A., McMillan, H., Characklis, G., Pang, Z., and Belyaev, V. (2013). Panta RheiEverything Flows: Change in hydrology and societyThe IAHS Scientific Decade 20132022. *Hydrological Sciences Journal*, 58(6):1256–1275.

Mukolwe, M. M., Baldassarre, G. D., Werner, M., and Solomatine, D. P. (2014). Flood modelling: parameterisation and inflow uncertainty. *Proceedings of the ICE - Water Management*, 167:51–60.

Neal, J., Schumann, G., and Bates, P. (2012). A subgrid channel model for simulating river hydraulics and floodplain inundation over large and data sparse areas. *Water Resources Research*, 48(11):1–16.

Néelz, S. and Pender, G. (2013). Delivering benefits through evidence - Benchmarking the latest generation of 2D hydraulic modelling packages. Technical report, Environment Agency, Bristol, UK.

Neumayer, E. and Barthel, F. (2011). Normalizing economic loss from natural disasters: A global analysis. *Global Environmental Change*, 21(1):13–24.

Orlandini, S., Moretti, G., and Albertson, J. D. (2015). Evidence of an emerging levee failure mechanism causing disastrous floods in Italy. *Water Resources Research*, 51(10):7995–8011.

Ortega-Guerrero, A., Rudolph, D. L., and Cherry, J. A. (1999). Analysis of long-term land subsidence near Mexico City: Field investigations and predictive modeling. *Water Resources Research*, 35(11):3327–3341.

Papaioannou, G., Loukas, A., Vasiliades, L., and Aronica, G. T. (2016). Flood inundation mapping sensitivity to riverine spatial resolution and modelling approach. *Natural Hazards*, 83(1):117–132.

Pappenberger, F., Matgen, P., Beven, K. J., Henry, J. B., Pfister, L., and Fraipont, P. (2006). Influence of uncertain boundary conditions and model structure on flood inundation predictions. *Advances in Water Resources*, 29(10):1430–1449.

Penning-Rowsell, E., Johnson, C., Tunstall, S., Morris, J., Chatterton, J., Green, C., Koussela, K., and Fernandez-bilbao, A. (2005). *The Benefits of Flood and Coastal Risk Management: A Handbook of Assessment Techniques*. Middlesex University Press, London, UK.

Penning-Rowsell, E., Viavattene, C., Pardoe, J., Chatterton, J., Parker, D., and Morris, J. (2010). *The Benefits of Flood and Coastal Risk Management: A Handbook of Assessment Techniques*. Middlesex University Press, London, UK.

Petrow, T. and Merz, B. (2009). Trends in flood magnitude, frequency and seasonality in Germany in the period 19512002. *Journal of Hydrology*, 371(1-4):129–141.

Phien-wej, N., Giao, P., and Nutalaya, P. (2006). Land subsidence in Bangkok, Thailand. *Engineering Geology*, 82(4):187–201.

Pielke Jr., R. a., Gratz, J., Landsea, C. W., Collins, D., Saunders, M. A., and Musulin, R. (2008). Normalized Hurricane Damage in the United States: 19002005. *Natural Hazards Review*, 9(February):29–42.

Pielke Jr., R. A. and Landsea, C. W. (1998). Normalized Hurricane Damages in the United States: 1925 95. *Wea. Forecasting*, 13(Landsea 1993):621–631.

Potok, A. J. (1991). A Study of the Relationship between Subsidence and Flooding. In *Proceedings of the Fourth International Symposium on Land Subsidence*, number 200, pages 389–396, Houston, Texas, USA.

Quiroga, V., Popescu, I., Solomatine, D., and Bociort, L. (2013). Cloud and cluster computing in uncertainty analysis of integrated flood models. *Journal of Hydroinformatics*, 15:55–70.

Refice, A., D'Addabbo, A., Pasquariello, G., Lovergine, F. P., Capolongo, D., and Manfreda, S. (2015). Towards high-precision flood mapping: Multi-temporal SAR/InSAR data, Bayesian inference, and hydrologic modeling. *International Geoscience and Remote Sensing Symposium (IGARSS)*, 2015-November:1381–1384.

Refice, A., Pasquariello, G., D'addabbo, A., Bovenga, F., Nutricato, R., Capolongo, D., Lepera, A., Pietranera, L., Manfreda, S., Cantisani, A., and Sole, A. (2013). Inundation monitoring through high-resolution SAR/InSAR data and 2D hydraulic simulations. *Proc. 33rd EARSel Symposium*, pages 15–22.

Rodolfo, K. S. and Siringan, F. P. (2006). Global sea-level rise is recognised, but flooding from anthropogenic land subsidence is ignored around northern Manila Bay, Philippines. *Disasters*, 30(1):118–139.

Samela, C., Manfreda, S., Paola, F. D., Giugni, M., Sole, A., and Fiorentino, M. (2015). DEM-Based Approaches for the Delineation of Flood-Prone Areas in an Ungauged Basin in Africa. *Journal of Hydrologic Engineering*, 21(August):06015010.

Sampson, C. C., Smith, A. M., Bates, P. D., Neal, J. C., Alfieri, L., and Freer, J. E. (2015). A high-resolution global flood hazard model. *Water Resources Research*, pages 7358–7381.

Schmidt, C. W. (2015). Delta subsidence: An imminent threat to coastal populations. *Environmental Health Perspectives*, 123(8):204–209.

Schröter, K., Kreibich, H., Vogel, K., Riggelsen, C., Scherbaum, F., and Merz, B. (2014). How useful are complex flood damage models? *Water Resources Research*, 50:3378–3395.

Schröter, K., Lüdtke, S., Vogel, K., Kreibich, H., and Merz, B. (2016). Tracing the value of data for flood loss modelling. In *FLOODrisk 2016 - 3rd European Conference on Flood Risk Management*, volume 05005, pages 4–8.

Schubert, J. E., Sanders, B. F., Smith, M. J., and Wright, N. G. (2008). Unstructured mesh generation and landcover-based resistance for hydrodynamic modeling of urban flooding. *Advances in Water Resources*, 31(12):1603–1621.

Schultz, J. and Elliott, J. R. (2013). Natural disasters and local demographic change in the United States. *Population and Environment*, 34(3):293–312.

Schumann, G., Bates, P. D., Horritt, M. S., Matgen, P., and Pappenberger, F. (2009). Progress in integration of remote sensing-derived flood extent and stage data and hydraulic models. *Reviews of Geophysics*, 47(3):1–21.

Scorzini, A. R. and Frank, E. (2015). Flood damage curves: New insights from the 2010 flood in Veneto, Italy. *Journal of Flood Risk Management*, pages 1–12.

Settis, S. (2012). *Paesaggio Costituzione cemento. La battaglia per l'ambiente contro il degrado civile*. Einaudi edition.

Sivapalan, M., Savenije, H. H. G., and Blöschl, G. (2012). Socio-hydrology: A new science of people and water. *Hydrological Processes*, 26(8):1270–1276.

Smith, D. I. (1994). Flood damage estimation - a review of urban stage-damage curves and loss functions. *Water SA*, 20(3):231–238.

Solomon, T. and Liu, Z. (2010). Earthquake induced damage classification for reinforced concrete buildings. *Structural Safety*, 32(2):154–164.

Sudhira, H. and Ramachandra, T. (2007). Characterising Urban Sprawl From Remote Sensing Data and Using Landscape Metrics. In *10th International Conference on Computers in Urban Planning and Urban Management*, pages 1–12.

Svensson, C., Kundzewicz, W. Z., and Maurer, T. (2005). Trend detection in river flow series: 2. Flood and low-flow index series. *Hydrological Sciences Journal*, 50(5):811–824.

Tarquini, S., Isola, I., Favalli, M., Mazzarini, F., Bisson, M., Pareschi, M. T., and Boschi, E. (2007). TINITALY / 01: a new Triangular Irregular Network of Italy. *Annal of Geophysics*, 50(1):407–425.

Tarquini, S., Vinci, S., Favalli, M., Doumaz, F., Fornaciai, A., and Nannipieri, L. (2012). Release of a 10-m-resolution DEM for the Italian territory: Comparison with global-coverage DEMs and anaglyph-mode exploration via the web. *Computers & Geosciences*, 38(1):168–170.

Teatini, P., Ferronato, M., Gambolati, G., Bertoni, W., and Gonella, M. (2005). A century of land subsidence in Ravenna, Italy. *Environmental geology*, 47(6):831–846.

Thieken, A. H., Olschewski, A., Kreibich, H., Kobsch, S., and Merz, B. (2008). *Development and evaluation of FLEMOps - A new Flood Loss Estimation MOdel for the private sector*, volume 118. Wit press edition.

Tobin, G. A. (1995). The levee love affair: a stormy relationship? *Journal of the American Water Resources Association*, 31:359–367.

Tsakiris, G. (2014). Flood risk assessment: Concepts, modelling, applications. *Natural Hazards and Earth System Sciences*, 14(5):1361–1369.

van der Sande, C. (2001). River flood damage assessment using IKONOS imagery. Technical report, European Commission - Joint Research Center.

van Dyck, J. and Willems, P. (2013). Probabilistic flood risk assessment over large geographical regions. *Water Resources Research*, 49(6):3330–3344.

Villarini, G., Smith, J. a., Serinaldi, F., and Ntelekos, A. a. (2011). Analyses of seasonal and annual maximum daily discharge records for central Europe. *Journal of Hydrology*, 399(3-4):299–312.

Vis, M., Klijn, F., De Bruijn, K. M., and Van Buuren, M. (2003). Resilience strategies for flood risk management in the Netherlands. *International Journal of River Basin Management*, 1(1):33–40.

Vorogushyn, S. (2008). *Analysis of flood hazard under-consideration of dike breaches*. PhD thesis, Unniversity of Potsdam, Germany.

Vorogushyn, S., Lindenschmidt, K. E., Kreibich, H., Apel, H., and Merz, B. (2012). Analysis of a detention basin impact on dike failure probabilities and flood risk for a channel-dike-floodplain system along the river Elbe, Germany. *Journal of Hydrology*, 436-437:120–131.

Vorogushyn, S. and Merz, B. (2013). Flood trends along the Rhine: the role of river training. *Hydrology and Earth System Sciences*, 17(1):3871–3884.

Vorogushyn, S., Merz, B., Lindenschmidt, K. E., and Apel, H. (2010). A new methodology for flood hazard assessment considering dike breaches. *Water Resources Research*, 46(8):1–17.

Wang, Z., Lai, C., Chen, X., Yang, B., Zhao, S., and Bai, X. (2015). Flood hazard risk assessment model based on random forest. *Journal of Hydrology*, 527:1130–1141.

White, G. (1945). *Human adjustment to floods*. Department of Geography - University of Chicago, USA.

Wilby, R. L., Beven, K. J., and Reynard, N. S. (2008). Climate change and fluvial flood risk in the UK: more of the same? *Hydrological Processes*, 22:2511–2523.

Winsemius, H. C., Aerts, J. C. J. H., van Beek, L. P. H., Bierkens, M. F. P., Bouwman, A., Jongman, B., Kwadijk, J. C. J., Ligtvoet, W., Lucas, P. L., van Vuuren, D. P., and Ward, P. J. (2015). Global drivers of future river flood risk. *Nature Climate Change*, (December):1–5.

Winsemius, H. C., Van Beek, L. P. H., Jongman, B., Ward, P. J., and Bouwman, A. (2013). A framework for global river flood risk assessments. *Hydrology and Earth System Sciences*, 17(5):1871–1892.

Yin, J., Yu, D., Yin, Z., Wang, J., and Xu, S. (2013a). Modelling the combined impacts of sea-level rise and land subsidence on storm tides induced flooding of the Huangpu River in Shanghai, China. *Climatic Change*, 119(3-4):919–932.

Yin, J., Yu, D., Yin, Z., Wang, J., and Xu, S. (2013b). Multiple scenario analyses of Huangpu River flooding using a 1D/2D coupled flood inundation model. *Natural Hazards*, 66(2):577–589.

Zanchettini, D., Traverso, P., and Tomasino, M. (2008). Po river discharge: a preliminary analysis of a 200-year time series. *Climate change*, 88:411–433.

Zhang, K., Dittmar, J., Ross, M., and Bergh, C. (2011). Assessment of sea level rise impacts on human population and real property in the Florida Keys. *Climatic Change*, 107(1):129–146.

Acknowledgements

All institutions, agencies and public bodies that contributed in various ways to make this work possible are thankfully acknowledged. Part of the research activity was performed with the support and contribution of the Civil Protection Agency of Emilia-Romagna under a five-year framework research agreement with the Department of Civil, Chemical, Environmental and Materials Engineering (DICAM) of the University of Bologna (DICAM-PCREM, 2015). Moreover, an active and fundamental contribution was provided by the Po river Basin Authority (AdB-Po), which also contributed providing various data sets. This work is also part of the research activities carried out by the working group Anthropogenic and Climatic Controls on WateR AvailabilitY (ACCuRAcY) of Panta Rhei Everything Flows Change in Hydrology and Society (IAHS Scientific Decade 2013-2022).

The present Dissertation represents the result and the arrival point of three stimulating and fruitful years of PhD activity. I really want to thank my supervisor, Prof. Attilio Castellarin, for his professional and caring guidance, and for providing me with important insights to carry on my work. I would like to express my deepest and sincere gratitude to my "unofficial" co-supervisor, Dr. Alessio Domeneghetti, for being constantly very patient, helpful and motivating whenever I needed. It was really a honour and a pleasure to work with you. Special thanks to Prof. Brath, for involving me in many of his interesting ongoing projects.

I am thankful towards all my colleagues, the "old" and the "new" ones. Thank you Alberto, Elena, Cristiana, Marco, Andrea, Serena, Sara, Emanuele, Alessio, Matteo, Simone, Umberto, Federica, Iuliia, Mattia, Gabriella, Silvia and Arianna. Thank you for sharing all these PhD months, supporting me during either good and bad moments, inside and outside the office. Also a big thank to all the "water" PhD students and young researchers all over Italy, with whom I spent wonderful moments and who made me feel in good company in dealing with the numerous research-related issues.

Many thanks are owed to Prof. Heidi Kreibich, because of her really welcoming reception and valuable supervision during my stay at GFZ Potsdam, Germany. I would also like to thank all the researchers I met at GFZ, especially Prof. Bruno Merz and Dr. Kai Schröter for their helpfulness and precious collaboration in my PhD abroad activity.

Acknowledgements

But this works has been possible also thanks to many people outside the academic world, who encouraged this life path with their true enthusiasm and friendship, from the closest to the farthest ones (but still present in my life). However, in this context I would only say a big "Thank you" to everyone. Every person who has supported me in many different ways deserves to be thanked properly and I promise to do it personally.

Last but not least, I would like to warmly thank my family, which always supported me without hesitation in every decision I took, with love, patience and understanding. Thank you Riccardo for being a wonderful dad and life partner and, most important of all, my not-so-little-anymore Emanuele, for being the best gift that life gave me.